THE MECHANISM OF HUMAN APOLIPOPROTEIN L1 KILLING OF AFRICAN TRYPANOSOMES

by

AMY STYER GREENE

(Under the Direction of STEPHEN HAJDUK)

ABSTRACT

Trypanosoma brucei brucei parasites are rapidly lysed by human serum due to innate immune factors called trypanosome lytic factors (TLFs). Related parasites *T. b. rhodesiense* and *T. b. gambiense* evolved resistance to the TLFs and cause the deadly disease human African trypanosomiasis. My work focused on TLF-1, a high density lipoprotein particle (HDL) containing the pore-forming toxin Apolipoprotein L1 (ApoL1) and hemoglobin-binding protein haptoglobin related protein (Hpr). I found that TLF-1 and ApoL1 cause rapid changes at the plasma membrane, including dissipating the plasma membrane potential and inducing sensitivity to hypotonic lysis. ApoL1-induced osmotic stress at the plasma membrane leads to water influx and eventual lysis. Moreover, osmotic lysis is exacerbated by oxidizing agents and molecules which bind to free thiols in proteins. My work suggests that ApoL1 in TLF-1 traffics to the plasma membrane of *T. b. brucei*, facilitating sodium influx, ionic imbalance, oxidation of osmoregulatory proteins, cell swelling, and trypanosome lysis.

INDEX WORDS: Trypanosome, *Trypanosoma brucei*, ApoL1, HDL, cell death, oxidative stress, osmotic stress, plasma membrane potential

THE MECHANISM OF HUMAN APOL1 KILLING OF AFRICAN TRYPANOSOMES

by

AMY STYER GREENE

B.S., University of Delaware, 2010

A Dissertation Submitted to the Graduate Faculty of The University of Georgia in Partial Fulfillment of the Requirements for the Degree

DOCTOR OF PHILOSOPHY

ATHENS, GEORGIA

2016

THE MECHANISM OF HUMAN APOLIPOPROTEIN L1 KILLING OF AFRICAN TRYPANOSOMES

by

AMY STYER GREENE

Major Professor:	Stephen Hajduk
Committee:	Robert Sabatini
	Kojo Mensa-Wilmot
	Zachary Wood
	Amy Medlock

Electronic Version Approved:

Suzanne Barbour
Dean of the Graduate School
The University of Georgia
May 2016

DEDICATION

I dedicate this thesis to those I have known and lost during my six years at UGA: Howard Styer “Poppop”, Aunt Miriam Ruth, Dr. Laura Cliffe, Dr. Tariq Perwez, Father Tom Vigiolatta, Dr. Oliver Ludwig, Snizhana Radzetska, Kortney Gordon and her pre-born baby Sophie, Jon Scarfenberger, Dr. Paul Grutsch, and Dr. Martin Kleiber.

ACKNOWLEDGEMENTS

Thanks to everyone! All praise to the Eucharistic Jesus who comes down to earth to be with my sinful, stressed-out self. I especially thank my husband Fadi Greene who put off his career to come down to GA and support me as I finished my Ph.D. a semester later than originally planned. I'm also very thankful for the many hours Fadi saved me by helping to format and edit this dissertation. Numerous friends, family, and lab co-workers have encouraged me and given me great ideas during this work.

My committee is made up of a diverse group of professors who have contributed to my development in different ways. Steve Hajduk is a great scientist to have as a Ph.D. mentor. He is always creative and willing to support my ideas and models. He generously sent me to the biology of parasitism course and several conferences which were highlights of my time here. I am also thankful to have a boss who is supportive of my pursuit of a teaching-oriented career. Bob Sabatini always asks questions to ensure that I can articulate ideas well. Zac Wood thinks about things in terms of structure and kinetics, and he brings a joyful optimism about science to committee meetings. Kojo thinks outside the box, and asks questions that make me think. His perspectives on curing African trypanosomiasis as a disease is also helpful. Amy Medlock's expertise was helpful in my introductory work on reconstituting globins with heme, and I am thankful that she always takes the time to ask about me as a person as well as about my science.

There are other professors at UGA who deserve recognition. I must thank CTEGD professor Dr. Roberto Docampo and Dr. Silvia Moreno for helpful discussions about the plasma membrane potential and osmotic stress in trypanosomes. Dr. Paula Lemons has been a wonderful mentor and resource for my interest in teaching and learning. I have spent many hours with her working together on teaching projects and discussing career plans. Dr. Paula Lemons and Dr. John Rose have also been extremely helpful in writing dozens of letters of recommendation for teaching positions I have applied for. Thanks to Dr. Jon Rose and Dr. Allan Pryzbyla for allowing me to give guest lectures in their biochemistry classes. It has also been a joy to work with Dr. Kris Miller who co-ordinates biology lab instructors. She gives me the freedom to teach and assess my students in creative ways, making my time in the biology 1108 lab a highlight of my Ph.D.

I have had the joy of working with two talented undergraduates in the lab: Allen Witt and Savanah-Rose Pena. Both worked on the biogenesis of TLF-2 project, which I have unfortunately not been able to pull into a publication-style chapter for this dissertation. They are now both in medical school, and I hope that the experience they had performing experiments, reading articles, and writing about their results helped them to become better doctors and collaborators with scientists.

TABLE OF CONTENTS

Page

LIST OF TABLES

Page

LIST OF FIGURES

Page

CHAPTER 1

INTRODUCTION AND LITERATURE REVIEW

INTRODUCTION TO TRYPANOSOMES

Humans are innately resistant to infection by most African trypanosome parasites because of primate-specific lipoprotein particles called trypanosome lytic factors (TLFs). Later chapters detail work I have contributed to understanding how *Trypanosoma brucei brucei* parasites are killed by the TLFs. Understanding how innate immunity kills these parasites may lend insights into promising drug targets. Therefore, this introduction will begin by discussing the disease human African trypanosomiasis and basic trypanosome biology. In subsequent sections, the structure and mechanism of TLF will be discussed, follow by the TLF resistance mechanisms of human-infective trypanosomes, other biology helpful for understanding TLF-1 mechanisms, and roles for the TLFs in human biology.

The Disease: Human African Trypanosomiasis

The deadly disease Human African Trypanosomiasis (HAT) and the economically debilitating cattle disease Nagana are caused by African trypanosome parasites. Tsetse flies serve as the vector for both human and animal parasites, and transmit the infection through biting and release of parasites in the saliva. The geographic range of African trypanosomiasis is restricted to the tsetse fly range and forms a belt across central Africa.

Over the last century, the death toll from Human African Trypanosomiasis has fluctuated due to epidemics and control efforts (1). At the turn of the 20th century, an epidemic killed hundreds of thousands of people in Uganda and Congo. The development of drugs by scientists from the colonizing nations helped curb another epidemic in the 1920s and 1930s. Later, effective detection and treatment efforts by mobile teams of doctors nearly eliminated *T. b. gambiense* transmission in some areas. Cases of human trypanosomiasis reached a historical low in the 1960s. Following de-colonization, the incidence of disease increased and another epidemic began. Currently, control efforts have reduced cases of human sleeping sickness to less than ten thousand reported cases per year.

Two sub-species of human-infective trypanosomes have different clinical manifestations. The West African Parasite, *T. brucei gambiense* infects primarily humans and is responsible for 98% of clinical HAT cases(2). Neurological symptoms from *T. b. gambiense* may take years to develop. The other human-infective parasite, *T. b. rhodesiense,* causes acute HAT and is endemic in the eastern part of the tsetse fly's range. *T. b. rhodesiense* induces acute neurological symptoms in infected people. As a zoonotic parasite, *T. b. rhodesiense* does not depend on a human reservoir for survival.

Parasite infection with either *T. b. gambiense* or *T. b. rhodesiense* initially causes flu-like symptoms as the parasite expands in the bloodstream (3). Without careful monitoring, trypanosomiasis is often misdiagnosed at the early stage. Diagnosed cases are relatively easily treated with pentamidine for *T. b. gambiense* infection or suramin for *T. b. rhodesiense* infection. After weeks to years of dormancy during an untreated

first stage infection, parasites re-emerge in the cerebral spinal fluid and cause the neurological symptoms including the unusual sleep/wake cycles which give African Sleeping Sickness its' name. If untreated, most people with neurological sleeping sickness succumb to coma and eventually death. Current drugs are difficult to administer, and toxic, with few options for resistant parasites. Understanding mechanisms of cell death in trypanosomes may lead to better drugs in the future.

Trypanosome Morphology and Life Cycle

African trypanosome parasites are single-celled flagellated eukaryotes, whose name reflects the corkscrew motion with which they move. They adapt to different niches in the mammalian bloodstream and tsetse fly by changes in morphology and metabolism. Because this work focuses on human innate immunity to trypanosomes, all of my experiments were performed in the mammalian bloodstream form parasites. However, it is important to appreciate that African trypanosomes participate in a complex life cycle which explains unique aspects of parasite biology and evolution.

Parasites first enter the mammalian host as through the bite of a tsetse fly. The metacyclic form parasites in the tsetse saliva are pre-adapted to survive in the mammalian bloodstream. For instance, *T. b. rhodesiense* metacyclic parasites express the Serum Resistance Associated (SRA) protein which confers resistance to TLF (4). After migrating from the site of the tsetse fly bite into the bloodstream, the non-dividing metacyclic form parasites shift into long slender bloodstream form parasites which have the ability to express millions of different of variable surface glycoproteins. The human immune system recognizes the variable surface glycoproteins as foreign antigens, and

VSGs becomes the target of the humoral immune response within a few weeks of infection. In pleomorphic field strains of the parasites, before the immune response overwhelms the parasites, the majority of bloodstream parasites shift into non-dividing short stumpy parasites. The metabolic signal for the long slender to short stumpy switch is unknown. Although short stumpy parasites are more resistant to the mammalian immune system than long slender parasites, they only survive if ingested by a tsetse fly.

After clonal expansion of anti-VSG IgG-producing B cells, most long slender bloodstream parasites are killed by the complement system (5). However, the few parasites which switched to expressing a different VSG coat are not recognized by the anti-VSG immune response, and these parasites survive to cause future waves of parasitemia. After several weeks to years, parasites disseminate from the bloodstream into the relatively protected environment of the cerebral spinal fluid of the central nervous system. Though it is clinically important to understand the source of neurological symptoms for sleeping sickness, the process by which parasites traverse the blood brain barrier is not understood.

Because bloodstream form *T. b. brucei* can be cultured *in vitro* in serum-containing media, most recent studies of parasite biochemistry have utilized cultured bloodstream *T. b. brucei*. Bloodstream parasites have unusual metabolism due to their unique niche in mammalian serum. In the high-glucose environment of the bloodstream, parasites metabolism relies entirely on substrate level glycolysis for energy production. Most glycolytic enzymes are packaged into specialized organelles called glycosomes, and electrons from glycerol-3-phosphate reduction are passed

through ubiquinol to trypanosome alternative oxidase in the mitochondrial inner membrane (6).

The bloodstream form *T. b. brucei* contains a single mitochondrion which is smaller and less metabolically active than in procyclic forms. The mitochondrion does not use an active electron transport chain, and the mitochondrial membrane potential is maintained primarily for protein and tRNA transport rather than ATP production. In fact, the terminal ATP synthase of the electron transport chain works backwards, hydrolyzing ATP to drive the proton gradient necessary for mitochondrial membrane potential maintenance (7). This simplification of bloodstream *T. b. brucei* mitochondrial function is important to keep in mind later, when the mitochondria's role in TLF lysis is discussed.

In the tsetse fly, short stumpy parasites rapidly differentiate into procyclic forms. Of the many diverse lifecycle stages the parasites assume in the fly, only the procyclic form can be consistently cultured *in vitro.* In the fly midgut, short stumpy parasites differentiate into procyclic forms. These migrate through multiple tissues to the salivary glands, where they differentiate into epimastigotes. Sexual recombination has also been demonstrated in the salivary gland, though the mechanism and prevalence of trypanosome sex is not well understood (8). In the salivary glands, parasites differentiate into human-infective metacyclic forms which are pre-adapted for survival in the mammalian host.

TRYPANOSOME LYTIC FACTORS (TLFS)

Trypanosome lytic factors (TLFs) are innate immune particles in human blood which rapidly and effectively kill *Trypanosoma brucei brucei* parasites. The goal of my

work is to understand how the TLFs are able to kill trypanosomes so effectively. This section will introduce TLF history and structure.

Discovery of the TLFs

In 1902 Laveran discovered that normal human serum cured *T. b. brucei* infected mice. Other historical work noted that most species of African trypanosomes (*T. evansi, T. equinum, T. equiperdum, T. congolense, T. b. brucei*) but not the human infective subspecies *T. b. gambiense* and *T. b.* rhodesiense were sensitive to human serum lysis (9). These experiments became the basis of the blood infectivity test which was used prior to the genomic era to distinguish *T. b. gambiense* and *T. b. rhodesiense* from the other parasite species in the field. In order to understand what factor in human blood was responsible for trypanosome lysis, biochemists in the 1970's and 1980's began to fractionate blood by various methods to discover the trypanolytic molecule and its properties. In 1978, Rifkin published the discovery that the high density lipoprotein fraction of human serum was trypanolytic (10). The ubiquitous HDL protein Apolipoprotein A1 was found not to be responsible for lytic activity, suggesting that a more specific lipoprotein was important (11, 12). Soon afterwards, haptoglobin related protein (Hpr) was determined to be an essential part of the the trypanolytic particle (13). Another essential TLF-1 component, apolipoprotein L1 (ApoL1), was not originally thought to be an integral component of TLF-1, and its lytic activity was not discovered until 2003 (14).

ApoL1 Activity and Structure

The ApoL1 protein is related to intracellular pro-apoptotic proteins and pore-forming bacterial colicin toxins (15). It is the only protein in its class which is secreted, and therefore contains a signal peptide on its N-terminal region. The pore-forming domain of ApoL1 forms pores which are cation-selective and acid-gated, meaning ApoL1 is most active in neutral (not acidic) environments (16). A membrane addressing domain not part of the modelled channel itself is critical for membrane insertion. The C-terminal domain of ApoL1 is called the SRA-interacting domain because it binds to the *T. b. rhodesiense* serum resistance associated (SRA) protein.

Like other pro-apoptotic proteins, ApoL1 contains a BCL2 homology 3 (BH3) domain (Figure 1.1). It is tempting to speculate that the BH3 domain of ApoL1 might initiate apoptotic-like cell death in trypanosomes. However, the BCL2 protein family is not well conserved in trypanosomes, so it is unclear how such signaling would proceed. For instance, expression of mouse BCL2 in *T. b. brucei* did not rescue apoptotic-like cell death induced by ROS, demonstrating a structurally divergent programmed cell death machinery in trypanosomes (17). ApoL1 constructs with mutated or deleted BH3 domains have been tested for trypanolytic activity. When the BH3 domain is deleted, or when a lysine and an alanine within the BH3 domain are replaced with glutamate residues, the resulting ApoL1 loses trypanolytic activity (18, 19). However, when other BH3 residues are mutated to alanines or lysines, the ApoL1 retains trypanolytic activity (18, 19). It was not shown whether each mutated ApoL1 retained ion channel activity or localized to the same regions of *T. b. brucei,* though some mutants were shown to insert into mitochondrial membranes (18). Therefore, the role of the BH3 domain of ApoL1 in trypanolysis remains to be elucidated.

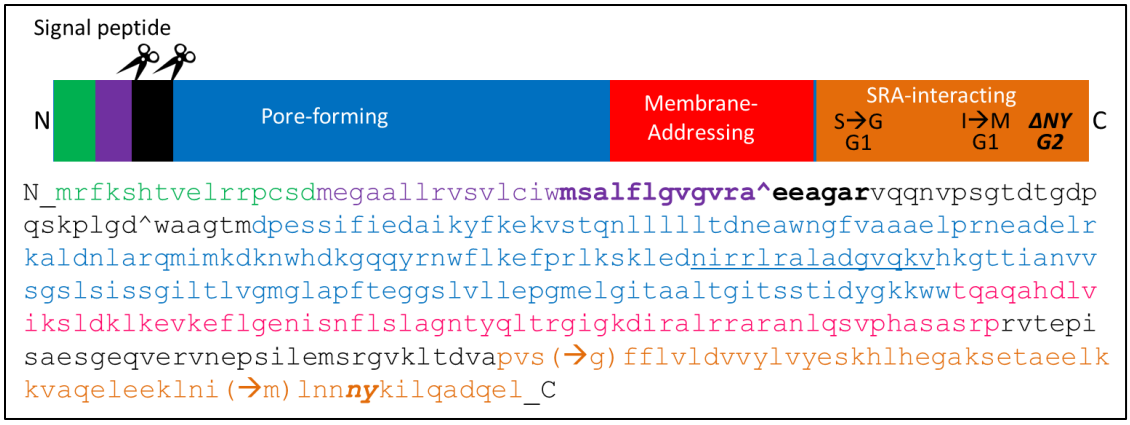

Figure 1.1: **ApoL1 primary structure.** Alternative splicing isoforms of ApoL1 are shown with the longer isoform in green, and regions deleted in the alternative splicing isoform are bold. Protein cleavage sites are indicated by ^ and scissors in the top diagram. The secreted signal peptide is shown in purple, the pore-forming domain is blue with the BH3 domain underlined, the membrane-addressing domain is red, the SRA-interacting domain is brown, with the G1 amino acid substitutions indicated with arrows (S→G and I→M) and the *G2 deletion bold and italicized (ΔNY).* N_ is shown for the N-terminal and _C for the C-terminal end of the protein.

Although no structural data is available for ApoL1, mutational studies and homology data have elucidated several different functional domains in the protein. ApoL1 has several different functional domains which are indispensable for its trypanolytic activity (Figure 1.1). First, as the only member of the ApoL family which is secreted, it contains a cleaved N-terminal signal peptide. Secondly, the pore-forming domain shares homology with bacterial colicin pore-forming toxins and contains hydrophobic helices (15). Thirdly, a double-helical membrane addressing domain is required for insertion of the ApoL1 ion channel into membranes (15). The SRA-interacting domain is defined by the region of the protein which is necessary for inactivation of ApoL1 by *T. b. rhodesiense* (20). In fact, ApoL1 was discovered through a pull-down of parasite lysates using the *T. b. rhodesiense* resistance protein SRA as bait (14). Importantly, the two human polymorphisms in ApoL1 which confer resistance to *T. b. rhodesiense* are

located in the SRA-interacting domain, and prevent SRA binding, freeing up ApoL1 to induce lysis of the human-infective *T. b. rhodesiense*.

Hpr activity and structure

Hpr is a defining component of the TLF particles with an important role in the TLF-1 lytic mechanism. Like the serum protein haptoglobin (Hp), Hpr binds to dimers of hemoglobin (Hb) in blood. When bound to hemoglobin, Hpr binds to the haptoglobin hemoglobin receptor (HpHbR) in *T. b. brucei,* facilitating high affinity uptake into the parasite.

There is disagreement in the literature about whether Hpr itself is toxic to trypanosomes. When native Hpr protein was purified from TLF-1, the purified protein induced lysis of *T. b. brucei* (21). However, TLF-1 has such high activity that amounts of TLF-1 undetectable on Western blot could be responsible for the lytic activity reported for Hpr. To test this hypothesis, I purified Hpr and assessed its ability to lyse SRA-expressing trypanosomes. SRA is expected to inactivate ApoL1 and the TLF-1 particle, but not purified Hpr. While variable results were obtained for Hpr killing of WT *T. b. brucei,* none of the *T. b. brucei* expressing SRA were killed by purified Hpr (Figure 1.2). Thus, while Hpr is required for high activity TLF-1 by facilitating uptake into the parasite, it appears that Hpr by itself is not lytic. Supporting this hypothesis, mice expressing Hpr without ApoL1 were not able to clear trypanosome infection (22). To complicate matters, the hydrophobic signal peptide of Hpr, if expressed without the rest of the protein, is an effective and specific anti-trypanosomal agent, though it kills *T. b. brucei* by a different

mechanism than TLF-1 (23, 24). It is not known whether this signal peptide is involved in TLF-1 induced lysis of *T. b. brucei.*

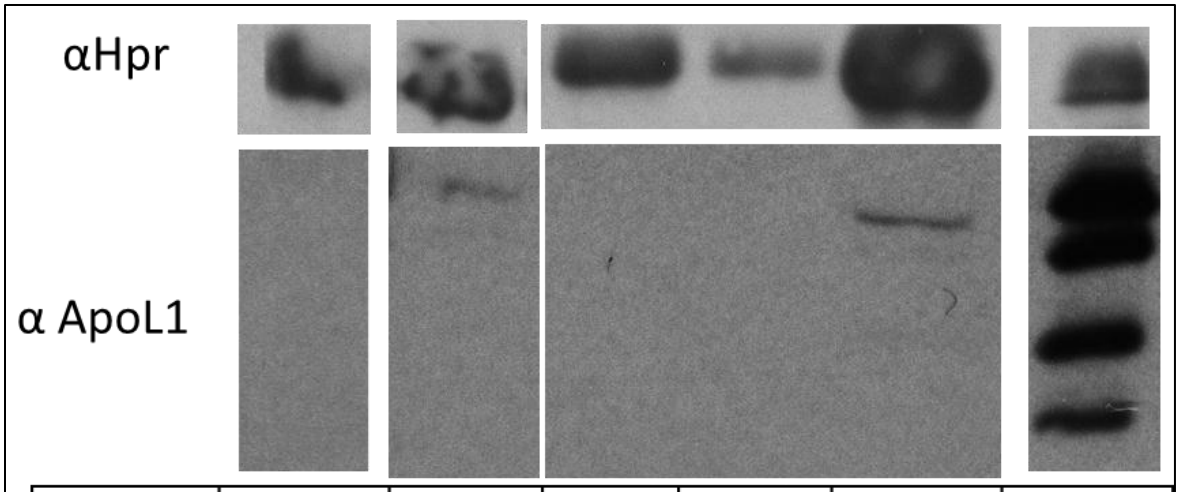

Sample	Hpr a	Hpr b	Hpr c	Hpr d	Hpr e	TLF-1
% survival after 24 hr WT *T.b.b.*	0±0	32±14	66±27	101±45	28±12	0
% survival after 24 hr SRA-*T.b.b.*	104±21	100±22	82±18	111±23	112±30	122±25

Figure 1.2**: Hpr alone does not kill *T. b. brucei.*** Top: Western blot preparations of Hpr (a through e) and TLF-1. Blots of native Hpr (lanes 1-5) or TLF-1 (lane 6) were probed with either anti-Hpr IgG (top) or anti-ApoL1 IgG (bottom), and visualized using horseradish peroxidase conjugated secondary antibody. Native Hpr was purified by dissolution of HDLs in CHAPS detergent, ApoL1 was removed by flowing over an anti-ApoL1 sepharose resin, and Hpr was eluted from an αHpr column as described previously (25). Only the Hpr preparations "b" and "e" had any contaminating αApoL1 visible on the Western blot. The control, TLF-1 (final lane) reacted with both αApoL1 and αHpr antibodies as expected. Bottom table: 24 hour survival assays were performed with the different Hpr preparations at concentrations equivalent to those run on the Western blot. Survival assays were performed with either SRA-expressing *T. b. brucei* (SRA-*T.b.b.*) or wild-type *T. b. brucei* (WT *T.b.b.*). Variable survival rates in the wild-type *T. b. brucei* treated with Hpr seem to represent contaminating ApoL1 (or TLF-1) in the Hpr preparations. No SRA-expressing *T. b. brucei* were killed by any Hpr preparation. A. S. Greene unpublished data.

No crystal structure of Hpr is available. However, Hpr is 91% identical to human haptoglobin, and a crystal structure of the related porcine HpHb complex is published (26). The amino acid sequence alignment of human Hp1 and Hpr is shown Figure 1.3.

Like Hp, Hpr is composed of alpha and beta chains which undergo intramolecular cleavage from a single polypeptide chain before assembling into a mature protein. Unlike Hp, Hpr does not contain a cysteine in the alpha chain which forms a disulfide linkage between two Hp alpha-beta dimers (27). On non-reducing gels, Hpr runs as a combination of dimers and tetramers, possibly because of intermolecular disulfide formation between un-conserved cysteins on in the beta chain of Hpr (27). The alpha chains of Hp or Hpr bind tightly to Hb dimers through multiple interactions with both alpha and beta chains of Hb (26).

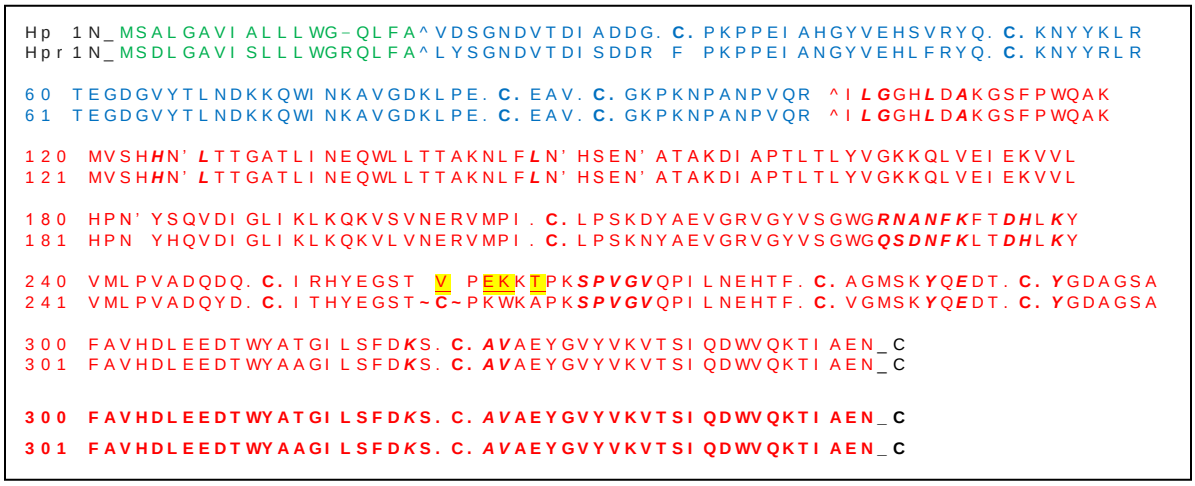

Figure 1.3**: Sequence Alignment of Human Haptoglobin (Hp1) and Hpr**. The signal peptide is green with the cleavage site indicated by a caret ^, the alpha chain is blue, the beta chain is red with CD163 binding sequence underlined and highlighted and **Hb-interacting amino acids bolded,** cysteines involved in disulfide bonds are bolded **.C.**, and **~C~** shows the free cysteine. Putative glycosylation sites are marked with an apostrophe ‘, and N_ and _C represent the amino and carboxyl termini of the proteins. Figure based on reference (27).

Unlike most secreted proteins, the N-terminal signal sequence of Hpr is not cleaved. This signal peptide alone anchors Hpr into the hydrophobic lipids of the TLF-1 HDL particle (28). The specific interaction of Hpr with ApoL1 containing TLF-1 particles

is likely dictated by biophysical interactions with anionic and fluid lipid environments rather than protein-protein interactions (28, 29).

TLF-2 Structure and Mechanism

There are two related trypanolytic fractions of human serum (Figure 1.4). TLF-1 is an HDL particle, as described previously. TLF-2 is found in a denser lipoprotein fraction which also contains Hpr, ApoL1, and ApoA-1, in addition to IgM molecules (30). It is relatively lipid-poor and therefore may be a nascent HDL. However, nascent HDLs do not normally associate with IgM molecules, suggesting a different mode of biogenesis as detailed later in this introduction. It has not been resolved whether Hpr in TLF-2 retains Hb-binding activity, and whether TLF-2 carries Hb under normal conditions. The origin of the IgM molecules has also not been addressed.

The relative roles of TLF-1 and TLF-2 in immunity against trypanosomes are unclear, but TLF-2 may be more physiologically relevant in human immunity to *T. b. brucei* (31). Little to no data is available on the relative levels of circulating TLF-1 and TLF-2 serum under different conditions. In one study of human serum, TLF-1 and TLF-2 are both present at similar levels (several mg/L serum) (30).

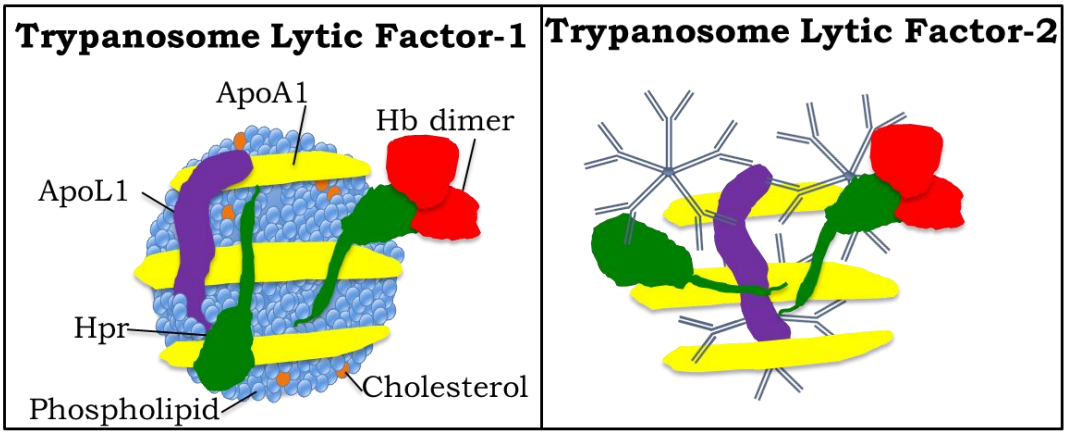

Factor	HDL	Lipid	ApoA1	Hpr	ApoL1	Hb	IgM	Receptor
TLF-1	Yes	40% by mass	Yes	Yes	Yes	Yes	No	HpHb
TLF-2	No?	No	Yes	Yes	Yes	?	Yes	?

Figure 1.4: **Comparison between TLF-1 and TLF-2.** Diagram for TLF-1 (top left) and TLF-2 (top right). Bellow the diagrams is a table comparing TLF-1 and TLF-2.

TLF-2 can efficiently bind to the parasites through uncharacterized receptors as well as the HpHbR (31-33). Researchers have been unable to identify a single, saturable TLF-2 receptor. It is possible that IgMs in TLF-2 might simply stick to the *T. b. brucei* VSGs (34, 35). Therefore, physiological HpHb does not prevent TLF-2 from entering *T. b. brucei,* allowing TLF-2 to kill parasites in the presence of HpHb in serum.

Contradictory studies were published in the 1990's arguing about whether Hp inhibited human serum lysis of *T. b. brucei* (31, 36, 37). It is now known that Hpr in TLF-1 requires Hb for binding to the *T. b. brucei* HpHbR, and that serum HpHb competes away TLF-1 binding and uptake via the HpHbR (38, 39). In humans blood, however, the HpHb complex is rapidly removed from circulation, depleting the amount of

competitor available (40, 41). Hpr-Hb in TLF-1 is not removed by the macrophage receptor CD163, theoretically allowing for the accumulation of Hb-bound TLF-1 and TLF-2 (27, 42). Therefore, it is perplexing that Hb has never been detected bound to TLF-1 purified from human blood, and must be added to *in vitro* assays to increase trypanolytic activity (43). The effects of physiological Hp and Hb on the functions of TLF-1 and TLF-2 immune function remains open for investigation.

TLF-2 is much more labile than TLF-1, requiring extensive purification processes that deplete activity. Thus, very little biochemical work has been done to elucidate the mechanism by which TLF-2 kills parasites. In fact, most of the interest in TLF-2 occurred two decades ago when researchers were still working out what components of human serum were trypanolytic. Currently, it is common for authors to assume that recombinant ApoL1 kills trypanosomes the same way as the TLF-1, TLF-2, or human serum. However, there is no evidence that this assumption is correct. As the literature on the toxicity of human polymorphisms of ApoL1 grows, it is critical that TLF-2 and its physiological roles are no longer ignored.

MECHANISMS OF TRYPANOSOME LYSIS BY TLF-1

The goal of my work is to understand the mechanism human innate immune molecules (TLFs) utilize to kill African trypanosomes. The field's understanding of the mechanism of trypanosome lysis induced by the TLFs has changed dramatically over the course of my thesis work. This section of the introduction will detail the prevailing models for TLF lysis of trypanosomes and the data that supports those models.

There are three major models of TLF-1 induced trypanosome lysis based on proposed or inferred localization for the TLF-1 and ApoL1 activity within the parasite.

Apolipoprotein L1 (ApoL1) is a pore-forming toxin in TLF which is important for initiating cell death. The three proposed organelles targets TLF-1 and ApoL1 activity are the lysosome, the mitochondrion, and the plasma membrane (see Figure 1.5). In this section basic TLF biology is introduced and then the three major models (lysosome, mitochondria, and plasma membrane) are unpacked.

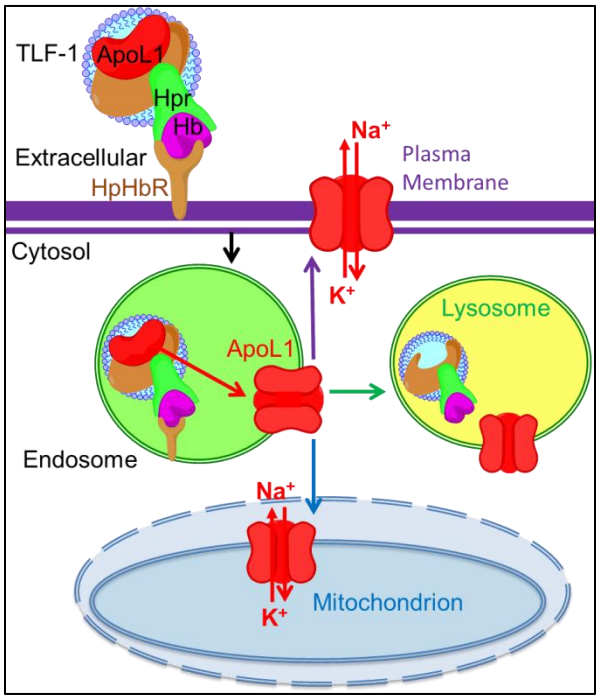

Figure 1.5: **Three Organelles for TLF activity.** After high-affinity endocytosis into an acidic endosome or lysosome of *T. b. brucei*, ApoL1 inserts into the vesicle membrane and forms an ion channel. The membrane-associated ApoL1 may traffic to the lysosome along with the rest of the TLF complex, recycle to the plasma membrane, or traffic to the mitochondrion. Models associated with each subcellular localization are detailed in subsequent figures.

Lysosomal Models: TLF-1 induces lysosomal damage

Abundant data led to various models where TLF-1 induces lysis of *T. b. brucei* via the lysosome. In multiple studies, TLF-1 and ApoL1 have been found to localize primarily to the lysosome (15, 44). Also, TLF-1 requires endocytosis to kill *T. b. brucei*,

and acidification of the endolysosomal pathway is a requirement for lysis. Consistently, *in vitro* data on ApoL1 shows preferential insertion into membranes at low pH (16, 29). Moreover, knocking down the late endosomal protein Rab7 which facilitates cargo trafficking to the lysosome, or knocking down the lysosomal p67 protein, confers some resistance to TLF-1 (45, 46). However, recent data from my work and others have suggested that the lysosome damage is not important for *T. b. brucei* cell death (18, 47). Nevertheless, it is important to understand the context and data support for the lysosomal models before understanding more recent developments in the lytic mechanism.

Lysosomal models: HpHb-induced peroxidative damage

Prior to the discovery of ApoL1 as a component of the TLFs, Hpr was the defining protein in TLFs and was thought to be solely responsible for trypanosome lysis. The prevailing hypothesis became that Hpr, along with hemoglobin bound, acted as a peroxidase causing oxidation and breakdown of the *T. b. brucei* lysosome (13, 48). There were several pieces of evidence supporting oxidative lysis of trypanosomes, but how the TLF-1 molecule initiated oxidative stress was not clearly shown.

The formation of oxygen radicals from redox cycling of iron (including heme iron) is catalyzed by low pH, in a process often termed Fenton chemistry (49). In support of a role for Fenton chemistry in TLF-1 lysis of *T. b. brucei,* addition of exogenous catalase or the antioxidant DPPD also inhibited TLF-1 lysis of *T. b. brucei* (13, 48). Furthermore, raising the pH of the lysosome via ammonia, chloroquine or monesin ablated TLF-1 lysis, possibly through inhibition of Fenton chemistry (44). One paper found no

evidence for peroxidation during TLF-1 lysis, but in those studies a Hb-free buffer was utilized (50).

Peroxidation of lysosomal lipids might be facilitated by HprHb interaction with the lysosomal membrane. In fact, Hpr, ApoL1, or entire TLF-1 molecules bind to liposomes in a low pH environment (29). Moreover, ApoL-1, TLF-1, and Hpr each permeabilized the liposome membranes at low pH, that Hpr as well as ApoL1 may insert into trypanosome membranes. In the trypanosome lysosome, however, lipid composition, buffering molecules, and proteolytic enzymes may affect the insertion or stability of Hpr in the lysosomal membrane.

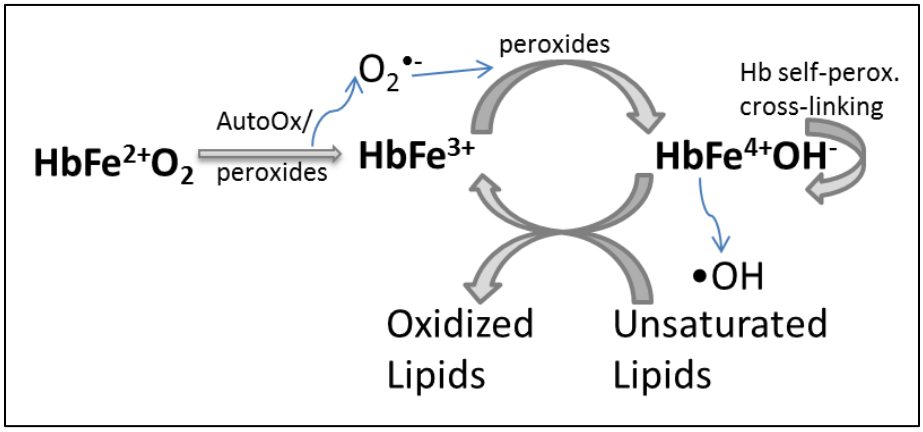

Figure 1.6**: Schematic for Hb-initiated Lipid Peroxidation.** Initiation of the peroxidation cycle may occur via auto-oxidation from oxyhemoglobin for release superoxide, or via reaction with hydrogen peroxide. The oxygen radical or hydroxide radicals may diffuse to spread oxidative damage. Diagram modified from (26, 51).

The peroxidative activity of HprHb can be inferred based on an extensive literature on HpHb as a peroxidase (52-54). A simple schematic for Hb peroxidase activity is shown in Figure 1.6. Binding of oxyHb dimers to Hp does not change the basic peroxidative chemistry of Hb. Unlike enzymatic peroxidases, Hb didn't evolve to stabilize radical intermediates, and therefore ends up peroxidizing reactive amino acids

proximal to heme (55). When Hb is bound to Hp, amino acids in Hp rather than Hb receive the brunt of the oxidative damage. While HprHb doesn't differ significantly from HpHb in terms of amino acids available for oxidation, its presence in an embedded in an HDL particle with closely packed proteins and lipids and cholesterol facilitates proliferation of radicals throughout the particle. Extensive peroxidation can initiate covalent crosslinking between Hb subunits and adjacent proteins, which initially may facilitate rather than hinder the peroxidation cycle (53). While lipids are unlikely to be direct substrates of Hb peroxidation, they are highly susceptible to damage by free radicals released nearby.

In the second chapter of this dissertation, I show that that peroxidase activity of HprHb is not important for the lytic activity of TLF-1. Instead, peroxide-mediated oxidation of sensitive thiol(s) impairs the ability of *T. b. brucei* to osmoregulate, leading to osmotic lysis (18). Although the details of the lysosomal peroxidation model were not supported by my work, the overall conclusion that oxidative processes are involved in lysis remains valid.

Lysosomal Models: TLF-Induced Lysosomal Swelling or Permeabilization

Two competing models for TLF-1 induced lysosomal activity have been proposed (Figure 1.7 and Figure 1.8). In the one model (Figure 1.7), TLF-1 was proposed to initiate oxidative breakdown of the lysosomal lipid membrane via the HprHb complex, as described in the previous section. TLF-1 induced lysosomal membrane breakdown makes the lysosome permeable to proteins and fluorescent dextrans, and the leaking of lysosomal content was proposed to cause cell death (43, 44). In the other model (Figure 1.8), ApoL1 insertion into the lysosomal membrane was proposed to cause an

influx of chloride ions leading to osmotic swelling of the lysosome (15, 56). At the point when lysosomal models were being tested, publications from two different groups disagreed about whether ApoL1 was a Na^+ or Cl^- channel (15, 57).

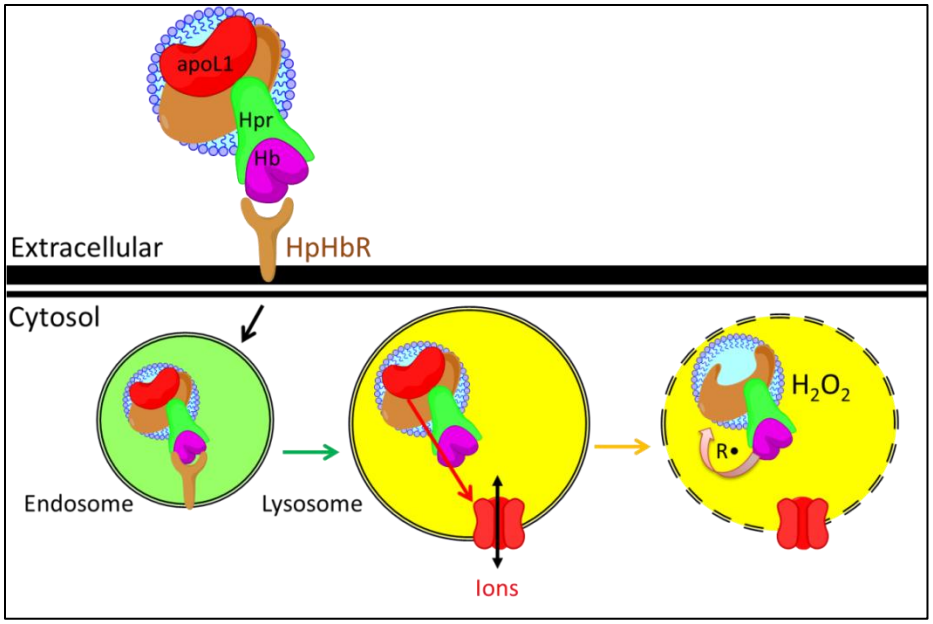

Figure 1.7**: Model for TLF-1 induced peroxidation and lysosomal permeabilization.** ApoL1 insertion into the lysosomal membrane induces anion or cation influx. The heme iron in Hpr-Hb initiates peroxidation of lysosomal lipids. Peroxidation of lysosomal lipids coupled leads to permeabilization of the lysosomal membrane. HpHbR is haptoglobin hemoglobin receptor.

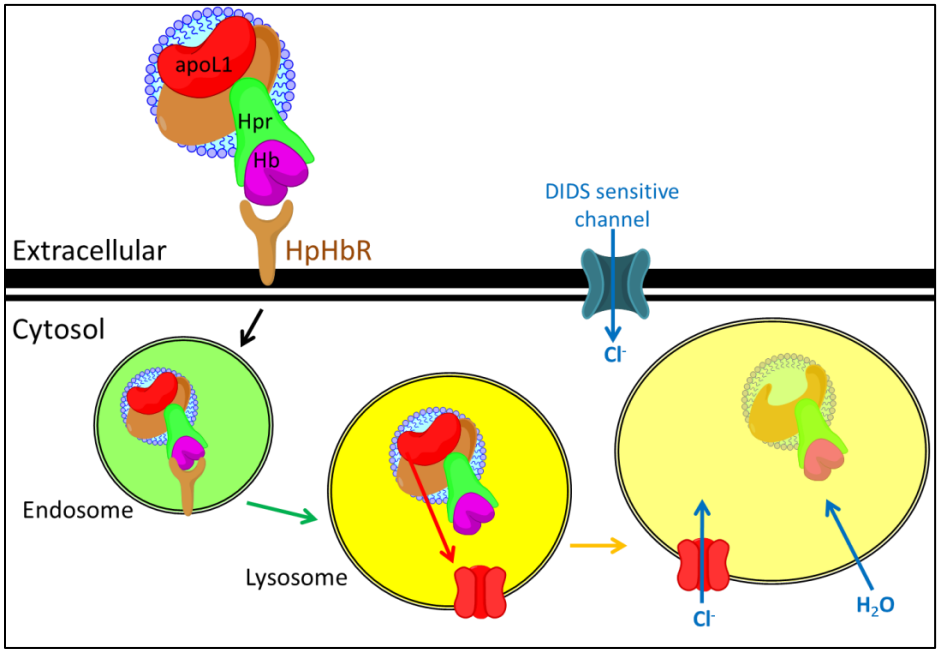

Figure 1.8**: Model for ApoL1-induced Lysosomal Swelling.** ApoL1 inserts into the lysosomal membrane and induces osmotic swelling due to Cl^- influx. Chloride enters

the cytoplasm via an outer membrane DIDS-sensitive Cl^- channel. HpHbR is haptoglobin hemoglobin receptor.

Lysosomal osmotic swelling due to ion influx is incompatible with lysosomal permeabilization to proteins, though permeabilization could occur after osmotic swelling. In addition to osmotic swelling, however, an increase in lysosomal size could be associated with the autophagic vacuole in *T. b. brucei,* as seen in neuropeptide treated *T. b. brucei* (58). In that case, the increased size would come not from osmotic swelling but from fusion of autophagic vesicles with the lysosome. In unpublished work from our lab, lysosomal swelling is rarely observed unless *T. b. brucei* is treated with low activity or heat-inactivated human serum or TLF-1 (Figure 1.9) (98). High acitivity TLF-1 or human serum always yielded swollen cells with relatively normal lysosomal size. These data suggest that lysosomal swelling may be an artifact of the method of storage and purification of human serum and TLF-1. The phenotype of whole cell swelling, as observed by us and other researchers, is likely the more biologically relevant mechanism for TLF-1 killing of *T. b. brucei.*

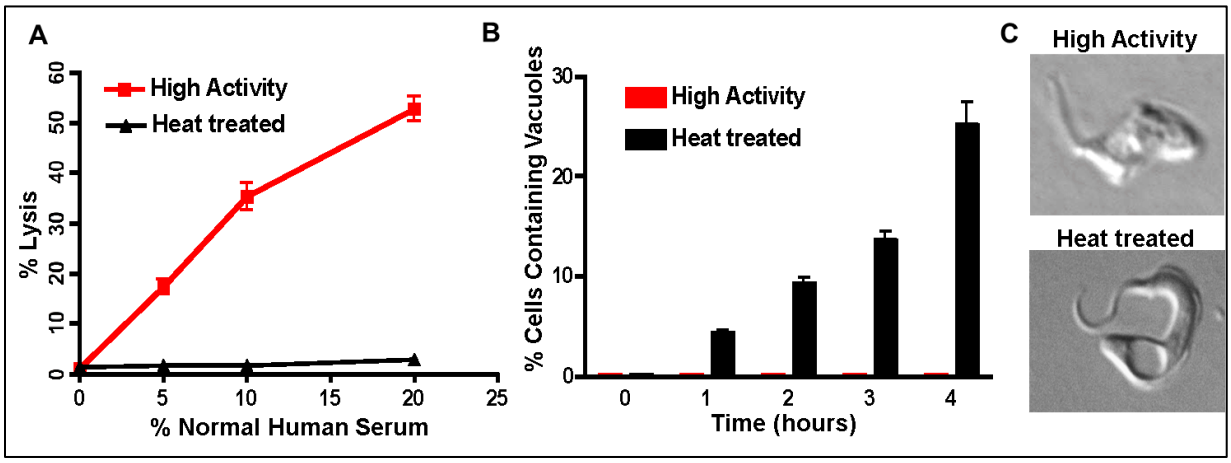

Figure 1.9: **Low Activity Human Serum Produces Swollen Lysosomes.** (**A**) Heat treatment of human serum (62°C for 30 min) results in a significant decrease in lytic activity of human serum. *T. b. brucei* cells were incubated with increasing

concentrations of high activity human serum and heat treated serum at 37°C. Percent lysis was determined after 2 hrs. (**B**) Decreased lytic activity of human serum due to heat treatment leads to an increase in the appearance of swollen vacuoles over time. Cells were incubated with 20% human serum at 37°C. The percentage of swollen vacuoles was determined at 1 h time points for a total of 4 hrs. (**C**) Differential interference contrast (DIC) image from live cell microscopy video taken of *T. b. brucei* incubated with high activity or heat treated human serum. Data from Natalie A. Stephens, Carla Rutherford and Stephen L. Hajduk, unpublished.

Recent data including my own suggest that localization of TLF-1 and ApoL1 to the lysosome is not important for lysis of *T. b. brucei* (18). For instance, the loss of mitochondrial membrane potential as well as lysosomal membrane permeabilization were observed under a variety of conditions. It was found that loss of lysosomal integrity could occur independently of mitochondrial phenotypes, and that cells only experiencing loss of lysosomal integrity did not lyse (18). Furthermore, the varied lysosomal phenotypes observed by different labs and under different treatment conditions suggest that TLF-1 effects to the lysosomal are not cause of cell death in *T. b. brucei*.

Mitochondrial model: ApoL1-induced Apoptosis-like cell death

Recently, ApoL1 was found to associate with the mitochondrion of *T. b. brucei* and an apoptotic-like mechanism for lytic cell death was proposed (Figure 1.10) (18). On fluorescence microscopy, ApoL1 co-localized with mitochondrial membrane markers. Within 20 minutes of human serum or recombinant ApoL1 addition to *T. b. brucei* their mitochondrial membrane potential was dissipated. Within one hour after ApoL1 addition, endonuclease G (endoG) was released from the mitochondrion, presumably causing the observed nuclear DNA fragmentation. Furthermore, dramatic changes in mitochondrial morphology occurred following ApoL1 addition, suggesting

direct damage to this organelle. No experiments elucidated whether ApoL1 was localized to the outer or the inner membrane of the mitochondria. It is not known how proteins may move from trafficking vesicles into mitochondrial membranes in any cell type(59).

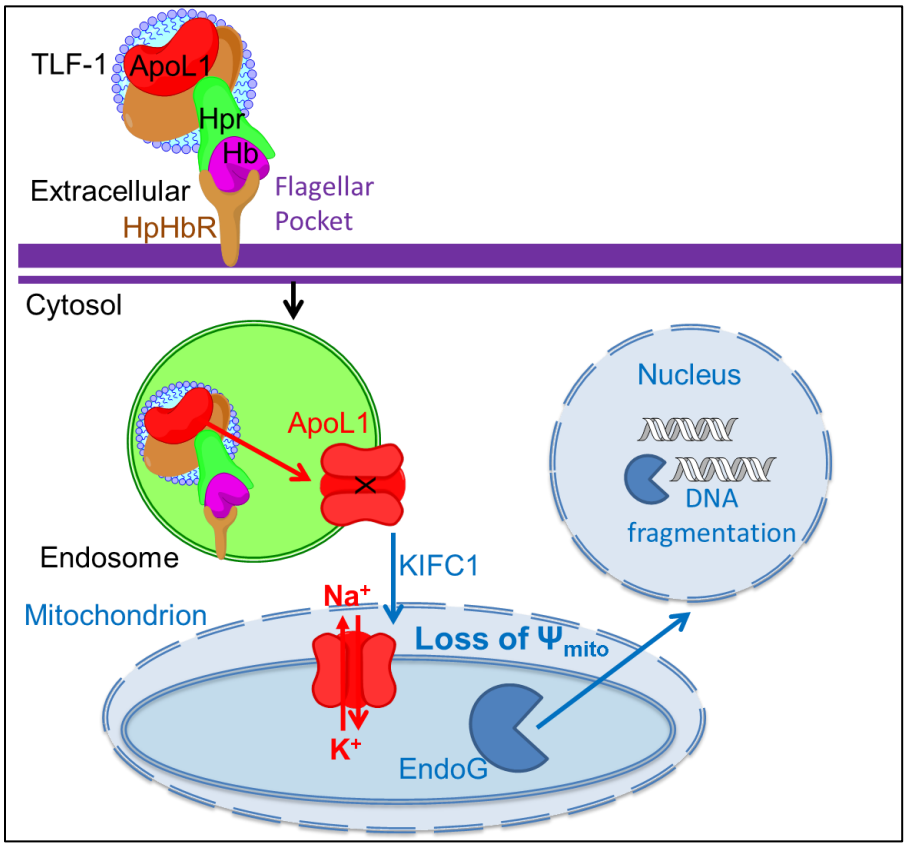

Figure 1.10**: Model for Apoptosis-like Cell Death initiated by ApoL1 at the Mitochondria.** Ψ_{mito} is the mitochondrial membrane potential. EndoG is endonuclease G. The "X" over the ApoL1 pore indicates a closed channel under acidic pH. HpHbR is haptoglobin hemoglobin receptor.

The kinesin KIFC1 was found to be involved in trafficking ApoL1 from the endo-lysosomal vesicles (18). RNAi against KIFC1 caused ApoL1 to accumulate only in the lysosome. Importantly, depleting KIFC1 by RNAi led to moderate resistance to mitochondrial membrane potential loss and lysis. However, KIFC1 knockdown did not

prevent the lysosomal phenotypes such as ApoL1-induced lysosomal membrane permeability. Thus, the authors concluded that lysosomal membrane permeability, while induced by ApoL1, does not directly initiate TLF-1 lysis.

The authors did not address localization of ApoL1 to non-mitochondrial locations including the plasma membrane or flagellar pocket (18). In their microscopy pictures, no markers for the flagellar pocket were used to determine if ApoL1 puncta near the kinetoplast represents ApoL1 at the flagellar pocket versus on the mitochondrial membrane. It is also not known whether KIFC1 may be involved in recycling ApoL1 and other cargo to the flagellar pocket or other cellular membranes. Interestingly, knockdown of KIFC1 leads to defective calcium signaling in *T. b. brucei* (60). Calcium signaling might be involved in multiple mechanisms of cell lysis, including the osmotic lysis initiated at the plasma membrane, so the effects of the KIFC1 knockdown on ApoL1 toxicity may be multi-faceted.

Plasma Membrane Model: ApoL1-induced osmotic lysis of *T. b. brucei*

Cytoplasmic swelling of *T. b. brucei* with water is has been consistently recognized as a major phenotype of TLF-1 lysis. Importantly, blocking the osmotic influx of water with high concentrations of cell impermeable sucrose prevents TLF-1 induced lysis (61). Furthermore, the flux of ions measured across the plasma membrane during TLF-1 lysis mirror the flux of ions that occur in cells under hypotonic stress. Sodium ion influx, potassium ion efflux, and calcium ion influx are all hallmarks of both TLF-1 treated and hypotonically stressed *T. b. brucei* (57, 61). Calcium influx might be important for TLF-1 induced lysis of *T. b. brucei,* because removal of Ca^{2+}

from human serum depletes lytic activity, and lysis is rescued by re-addition of Ca^{2+} (but no Mg^{2+}) to the cells (62).

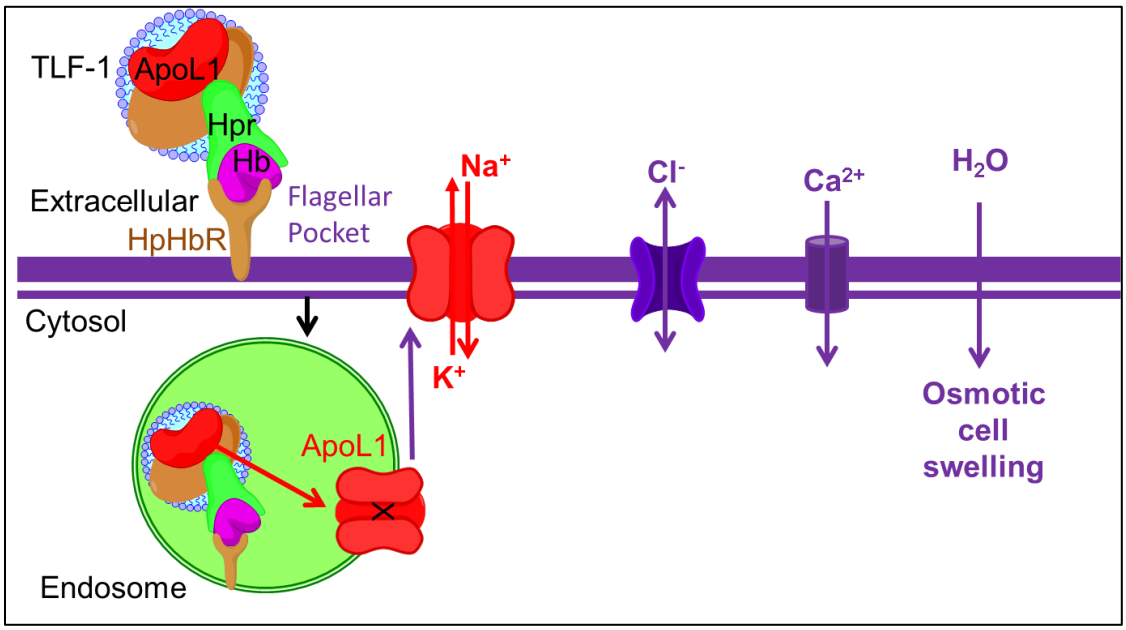

Figure 1.11**: Model for Osmotic Lysis of *T. b. brucei* Initiated by ApoL1 at the Plasma Membrane.** The "x" over the ApoL1 ion channel (red) in the lysosome represents a closed channel at acidic pH. HpHbR: haptoglobin hemoglobin receptor.

Direct interaction of ApoL1 with the plasma membrane could lead to cell swelling (Figure 1.11). Early phenotypic observations of trypanosome swelling induced by human serum led to the hypothesis that human serum disrupted the plasma membrane of *T. b. brucei* (61). Soon afterwards, however, experiments showed that endocytosis of the molecule is required for trypanosome lysis, so the plasma membrane hypothesis was rejected (44). Recently, an *in vitro* study of ApoL1 proposed the model that after endocytosis, ApoL1 could traffic through recycling endosomes back to the plasma membrane (16). ApoL1 cation channel formation into the plasma membrane would account for the observed phenotype of osmotic lysis induced by TLF-1.

Chapters 2 and 3 of this dissertation detail my work elucidating the role of osmotic cell swelling during TLF-1 lysis of *T. b. brucei.* My research has built on existing data to support the plasma membrane model for osmotic swelling as the best simple model for TLF-1 lysis of *T. b. brucei.* In fact, TLF-1 treated trypanosomes probably experience overlapping effects from ApoL1 in the lysosome, mitochondrion, and plasma membrane. Future research may elucidate the connections between stress signaling and cellular damage due to ApoL1 in the different *T. b. brucei* organelles.

MECHANISMS OF TLF RESISTANCE

Thousands of humans die every year from African trypanosome infection. Clearly, the humans are not innately immune against all trypanosome species. In a remarkable example of co-evolution, the two species of human-infective trypanosomes have evolved distinct resistance mechanisms to the TLFs in human serum. The mechanisms of resistance developed by *T. b. rhodesiense* and *T. b. gambiense* lend insight into the mechanisms by which the TLFs kills susceptible parasites. *T. b. rhodesiense* evolved to infect primates relatively recently in evolutionary history, and expresses a single serum resistance associated (SRA) protein. *T. b. gambiense* resistance is multi-factorial and more research is necessary to fully understand how these parasites defend themselves against the TLFs. The mechanisms of resistance evolved by *T. b. rhodesiense* and *T. b. gambiense* lend insight into how the TLFs kill susceptible trypanosome species.

Mechanisms of Resistance in *T. b. rhodesiense*

The human sleeping sickness parasite *T. b. rhodesiense* is resistant to human serum due to expression of the serum resistance associated protein (SRA), the expression of which is used to distinguish *T. b. rhodesiense* from other subspecies in the field. Heterologous SRA expression in *T. b. brucei* confers complete resistance to human serum (63, 64). In fact, a parasitologist developed trypanosomiasis after becoming accidentally infected with SRA-expressing *T. b. brucei* (65). Expressing SRA probably caries a fitness cost because strains that have not been challenged with human serum begin to lose SRA expression, and field strains have variable SRA expression levels and correlating variable resistance to TLF-1 (63, 66). The plasticity of SRA expression may reflect the fact that *T. b. rhodesiense* is a zoonotic parasite infecting domestic and wild animals and therefore human transmission is not critical for parasite persistence. In animals, gene exchange between *T. b. rhodesiense* and *T. b. brucei* strains can lead to expansion of TLF resistance among zoonotic parasite populations (67).

The N-terminal region of SRA binds to a C-terminal region on ApoL1 with strong and specific binding; in fact, SRA can be used to pull down ApoL1 from trypanosome lysate (and vice versa) (14). SRA binding occurs at low pH, and the two proteins dissociate at neutral pH (16). SRA does not totally prevent interaction of ApoL1 with membranes, but prevents the channel from opening at neutral pH, and makes the membrane insertion less stable (16). SRA is found in the flagellar pocket and the endosomes of trypanosomes where it can bind to ApoL1, preventing ion channel formation and facilitating ApoL1 degradation in the lysosome (68, 69).

Recently, it was discovered that SRA is excreted from trypanosomes in extracellular vesicles, suggesting that the SRA resistance mechanism might be more nuanced than it was formally thought (70). In fact, SRA-containing extracellular vesicles may be internalized by TLF-sensitive trypanosomes to confer transient TLF-1 resistance (70). Extracellular vesicle transfer provides a mechanism for human co-infections between SRA-expressing resistant parasites and human serum sensitive parasites. Moreover, recent unpublished work from our lab suggests that SRA may facilitate ApoL1 excretion via extracellular vesicles.

Mechanisms of resistance in *T. b. gambiense*

The prevalent human sleeping sickness parasite *T. b. gambiense* has a complex and lengthy evolutionary relationship with primates (71). Importantly, there are two classified strains of *T. b. gambiense,* type I and type II. Type I *T. b. gambiense* resistance is fairly well characterized, but type II *T. b. gambiense* resistance is not well understood (72).

One aspect of resistance involves preventing high-affinity uptake of TLF-1. The *T. b. gambiense* HpHbR has mutations which make it non-functional, and the mRNA and protein expression is subsequently down-regulated (39, 73). However, due to the high rate of endocytosis in bloodstream form trypanosomes, depleting receptor-mediated uptake is not sufficient to confer human serum resistance, so additional mechanisms of resistance were sought (32).

RNAi screens for TLF-resistance *T. b. brucei* have been employed to look for genes possibly involved in TLF resistance pathways (74, 75). Of these genes,

lysosomal cysteine protease inhibitor (ICP) modulates TLF-1 activity by inhibiting a cathepsin L, which may facilitate TLF-1 degradation (75, 76). Not surprisingly, genes involved in endosomal acidification as well as vesicular trafficking were found to confer partial human serum resistance (74). It is not clear what role, if any, these proteins play in resistance in field isolates of *T. b. gambiense.*

Recently, a *T. b. gambiense* species-specific protein TgsGP was shown by two different groups to be important to *T. b. gambiense* resistance to human serum(76, 77). TgsGP is a glycoprotein associated with the endolysosomal system of the parasites. Unlike SRA, TgsGP does not seem to bind directly with TLF-1 or SRA (76). Rather, resistance appears to work by rigidifying endosomal membranes, perhaps preventing ApoL1 insertion(76). Heterologous expression of TgsGP in *T. b. brucei* did not make confer resistance to TLF-1 lysis suggesting the protein may interact with other gambiense-specific proteins (77).

Mechanisms of Resistance in Procyclic Trypanosomes

Procyclic *T. b. brucei* parasites, unlike bloodstream forms, are resistant to human serum (78, 79). Many reasons have been postulated for their resistance, and there is no definitely answer. Firstly, procyclic parasites do not express the haptoglobin hemoglobin receptor, and their bulk phase endocytosis is much slower than in bloodstream form parasites (33). In laboratory conditions, however, high concentrations of TLF-1 are still unable to overcome procyclic resistance, suggesting more specific inhibition (80). The biophysical properties of procyclic endosomal membranes may preclude ApoL1 insertion, because ApoL1 only inserts into anionic membranes (29). If

ApoL1 traffics to the plasma membrane as proposed, less streamlined recycling in procyclic cells may prevent ApoL1 from reaching its site of action. The mitochondrion of procyclic *T. b. brucei* is highly metabolically active in contrast to the reduced mitochondrion of bloodstream form parasites. Therefore, mitochondrial trafficking and apoptosis-like cell death pathways are very different in procyclic compared to bloodstream form *T. b. brucei*, possibly accounting for a lack of ApoL1 toxicity to procyclic *T. b. brucei.*

Mechanisms of Resistance in Human Cells

Humans evolved to have toxic TLFs circulating constantly in the serum. Therefore, human cells must have characteristics that make them refractory to lysis by ApoL1. On the other hand, human diseases states associated with ApoL1 polymorphisms represents aberrant destruction of human cells by ApoL1 variants, as will be discussed at the end of this introduction. There are many reasonable hypotheses for TLF resistance in humans, but none have been carefully tested. At the most simplistic level, compared to *T. b. brucei,* human cells have much slower endocytic rates and no known high affinity receptors of TLF-1. Thus, ApoL1 does not enter the endo/lysosomal systems of mammalian cells nearly as effectively as in *T. b. brucei.* Another relevant question is whether only human cells are immune to TLF, or whether all mammalian cell types of refractory to the toxic effects of TLF. Prolonged expression of ApoL1 in mice is has not been possible, due to toxicity from expression (22). ApoL1 toxicity to primate versus mammalian tissue has not been directly compared. Discovering the unique features of cells which are susceptible and refractory to ApoL1

will help unravel the mechanisms by which ApoL1 induce damage to both trypanosomes and human cells.

BIOLOGY BEHIND TLF UPTAKE

In order to better understand biochemical basis for the different models for TLF lysis, it useful to review what is known about aspects of trypanosome biology that are implicated in the TLF lytic mechanisms discussed above. This section will discuss on endocytosis and exocytosis of TLF-1 via the HpHbR in *T. b. brucei*. The high-affinity uptake of TLF-1 plays an important role in facilitating rapid and effective cell death in *T. b. brucei* as I show in chapter 2 and chapter 3. In the absence of the HpHbR, TLF-1 lysis occurs with much slower kinetics and requires higher concentrations to kill *T. b. brucei*. Also, as discussed, preventing endocytosis of TLF-1 is one of the resistance mechanisms employed by the human-infective *T. b. gambiense* parasites.

Endocytosis and Exocytosis in trypanosomes

To survive in the mammalian bloodstream, parasites much evade complement mediated lysis. Endocytosis and clearance of immunoglobulins from the parasite surface occurs via one of the fastest endocytosis rates known in nature. In fact, every 12.5 minutes the entire cell surface VSG is endocytosed and recycled, effectively removing and degrading any bound host immunoglobulins (81). Within the parasite, recycling of VSG from the endosomes back to the surface takes only one minute.

Both endocytosis and exocytosis are restricted to a specialized region at the posterior of the cell called the flagellar pocket. Unlike other Eukaryotic cells which contain multiple lysosomes, trypanosomes have a streamlined endocytic system

terminating in a single lysosome proximal to the cell nucleus. Thus, all endocytic and exocytic cargo cycle between the flagellar pocket and the ER/golgi/lysosome near the nucleus. In trafficking studies, fluorescent proteins may be visualized as if traffics in punctate vesicles between the posterior flagellar pocket and the central lysosome.

Efficient endocytosis of nutrients from human serum may occur via receptor-mediated endocytosis or fluid-phase endocytosis. The trypanosome cell surface is uniformly carpeted with VSGs, but the flagellar pocket contains receptors whose ligand-binding sites are accessible to the extracellular milieu. Receptors studied in the flagellar pocket include the haptoglobin hemoglobin receptor (HpHbR) which facilitates HpHb uptake for heme acquisition, the transferrin receptor which facilitates iron uptake, and a low affinity LDL receptor for lipid uptake. The fast rate of endocytosis of fluid phase cargo facilitates efficient uptake of nutrients with no receptors.

From the flagellar pocket, clathrin-coated vesicles bud off and begin to acidify. After shedding of their clathrin coat, early endosomes arise as defined by the marker GTPase Rab5. Early endosomes may re-direct cargo back to the flagellar pocket via recycling endosomes, or continue on to late endosomes, which are defined by the GTPase Rab7 and homologs of early ESCRT (Endosomal Sorting Complex Required for Transport) machinery VSP4 and VSP23 (82). Again, late endosomes can send cargo back through recycling endosomes, or pass cargo on to the lysosome. In the single terminal lysosome, proteases degrade protein cargo, and transporters facilitate nutrient intake into the cytosol. A lysosomal glycoprotein of unknown function, p67, is a common marker used to label the lysosome in immuno-fluorescent studies.

Trafficking of VSG through the parasite is well studied. After protein synthesis in the ER, The ER translocon (Sec61) recognizes hydrophobic N-terminal ER targeting sequences on VSG and other plasma membrane proteins (83). In the ER, VSG is extensively glycosylated and a GPI (glycosylphosphatidylinositol) anchor is attached, anchoring VSG to the ER membrane. If the GPI signal is deleted, VSG accumulates in the ER and is trafficked to the lysosome for degradation. Otherwise, VSG exits the ER for the golgi, where further glycosylation occurs. From the golgi, VSG traffics to the plasma membrane through poorly defined Rab11 and actin-independent vesicles (83).

The signals for recycling of endosomal cargo to the plasma membrane versus delivery to the lysosome for degradation have not been fully characterized. The simplest model is that membrane associated proteins such as VSG and GPI-anchored receptors recycle to the flagellar pocket membrane, avoiding the lysosome, while most soluble cargo is delivered to the lysosome for degradation. This model is complicated by the existence of proteins such as the GPI-anchored SRA which traffic between the lysosome and endosomal compartments. In *T. b. brucei* cells expressing SRA with the GPI-addition site knocked out, the cells were still resistant to TLF-1 resistance, but SRA no longer trafficked efficiently to the flagellar pocket, though it was still localized to the endosomes and the lysosome (in the presence of protease inhibitors) (68). Ubiquitination of lysine amino acids in the cytoplasmic domains of invariant surface glycoproteins leads to a re-sorting of these transmembrane proteins from the plasma membrane to the lysosome (84-86).

The endocytic system of trypanosomes, like that of higher eukaryotes, is highly complex and comprised and many different trafficking vesicles, many of which are

poorly defined biochemically. There are several types of endosomal compartments in trypanosomes, which may sort different material. The early Rab5A endosomes contain VSG, endocytosed LDL, fluid-phase markers, and some transmembrane surface proteins, while Rab5B endosomes are only known to transport the membrane-bound ISG100 (invariant surface glycoprotein) (87, 88). Another type of poorly characterized endosomal vesicle is defined by Rab21 (89).

Recycling endosomes which carry cargo from both early and late endosomal compartments are defined by the Rab11 GTPase. Recycling endosomes also may be marked by the exocyst component Sec15, a conserved protein AZII, the ciliate-specific RBP74, and conserved 14-3-3 proteins (90). The ApoL1-binding *T. b. rhodesiense* protein SRA does not localize to recycling endosomes (69). Overexpression of constitutively active ATP-bound or constitutively inactive ADP-bound forms result in slowed recycling with negligible effects on rates of endocytosis (91). As recycling endosomes approach the flagellar pocket, they form discoidal morphologies and have been termed exocytic carriers because they directly fuse with the flagellar pocket (92). Recycling of different factors occurs at different rates. VSG quickly cycles between the early endosomes and recycling endosomes, but the transferrin receptor takes much longer (around 11 minutes) to cycle from the late endosomes back to the pocket (93).

Degradation of transferrin occurs in the lysosome, but not all of the amino acids are retained in the parasites – after 30 minutes half of the transferrin-associated radioactivity were present in the cell media (94). Similarly, IgG degradation products end up outside the cell, and degradation products of p67 can be found at the cell surface, indicating retrograde transport from the lysosome is possible (95). It is

unknown whether lysosome to plasma membrane transport involves Rab11 positive recycling endosomes, or intersects directly with the plasma membrane.

TLF-1 lysis requires many components of the endosomal and lysosomal system in *T. b. brucei*. ApoL1 and TLF-1 localize to early and late endosomal vesicles and the lysosome (44, 96). In RNAi screens for TLF-1 resistance, knockdown of the vacuolar H^+-ATPase prevented endosomal acidification and led to TLF-1 resistance (74). Knockdown of the lysosomal protein p67 also led to TLF-1 resistance but the mechanism of resistance is not well understood (45, 75). Preventing late endosome to lysosome trafficking of TLF-1 by either a 17˚C temperature block or knockdown of Rab7 slows or prevents *T. b. brucei* lysis (46, 97). The Rab7 data provided strong support for trafficking to the lysosome being necessary for TLF-1 lysis. However, it is not known whether Rab7 knockdown or the low-temperature block effects recycling to the plasma membrane or vesicular traffic to the mitochondrion. Recently, ApoL1 was found to co-localize with poorly define kinesin KIFC1 positive vesicles in puncta near the mitochondrion, suggesting that KIFC1 mediates vesicular transport between the endosomal system and mitochondrion (18). ApoL1 trafficking to the plasma membrane has not been studied. Recycling endosomes or KIFC1-positive vesicles may transport ApoL1 to the plasma membrane of *T. b. brucei.* My own preliminary data from a double-negative cell line of Rab11 suggests that classical Rab11 recycling endosomes are not important for ApoL1 trafficking to the plasma membrane.

The Haptoglobin Hemoglobin Receptor

The haptoglobin hemoglobin receptor (HpHbR) in the trypanosome flagellar pocket facilitates high affinity uptake of hemoglobin-bound TLFs. Therefore, understanding the HpHbR structure and trafficking may give insight into TLF-1 trafficking. It is important to note that high concentrations of hemoglobin-free TLF-1 or apoL-1 alone are able to kill cells, suggesting that receptor-mediated trafficking is not required for TLF-induced lysis (25, 32).

Aside from its role in deadly TLF-1 uptake, HpHbR is considered a nutrient receptor for heme uptake, because trypanosomes don't synthesize their own heme. Heme proteins expressed in bloodstream form trypanosomes include a variety of cytochromes which are involved in processes such as fatty acid desaturation (98). The role of heme uptake in trypanosomes is described in more detail in the next section of this introduction.

T. b. brucei HpHbR knockout cells show no growth defect *in vitro*, but in a mouse infection or in the presence of macrophages, HpHbR knockout parasites have decreased virulence and sensitivity to macrophage-induced oxidative stress (33). Protein-heme content was measured to be 2 ng/mL protein in HpHbR-containing *T. b. brucei* cells, but undetectable in HpHbR knockout cells, suggesting that heme proteins were responsible for the growth phenotype (33). Resistance in type I *T. b. gambiense* cells involves inactivating mutations and down-regulated expression of the HpHbR (39, 73). These parasites have successfully adapted to loss of heme uptake via the HpHbR in the field, confirming that the HpHbR receptor is non-essential in trypanosomes. Similarly, the plant trypanosome *Phytomonas serpens* completely lost the requirement for heme proteins (99). It remains an open question whether bloodstream form *T. b.*

gambiense can survive without heme, especially considering the relatively heme-poor environment of the cerebral spinal fluid in late-stage infection.

The HpHbR binds to the HpHb or HprHb complex and not to either of the individual proteins, with the ligand binding site making contact with amino acids of both the haptoglobin chain and the beta subunit of hemoglobin (including contacts with heme itself). The shape of the monomeric GPI-bound receptor is just long enough for the binding site of haptoglobin-hemoglobin to be accessible above the VSG coat. The mechanism by which the HpHbR and other GPI-bound receptors are restricted to the pocket is unknown, but approximately 200 HpHbR proteins populate the flagellar pocket (33). Because Hp1-1 is a tetramer with two hemoglobin binding sites, it has been postulated that the HpHbR may bind ligand in a divalent manner (41). TLF-1 contains around 5 hemoglobin binding sites on Hpr and therefore might bind with even higher valency depending on the conformational accessibility of the Hpr-Hb sites on TLF-1.

From the flagellar pocket, the HpHbR traffics into the endosomal compartments. When the pH reaches approximately 5.5, the receptor releases its HpHb ligand. The pH of early and late endosomes is not known nor has the proton pump responsible for acidification been definitively identified and localized. However, the pH of the lysosome has been measured to be 4.8, and trypanosome endosomes are likely rapidly acidified to below pH 6, as in other organisms (100, 101). Thus, it is unknown at what stage of endocytosis the HpHbR releases its ligand. In the case of transferrin, receptor disassociation does not occur until very acidic conditions below pH 5 are reached (94).

CELL DEATH PATHWAYS IN TRYPANOSOMES

The mechanism for TLF-induced cell death in *T. b. brucei* may involve the initiation of programmed cell death pathways. In particular, the recently published mitochondrial model for ApoL1 lysis involves initiation of apoptosis-like cell death in *T. b. brucei* (18). This section will review current knowledge of programmed cell death in trypanosomes, discussing apoptosis-like cell death, autophagic cell death, and the trypanosome-specific spliced leader silencing pathway. Finally, the mechanisms of cell death initiated by current drugs against human trypanosome infection will be discussed.

Programmed cell death was originally discovered in metazoans and thought to be an adaptation which evolved to facilitate multi-cellularity. However, it has become increasingly clear that trypanosomes and other non-metazoan life did, in fact, evolve complex programs for cell death analogous to those studied in metazoan organisms. The evolutionary drive for programmed cell death pathways in trypanosomes seem to be regulation of cell density, life cycle differentiation, and increasing the likelihood for survival and transmission of certain members of each clonal population (102). The pathways and triggers of programmed cell death in trypanosomes are very poorly characterized, with papers using terms like apoptosis and autophagic cell death without establishing clear definitions and markers. Therefore, distinguishing between necrotic cell death and different types of programmed cell death is difficult. Currently, some researchers still dispute the evidence that dedicated programmed cell death machinery exists in parasitic protozoa, and instead classify parasitic cell death as either necrotic or incidental (103).

Apoptosis-like cell death in trypanosomes

Apoptosis markers used in mammalian cells are not reliable markers for programmed cell death in bloodstream form *T. b. brucei*. Specifically, cytochrome c is absent from the mitochondria, so cytochrome c release is not observed. A complex pathway of caspase activation occurs in mammalian cells, but in trypanosomes, no apoptotic caspases have been discovered, though various alternative proteases including metacaspases may play a role in cell death. While some labs have reported phosphatidyl serine exposure due to induction of apoptosis, the VSG coat hinders binding of Annexin V, and dead *T. b. brucei* will bind Annexin V regardless of cell death mechanism (103, 104).

Apoptosis-like cell death in *T. b. brucei* has been initiated by prostaglandins, concanavalin A, ROS, various pro-oxidants, and a variety of drugs (105). The natural molecular inducers of apoptosis in *T. b. brucei* seem to be calcium influx into the mitochondria and oxidative stress (17). Importantly, both calcium influx and oxidative stress are associated with TLF-1 induced lysis of *T. b. brucei* (48, 61).

Apoptosis phenotypes observed in *T. b. brucei* include nuclear DNA fragmentation, loss of mitochondrial membrane potential, and intracellular calcium accumulation. In bloodstream form *T. b. brucei,* one of the only characterized molecular markers for apoptotic cell death is endonuclease G (endoG). During apoptosis, endoG is released from the mitochondria, and translocates to the nucleus where it induces DNA fragmentation (106). Recently, ApoL1 and human serum treated *T. b. brucei* were found to demonstrate these features, including a loss of plasma membrane potential, release of endoG, and DNA fragmentation (18). Apoptosis-induction factor knockdown also increased sensitivity of *T. b. brucei* to TLF-1 lysis (18).

Autophagic cell death in trypanosomes

Another form of programmed cell death described in trypanosomes is autophagic cell death. Autophagy probably evolved as a stress response pathway to prolong survival, but autophagic machinery may also be harnessed to execute programmed cell death. Autophagy protein components are well conserved in kinetoplastids, with proteins able to compensate for yeast mutants (107, 108). Central in the autophagy pathways are the ATG autophagy proteins, which are well conserved between yeasts and kinetoplastids (109). Suggestion a role for autophagic cell death, knocking down two of the three central ATG8 proteins in *T. b. brucei* led to decreased autophagic markers and increased survival of parasites under nutrient starvation. However, under exogenous stresses, it is often difficult to determine whether autophagic pathways are mobilized as a stress response to prolong survival, or whether autophagy is acting as a form of programmed cell death.

The universal phenotype of autophagy is the formation of acidic vesicles throughout the cytoplasm for the degradation of cellular components. Papers invoking autophagic cell death in *T. b. brucei* sometimes only have evidence of cytoplasmic vesicle formation and not any molecular indicators of autophagy (58). The formation of autophagosomes is a very rapid process. For instance, in procyclic form *T. b. brucei*, 30 min starvation in phosphate buffered saline solution led to the formation of ATG8 positive puncta in 100% of the cells(110). Importantly, in bloodstream form *T. b. brucei,* autophagy is associated with differentiation to the stumpy form parasites which are competent for tsetse fly transmission (110).

The role of autophagy during TLF-1 lysis of *T. b. brucei* has not been investigated. Lysosomal swelling in TLF-1 treated *T. b. brucei*, however, suggests addition of membrane from autophagic vesicles. In neuropeptide-treated *T. b. brucei*, similar lysosomal swelling and lysosomal permeability phenotypes were observed and attributed to autophagic cell death (58).

Spliced Leader Silencing Pathway in trypanosomes

The spliced leader silencing pathway (SLS) has been proposed to be a unique form of programmed cell death in kinetoplastids. Unlike most cell death pathways, which evolved from the stress response of the mitochondria, the SLS pathways evolved as a response to ER stress. The SLS pathways is thought to be related the trypanosome version of the unfolded protein response in other eukaryotes (111, 112).

Kinetoplastids transcribe polycistronic arrays of functionally unrelated genes, and the nascent RNA transcripts require unique processing before translation. During post-transcriptional processing all mRNAs in trypanosomes receive a spliced leader sequence upstream of their 5'UTR (5' untranslated region). The spliced leader RNA is derived from exons transcribed by RNA polymerase II. Production of spliced leader RNA may be silenced as a result of ER stresses, including knockdown of proteins involved in ER secretion and addition of reducing agents. These ER stresses cause phosphorylation of an ER resident kinase, PK3, which trans-locates to the nucleus and phosphorylates a protein in the SL translation complex, preventing transcription of SL (113).

SLS is associated with the common phenotypes of apoptotic cell death, including DNA fragmentation, loss of mitochondrial membrane potential, increases in cytosolic Ca^{2+}, ROS formation in the mitochondria, and phosphatidylserine exposure (114). Moreover, autophagosome formation is also observed associated with SLS, possibly to dispose of mis-functioning ER (114). Shutting down SL RNA transcription turns off all mRNA production, which eventually leads to cell death, making SLS a unique form of programmed cell death in kinetoplastids.

Until recently, SLS was studied mostly in procyclic form trypanosomes, with limited evidence for SLS in bloodstream form trypanosomes. A recent study of SLS in bloodstream form parasites failed to induce SLS despite numerous triggers, suggesting that the signaling pathways for SLS only exists in procyclic parasites (115). Induction of SLS has never been investigated in TLF-1 or human serum treated *T. b. brucei.*

Current Chemotherapy and Drug Mechanisms

When discussing the mechanisms of cell death in trypanosomes, it is important to think about the mechanisms of action of current chemotherapies against human trypanosome infection. The current drug repertoire for use in the field against human Sleeping Sickness includes a very short list of drugs with notoriously bad side-effects. Pentamidine is used for early stage *T. b. gambiense* infection, suramin for early stage *T. b. rhodesiense* infection, eflornithine/nifurtimox combination therapy for late stage *T. b. gambiense* infection, and melarsoprol for late stage *T. b. rhodesiense* infection (116). For most of these drugs the mechanism of action is poorly characterized.

Pentamidine is an aromatic amine-based compound for which the mechanism of action is not well understood. Because of its positive charge, pentamidine binds to DNA in the nucleus and kinetoplast (117). While DNA binding drugs seem intrinsically non-selective, the DNA-binding carcinogen ethidium bromide (and its derivatives) are used to treat *T. b. brucei* infection in cattle. Because pentamidine is associated with loss of mitochondrial membrane potential, its mode of action might involve inhibiting mitochondrial DNA or other processes (118). Pentamidine enters trypanosomes via the flagellar pocket transporter aquaglyceroporin 2 (AQP2), as well as a nucleotide transporter TbAT1 and another transporter HAT1 (119, 120). Pentamidine treatment requires a lengthy course of high concentrations (4mg/mg) of the drug administered intramuscularly. Its inability to cross into the CNS precludes its use against late-stage neurological disease.

Suramin is effective against various sub-species of *T. brucei*, but it only used against early stage *T. b. rhodesiense* infection because of the requirement for intravenous administration. For patients, suramin requires multiple intravenous administrations of high concentrations of drug (20 mg/kg) over a month-long period. Suramin is a derivative of the dye trypan blue, which Paul Ehrlich developed for African Sleeping Sickness at the turn of the 20th century. Like pentamidine, the mechanism of action of suramin is unclear and it is probably a promiscuous inhibitor of several classes of enzymes.

Trafficking of suramin within *T. b. brucei* is well characterized (121). In the serum, suramin is very stable due to association with low density lipoprotein particles (LDLs) which may facilitate drug uptake via LDL receptors (122). The parasite invariant

surface glycoprotein ISG75 is necessary for suramin entry into the parasite's endosomal pathway (123). Within the endosomes and lysosome, a number of different trafficking proteins are implicated in suramin susceptibility, including the lysosomal protein p67 which is also important for TLF-1 susceptibility (123, 124). Perhaps due to its effects on endosomal trafficking or binding to the TLF-1 molecule (analogously to an LDL), suramin prevented TLF-1 lysis of *T. b. brucei* (A. S. Greene unpublished data, Figure 1.12).

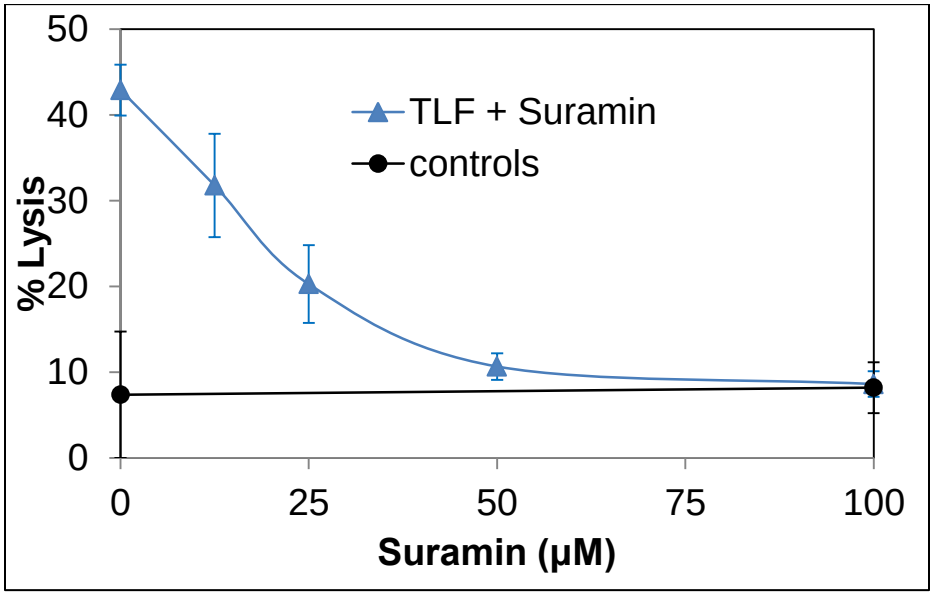

Figure 1.12: **Suramin Inhibits TLF-1 lysis of *T. b. brucei*.** The indicated concentrations of suramin were pre-incubated with 10^7 cells/mL *T. b. brucei* in serum containing culture media for 2 h at 37˚C before adding TLF-1 (8.8nM, with excess hemoglobin). After 2 hours with TLF-1 the % dead cells were counted as % lysis. Controls were treated with either 0 or 100μM suramin and no TLF-1.

Melarsoprol is another old drug, an organic arsenical introduced in the 1940s. The treatment regime for melarsoprol requires multiple intravenous injections over 10 days or several weeks. Compared to treatment with DFMO monotherapy, which requires multiple daily injections, melarsoprol treatment is more feasible, prolonging its

use for late stage *T. b. gambiense* until recent years. The drug is extremely toxic, causing the fatal side-effective in up to 10% of patients (125). In addition to toxicity, melarsoprol use over the last 70 years has led to the spread of parasite resistance among both *T. b. rhodesiense* and *T. b. gambiense* parasites, for which melarsoprol was a leading drug through the early 2000s. Resistance to melarsoprol comes from inhibition of drug import through some of the same transporters as pentamidine including aquaporin 2 and an adenosine transporter (126).

Melarsoprol promiscuously coordinates free thiols in trypanothione and proteins in *T. b. brucei*, shutting down redox regulation and leading to cell death (127, 128). My studies (chapter 2) show that thiol-binding agents exacerbate TLF-1 lysis. Therefore, melarsoprol dual therapy with an osmotic-stress inducing drug such as salinomycin may induce synergistic parasite lysis (47, 129).

Eflornithine, or dimethylornithine (DFMO), is an analog of the metabolic molecule ornithine. DFMO reversibly inhibits ornithine decarboxylase (ODC), an enzyme critical for producing the spermidine necessary for the synthesis of the antioxidant molecule trypanothione. Originally developed as an anti-cancer therapy, eflornithine shows no specificity for human over parasite OCD. In fact, the two enzymes are almost identical, and parasite ODC is thought to have arisen from horizontal gene transfer (130). The differences in enzyme half-life between human and parasite ODC is what makes DFMO an effective drug. Human ODC has an incredibly fast protein turn-over rate of around a half hour, so humans can tolerate very high concentrations of the drug without toxicity issues. In contract, ODC in *T. b. gambiense* takes hours to turn over and can be effectively inhibited, slowing cell division and harming the parasite's ability to respond to

oxidative stress. *T. b. rhodesiense* ODC has a faster turnover rate than *T. b. gambiense's* ODC, making these parasites innately resistant to DFMO (131). In *T. b. gambiense,* resistance against DFMO occurs if parasites lose a neutral amino acid transporter, TbAAT6, which facilitates drug import (132).

Worries about the development of DFMO resistance coupled with the difficulty delivering the full intravenous drug course prompted the development of the nifurtimox-DFMO combination therapy. Combination therapy decreased the 2x/day administration of DFMO from 14 days to 7 days along with a 10 day oral administration of DFMO (133). While the combination therapy did not result in significantly better treatment outcomes than DFMO monotherapy, it has become the treatment of choice due to decreased cost of administration. Nifurtimox is a drug developed for the South American intracellular parasite *Trypanosoma cruzi* which causes Chagas disease in humans. An active intracellular nitroreductase is necessary to activate the pro-drug for efficacy, and point mutations are associated with resistance in lab strains of *T. b. brucei* (134). Within the parasite, Nifurtimox depletes cellular small thiols including trypanothione which explain why it works with DFMO, which decreases trypanothione synthesis (135). Depleting trypanothione makes the parasites more sensitive to oxidative stress.

The ultimate hope for all infectious diseases research is the research results contribute to human health. Clearly, the current pharmaceutical options to treat African Sleeping Sickness are inadequate, and the development of drug resistant parasites will likely make the disease untreatable unless new drugs are developed soon. The TLFs are primate's naturally evolved drug against sleeping sickness. Comparing the

mechanism of action for small molecule drugs to TLF-1 killing of *T. b. brucei* may yield insights that can inform novel drug design.

OXIDATIVE STRESS AND THE LYSOSOMAL MODEL FOR TLF LYSIS

Oxidative stress is important for TLF-1 lysis of *T. b. brucei.* One model for lysosomal lysis suggested that HprHb within the TLF particle initiates oxidative damage to lysosomal lipids in the trypanosome. Chapter 2 of this dissertation details how I tested for TLF-1 induced damage in the lysosome using various methods. My experiments caused me to re-evaluate the role of oxidative stress in TLF-1 lysis, showing that oxidation was important not within the lysosome, but at the plasma membrane of the parasites (47). In this section, however, I will review the important background information on iron uptake and oxidative stress in trypanosomes which led me to perform the experiments detailed in chapter 2.

Iron Metabolism in Trypanosomes

The role and origin of oxidative stress in trypanosome lytic factor-induced cell death is a focus of this research. Heme-initiated oxidative stress in the lysosomal iron is critical especially for the lysosomal model of TLF-1 induced cell death. In trypanosomes and other organisms, heme and non-heme iron are major sources of oxidative stress to cells. This section will review the research on iron metabolism in trypanosomes, particularly in regard to oxidative stress in the lysosome. The following section will detail the systems trypanosomes have evolved to deal with oxidative stress.

Iron is an essential nutrient due to its role as a cofactor in numerous enzymes. In trypanosomes, iron transfer from the lysosome to the cytosol is facilitated by a lysosomal cation transporter (136). Internalized heme may be utilized for incorporation into heme-proteins or possibly catabolized as a source of iron. Although no predicted heme oxygenase gene is present in kinetoplastids, heme oxygenase activity has been observed , and heme uptake can rescue iron depravation in *Leishmania* amastigotes (137).

Trypanosomes and related kinetoplastid flagellates lack complete heme biosynthetic pathways and acquire heme from exogenous sources. *Trypanosoma brucei* and *T. cruzi* are missing the entire heme biosynthetic pathway, while *Leishmania spp.* have the last 3 enzymes which synthesize heme from protoporphyrinogen (138). *T. b. brucei* maintains a mitochondrial enzyme capable of modifying the heme b endocytosed from hemoglobin into heme a for use as a cofactor in different proteins (139).

Distinct environments and metabolic needs shaped the evolution of diverse uptake mechanisms for heme in each stage of the parasitic life-cycle. For instance, *Trypanosoma brucei* procyclic insect-stage parasites take up heme directly from the insect gut fluids. They utilize heme for oxidative metabolism in a classical cytochrome-mediated mitochondrial electron transport chain. Mammalian stages of both *T. b. brucei* and *Leishmania spp.* both acquire heme from Hb endocytosis via the flagellar pocket. In *Leishmania* (which resides in macrophages) the receptor is for Hb, while *T. b. brucei* take up HpHb with the HpHbR (140-142).

In the mammalian host, bloodstream *T. brucei brucei* have a reduced mitochondria and few heme proteins; however what heme is needed is acquired through the HpHb complex (33, 143). In *T. b. brucei,* the HprHb protein component is rapidly degraded in the lysosome, while the heme cofactor accumulates in the parasites for over two hours, and is incorporated into proteins (33). *T. b. gambiense* has evolved not to express active HpHbR, so it is unclear if or how heme uptake occurs in the bloodstream form of this human parasite. In a model for *T. b. gambiense* where the HpHbR has been knocked out of *T. b. brucei,* cells were viable but did not accumulate detectible levels of heme compared to wild-type *T. b. brucei* (33).

In the related kinetoplastid *Leishmania,* heme uptake requires Hb endocytosis and transport to the lysosome via Rab7 positive endosomes (144). Within the lysosome Hb is degraded and heme released at a rate unrelated to lysosomal pH, but regulated by free heme levels in the lysosome (144, 145). Uptake of Hb occurs through a heme transporter in the lysosome (146). The *T. cruzi* homolog of this heme transporter is found in the flagellar pocket, indicating that direct uptake of heme from the media may be possible in *T. b. brucei* as well as through the HpHb complex (143).

The identity and functions of heme-containing proteins in bloodstream *T. brucei* are unknown, though they are detectible on radioactive gels (33). The short list of annotated heme proteins includes a cytochrome b5-dependant oleate desaturase and a P450 sterol demethylase (33, 99). Neither of these proteins is likely to be essential, especially *in vitro* culture. Non-covalent heme chaperones, which are difficult to predict by bioinformatics, are required to safely traffic heme within the bloodstream cell (147). The function of heme-binding proteins in bloodstream *T. brucei* may be linked to

parasite defense against immune stresses. Heme-deficient HpHbR KO parasites showed increased susceptibility to macrophages (33). Inhibition of macrophage NO-production or NADPH oxidase caused HpHbR KO *T. b. brucei* to survive in the presence of macrophages, suggesting that uptake of heme is important in resistance to oxidative stress (33).

The presence of heme-binding proteins does not imply that heme is essential for an organism. Heme is not essential in the plant trypanosome *Phytomonas,* which has an oxidative metabolism based on alternative oxidase (99). Both *Phytomonas* and *T. brucei* contain a P450 sterol demethylase. In heme-free *Phytomonas* the demethylase activity was extinguished, creating parasites with only the enzyme's substrate lanosterol (99). It is possible that bloodstream *T. brucei* could survive loss of heme acquisition and changes to their sterol composition. However, *in vitro* cultured bloodstream *T. brucei* have 3 to 4 times more heme per cell (41pmol/10^9 cells) than *Phytomonas*, suggesting that they may have greater heme requirements than their vegetarian cousins (99). Comparatively, parasites with a normal oxidative metabolism such as the insect parasite *Crithidia* and procyclic *T. brucei* have hundreds of times more heme than bloodstream *T. brucei* (99, 148).

The Oxidative Defense Systems in Trypanosomes

If oxidative stress plays a role in TLF-1 induced trypanosome lysis, then it is critical to understand the oxidative defenses trypanosomes harbor. In one lysosomal model for TLF-1 lysis, the Hpr-Hb complex is proposed as an initiator of oxidative stress. Therefore, understanding the response of *T. b. brucei* to oxidative stress in the

lysosome is important for understanding later chapters. For instance, in chapter two of this dissertation, TLF-1 lytic activity is tested in *T. b. brucei* which have two cytosolic lipid peroxidases knocked out (Px I & Px II, see Figure 1.13).

Trypanosomes lack several canonical antioxidant enzymes present in other organisms. Most notably, catalase and selenium peroxidases are absent. Perhaps due to their divergent antioxidant system, trypanosomes are slightly more sensitive to oxidative stresses than most mammalian cell types (149, 150). The antioxidant enzymes in *T. b. brucei* have interesting properties which have made them prime targets for drug development for several decades (151).

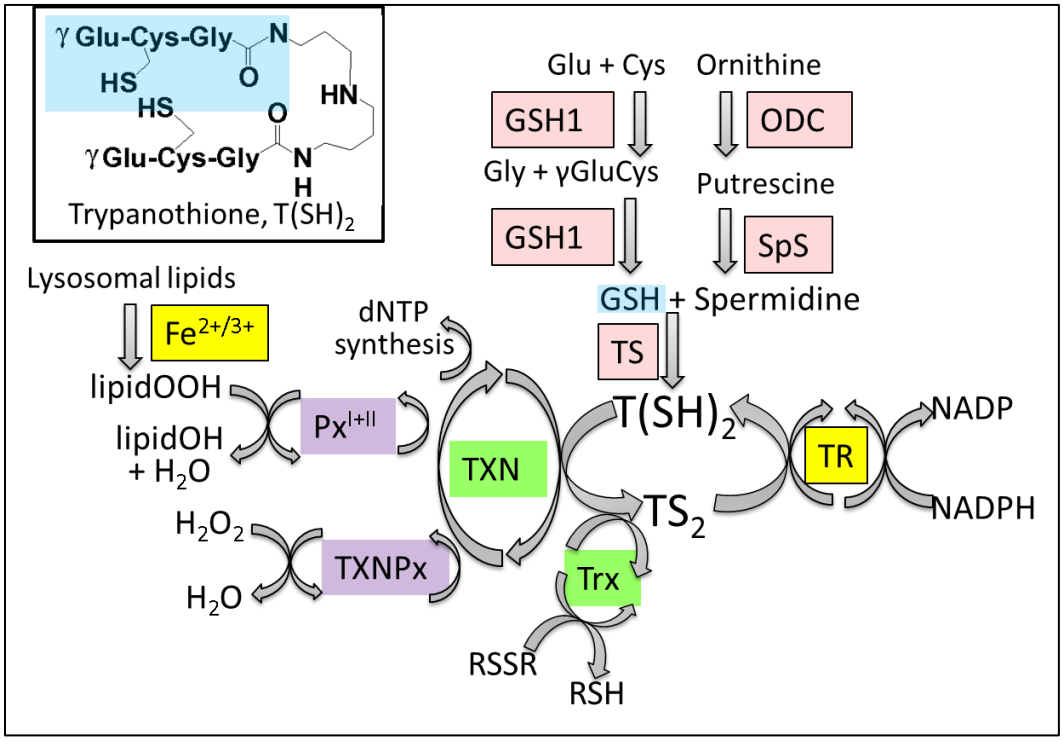

Figure 1.13: **Cytosolic Redox Enzymes in bloodstream form *T. brucei.*** GSH1: gluathionyl spermidine synthase, ODC: ornithine decarboxylase, SpS: spermidine synthase, TS: trypanothione synthase, TR: trypanothione reductase, Trx: thioredoxin,TXN: tryparedoxin, Px^{I+II}: lipid peroxidases I and II, TXNPx: peroxiredoxin-

type peroxidase, RSSR: protein dithiol. RSH: protein free thiol, TR: trypanothione reductase.

The redox biology of trypanosomes centers around a molecule unique to the kinetoplastids: the dithiol trypanothione, abbreviated $T(SH)_2$, or TS_2 for the oxidized form. Most organisms use the monothiol, glutathione, to maintain a reducing environment in the cytosol and shuttle electrons through antioxidant enzymes such as glutathione reductase. In contrast, $T(SH)_2$ has a less negative redox potential and a near-neutral pKa, allowing its thiols to be more easily oxidized than glutathione. Although bloodstream trypanosomes maintain millimolar levels of both glutathione and trypanothione, their redox enzymes are almost all trypanothione specific (152). The cytosolic enzymes and their interactions are diagrammed in Figure 1.13. Many of the enzymes in the trypanosome antioxidant defense system are essential for growth, or make *T. b. brucei* more resistant to oxidative stress (Table 1.1).

Table 1.1: **Redox Regulatory Enzyme in *T. brucei*.** The table lists the role of each enzyme in metabolism, the genetic knockdowns or knockout which have been constructed, the phenotypes of these cell lines, and any effects on sensitivity to peroxides.

Enzyme	Role	Cell lines made	Cell Line Phenotypes	Response to peroxides	Cita-tion
TXN tryparedoxin (cytosolic, mitochondrial)	Redox exchange with peroxidases	RNAi	Compensatory higher concentrations of small molecule thiols T(SH)2, Gsp, and GSH;	more sensitive to H_2O_2	(153, 154)
$T(SH)_2$ synthetase (TRYS) (cytosolic)	Links GSH and spermidine to make $T(SH)_2$	RNAi	Less Gsp and $T(SH)_2$ and GSH accumulation. Growth effect after a few days induction; Increased production of trypanothione reductase (TR)	more sensitive to H_2O_2	(155, 156)
		Single KO	Less GSH and $T(SH)_2$		(157, 158)
		Conditional double KO	Death after 6 days. free thiols ~50%		

			depleted at 3 days.		
		Over expressing cells	Less sensitive to inhibitor of $T(SH)_2$ synthase		
Non-selenium peroxidases (Px I, II, III) (cytosolic, mitohondrial)	Lipid peroxide metabolism, reduced by TXN	Double KO	Rapid cell death rescued by Trolox but not water-soluble antioxidants.		(159, 160)
2-Cys-peroxiredoxin (TXNPx) (cytosolic, mitochondrial)	Expression induced by H_2O_2 stress in *T. cruzi*; H_2O_2 but not lipid peroxides are substrates	RNAi	Death after 24 hr induction. Loss of H_2O_2/Trypanothione enzyme activity	more sensitive to H_2O_2	(154, 159)
Trypanothione reductase (TR) (cytosolic)	Reduces TS_2 to $T(SH)_2$ (center of redox metabolism)	dKO + conditional expression (1%-400% WT levels)	Less than 10% of WT levels still maintains reduced $T(SH)_2$	More sensitive to H_2O_2	(161)
Dithiol glutaredoxin Grx-1 (cytosolic)	De-glutathion-ylate proteins, ~2μM enzyme in cytosol	5-10 fold Overexpression Grx-1	Normal growth		(162)
Monothiol glutaredoxin (2and3) (cytosolic)	Upregulated during stationary phase or starvation				(163)
Monothiol glutaredoxin-1 1-C-Grx1 (mitochondria)	Reduces glutathione Fe-S protein	Over Expressing cells (5-10fold)	overexpression causes no growth phenotype WT cells + deferoxamine (Fe-chelator) causes 2-fold down regulation, WT + H_2O_2 causes 2-fold up-regulation;	more sensitive to deferoxamine and H_2O_2	(163)
Superoxide Dismutases (B1&B2) (cytosolic/glycosomal)	Superoxide anions are substrates	RNAi of B1 & B2	Growth defect after 24hr		(164)
		KO SOD B1 + conditional expression	Normal growth. Increased benznidazole, nifurtimox, paraquat susceptibility No difference in suramin susceptibility		(165)
		KO SOD B2	Normal growth		

The redox enzyme system may regulate the cell cycle and or increase drug resistance in kinetoplastids (151, 152, 166). For instance, the universal minicircle sequence binding protein (UMSBP) is oxidized by a mitochondrial TXNPx to regulate kinetoplastids DNA replication. After oxidation by H_2O_2, however, the UMSBP oxidation blocks kinetoplastid DNA replication, causing cell cycle arrest in response to oxidative stress (167). Also, TXN is necessary to reduce ribonucleotide reductase, thus regulating the dNTP pool of trypanosomes (168). In drug resistance, trypanothione may form conjugates with thiol-binding drugs, and exit the cell via the transporter MRPA. MRPA confers resistance to Melarsoprol in *T. brucei* and resistance to antimonial drugs in *Leishmania spp.*, including field isolates (169).

OSMOTIC STRESS AND THE PLASMA MEMBRANE MODEL FOR TLF LYSIS

The work presented in this dissertation leads to the conclusion that ApoL1-induced ionic imbalance at the plasma membrane of *T. b. brucei* leads to osmotic swelling and cell death. The molecular events associated with ionic disruption of the plasma membrane and cellular swelling are complex and involve poorly characterized plasma membrane ion channels and stress signaling pathways. This section will discuss what is known about the plasma membrane potential, endogenous plasma membrane channels, and the osmotic stress responses in trypanosomes.

Regulation of Plasma Membrane Potential in Trypanosomes

ApoL1 at the plasma membrane of *T. b. brucei* is predicted to disrupt ionic gradients leading to a loss of the plasma membrane potential in *T. b. brucei.* Chapter

three of this dissertation will show how TLF-1 initiates a loss of plasma membrane potential in *T. b. brucei.* This section reviews molecular details the molecular details of membrane potential regulation in *T. b. brucei.*

Maintaining a potential across the plasma membrane is critical for all living cells. A plasma membrane potential (Ψ_{PM}) is established because the plasma membrane is semi-permeable, entrapping large molecules and proteins inside the cells for a net negative charge internally. Furthermore, active ion transport is usually necessary to maintain a steep gradient of ions across the membrane (see Table 1.2). The magnitude of the potential difference across the membrane is determined by the concentration gradients of ions and molecules across the membrane and the permeability of each ion or molecular due to passive diffusion and active transport. Variations of the Nernst Equation can be used to calculate the Ψpm at steady state. Like most cells, the membrane potential of bloodstream form trypanosomes approaches the passive diffusion of potassium across the membrane, around -85mV (170, 171).

Table 1.2: **Concentration of Osmolytes in T. brucei and human serum**. The reported concentrations of different ions and molecules in both human serum and T. b. brucei are listed.

Molecule	**Human plasma or serum**	**Trypanosome cytosol (free)**	**Reference *H. sapiens***	**Reference *T. brucei***
Glucose	4-6mM	Low	(172)	(173)
Pyruvate	Pyruvate <50μM	26mM	(174)	(175)
trypanothione	NA	0.1-0.3mM		(152)
glutathione	1-5μM	0.2-1mM	(176)	(152)
TLF-1	~20nM	NA	(177)	
TLF-2	~12nM	NA	(177)	
H_2O_2	<1μM variable	<1μM	(178)	(150)
K^+	3.5-5mM	120mM	(179)	(170)
Cl^-	96-106mM	110mM		(170)
HCO_3^-	22-29mM	?	(180)	
Na^+	136-145mM	14mM		(170)
Ca^{2+}	2.1-2.7mM	70nM		(181)
Zn^{2+}	11-20μM	2mM		

H^+	pH 7.4	pH 7.4		(182)

The plasma membrane potential varies between the bloodstream form and the procyclic forms of the parasites. Procyclic parasites experience larger fluctuations to extracellular ion concentrations in the fly midgut and have robust mechanisms to maintain plasma membrane potential under different extracellular ion conditions. Bloodstream form *T. brucei* reside in the relatively constant environment of the mammalian bloodstream and are more sensitive to environmental changes than procyclic parasites. The membrane potential of bloodstream trypanosomes is depolarized by ice-cold temperatures, low pH or H^+-ATPase inhibitors, the Na^+ -ATPase inhibitor oubain, and potassium ionophores (171). There is conflicting data about whether high external potassium ion concentration cause spontaneous depolarization of bloodstream form *T. b. brucei* (170, 171, 183, 184).

Endogenous Channels at the Plasma Membrane of *T. b. brucei*

If ApoL1 forms a cation channel at the plasma membrane of *T. b. brucei,* endogenous plasma membrane channels will likely respond to the change in ion flux by activation or de-activation. Only a small proportion of the repertoire of channels regulating the plasma membrane potential, pH, and responses to osmotic stress have been studied in trypanosomes. Table 1.2 and Figure 1.14 depict some of the plasma membrane channels in *T. b. brucei* and available data on their functions.

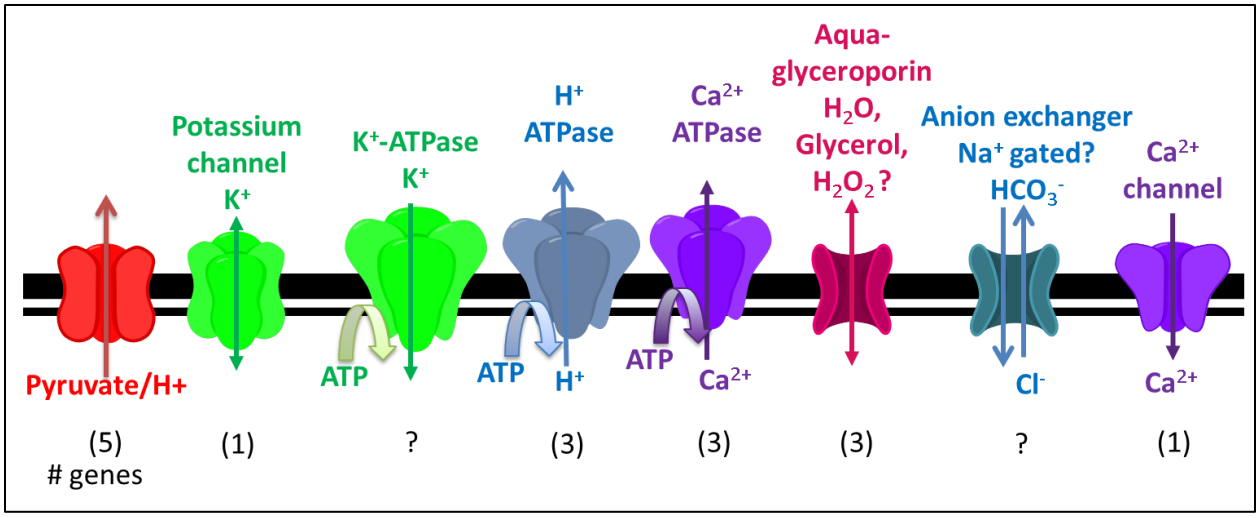

Figure 1.14: **Plasma Membrane Channels in *T. brucei***. The number of annotated genes per channel type is indicated below the schematic in parenthesis. The cartoons are not drawn to represent structural data.

The cytosolic pH of bloodstream form *T. brucei* is more sensitive to changes in the external environment than procyclic pH. The internal pH of bloodstream parasites may shift due to changes in extracellular pH, chlorine ion concentration, sodium ion concentration, glucose concentration, pyruvate concentration, and protonophores (182). The internal pH is regulated largely by pyruvate efflux. Because bloodstream form *T. brucei* rely on glucose metabolism rather than mitochondrial respiration for energy, they produce high concentrations of the metabolic end-product pyruvate. Export of pyruvate from the cytosol is essential for survival in *T. b. brucei* (175, 185). Blocking pyruvate export causes a rapid intracellular build-up of pyruvate, inhibition of glycolysis, cytosolic acidification, osmotic swelling, and cell lysis (175).

The chloride channel inhibitor DIDS may also inhibit monocarboxylate transporters such as pyruvate transporters (186). Therefore, it is possible that DIDS reversibly inhibitions the trypanosome pyruvate transporter. DIDS has been shown to

prevent lysis of *T. b. brucei* following ApoL1 treatment (15). Cytosolic acidification initiated by DIDS inhibition of pyruvate channels could inhibit ApoL1 pH gated channel activity, ameliorating lysis through a chloride-independent mechanism.

Trypanosomes are assumed to have DIDS-sensitive chloride channels in their plasma membranes. Unusual for eukaryotes, the chlorine concentration in bloodstream form trypanosome was measured to be similar to the extracellular chloride concentration, so it unclear whether the concentration gradient of chloride favors influx or efflux of chloride ions (170). Trypanosomes, like lymphocytes, may have a sodium-dependent chloride bicarbonate antiporter (187). In trypanosomes, one group found that bicarbonate channels are not important regulators of internal pH (182). However, another group found that DIDS treatment lowers the cytosolic pH of DIDS-treated *T. b. brucei,* and that DIDS-mediated acidification was rescued by the addition of bicarbonate to the media (182). If the ApoL1 channel insertion into the plasma membrane of *T. b. brucei* activated a chloride-bicarbonate antiporter, then an efflux of chlorine and an influx of bicarbonate would raise the internal pH. DIDS treatment of TLF-1 treated *T. b. brucei* would prevent bicarbonate influx resulting in internal acidification, perhaps decreasing ApoL1 pH gated channel activity and inhibiting lysis.

Table 1.3: **Plasma Membrane Channels in T. brucei**. Proven and putative [plasma membrane channels in T. b. brucei are listed with the gene annotation in 927 T. b. brucei cells, and experimental evidence for the channels. BSF stands for blood stream form *T. brucei,* PCF stands for procyclic form *T. brucei*

Plasma Membrane Channel	Gene(s) (Tb927)	Experimental evidence	Citation
Chloride channel(s)	unknown	DIDS saves cells from TLF lysis. 500μM DIDS lowers the cytoplasmic pH in BSF	(15, 182, 186)
Potassium channel	TbHKT1	In BSF no RNAi phenotype in low or normal K^+	(184)

	10.4300		
H^+-ATPase	TbHA1-3 10.12500, 10.12510 ?	RNAi of all 3 genes in BSF show a growth defect by 24 hours, 1&3 RNAi or only 2 RNAi slowed growth. Surface localized.	(188)
Pyruvate exporter (H+/pyruvate symporter)	TbTP1-5 3.4070,4080,4090,4100,4110	RNAi is lethal to BSF. Genes more upregulated in BSF than PCF. Also transports acetate & lactate. Plasma membrane localization.	(185)
Na+/K+-ATPase	?	Inferred from ouabain-induced plasma membrane depolarization.	(171)
K+-ATPase	TBCA1 9.15260	Related to yeast; no phenotype in RNAi (Annotated as Ca^{2+}-motive)	(170, 189)
Ca2+-activated K+ channel	CAKC 9.4820 and 1.4450	Putative.	(190)
Ca^{2+}ATPases	8.1160,8.1180, 8.1200	RNAi of PMC2 (8.1200 in Tb427 cells) leads to growth arrest. No difference in cytosolic Ca^{2+} in RNAi in PCF	(191)
Ca^{2+}channel	Tb927.10.11620 putative	Calcium influx from the buffer stimulated by amphiphilic peptides. Calcium influx prevented after depolarization of plasma membrane potential with gramicidin D.	(181, 190)
Volume-activated neutral amino acid channel	?	Inferred based on neutral amino acid efflux in response to hypo-osmotic stress.	(192)
Aqua-glyceroporin 1	6.1520	Flagellar membrane localization.	(193-195)
Aqua-glyceroporin 2	10.14160	Flagellar pocket localization. Facilitates uptake of pentamdine and melarsoprol. Associated with drug resistance in the field.	
Aqua-glyceroporin 3	10.14170	Plasma membrane localization.	

Trypanosome Volume Regulation under Osmotic Stress

Osmotic swelling of TLF-1 treated *T. b. brucei* is important to the lytic mechanism. Therefore, in this section we will investigate the osmotic stress responses of *T. b. brucei.* ApoL1 ion channel formation at the plasma membrane exhibits both similarities and differences to hypotonic stress conditions as described in my research in later chapters.

Unlike related kinetoplastids, *T. b. brucei* lack a contractile vacuole organelle for osmoregulation. African trypanosomes utilize signaling and energy storage from small

acidic organelles called acidocalcisomes for osmoregulation. Millimolar levels of polyphosphate fills the acidocalcisomes, presumably as a reservoir for energy storage. The negatively charged phosphates are balanced by high concentrations of cations, especially calcium, zinc, and magnesium in acidocalcisomes (196, 197). Active proton transporters in the acidocalcisome membrane keep the internal pH acidic and the internal calcium concentration high. Some of the transporters harness energy from the abundant pyrophosphatases in the organelle rather than ATP (191). Rapid hydrolysis of polyphosphate (especially long chain polyphosphate) accompanies the short-term cellular response to hypo-osmotic stress in *Trypanosoma cruzi* (198).

Regulatory volume decrease (RVD) following hypo-osmotic stress allows kinetoplastid parasites to quickly reach a steady state volume after initial swelling due to water influx. Efflux of neutral and negatively charged amino acids through volume sensitive channels is critical for RVD (199). In the trypanosomatid *Crithidia*, hypo-osmotic amino acid efflux can be inhibited by the thiol-binding inhibitor NEM, which among other substrates is known to inhibit H^+-ATPases in trypanosomes (192). An efflux of inorganic ions is important for osmoregulation, with cells losing internal chlorine, sodium, and potassium quickly during hypo-osmotic stress (196). Another hallmark of hypo-osmotic stress is calcium influx, which in *T. cruzi* enters the cytosol from the extracellular milieu rather than from intracellular calcium stores (199).

Calcium signaling is important in trypanosomes, and especially for their response to osmotic stress (190). Most of the cellular calcium is stored in acidocalcisomes. Calcium is released from acidocalcisomes following binding of IP3 to an acidocalcisome resident IP3 receptor (200). Intracellular calcium can mediate signaling between the

plasma membrane, the ER, and the mitochondria via IP3, calcium-binding proteins, and calcium transporters and channels (190).

There is a steep concentration gradient in calcium between the parasite cytosol and the external environment which is maintained by Ca^{2+}-ATPases (190). Arachidonic acid, the product of phospholipase A2 (PLA2), stimulates calcium influx from the external media into bloodstream form parasites (201). Calcium up-regulates PLA2 activity, increasing production of arachidonic acid (201). Conversely, the short chain saturated fatty acids myristate and palmitate inhibited PLA2-induced calcium influx (201). These signaling cascades may regulate the influx of calcium in osmotically stressed trypanosomes.

Aquaporins allow the passive diffusion of water into cells for osmotic regulation. Trypanosomes have three aquaglyceroporins (AQP) which are non-essential under isotonic conditions. Their localization differs, with AQP1 in the flagellar membrane, AQP3 in the plasma membrane, and AQP2 in the flagellar pocket. AQP2 has a unique more open selectivity filter allowing it to transport a range of substrates, including the clinically important drugs pentamidine and arsenical drugs. In field isolates of melarsoprol resistant *T. b. gambiense*, chimeric AQP2/3 mutations were found which prevent drug uptake by modifying the selectivity filter (119, 202).

In addition to transporting water molecules, aquaporin pores facilitate transport of other molecules, and commonly act as channels for hydrogen peroxide signaling (203). This represents one overlap between osmotic and oxidative stress in trypanosomes. In chapter two of this dissertation, I show that hydrogen peroxide makes *T. b. brucei* extremely sensitive to osmotic stress, perhaps reflecting some uptake through

aquaporins. However, ROS were not higher in trypanosomes treated with hydrogen peroxide under hypotonic stress than under normotonic conditions (47). Thus, differential opening of aquaporins during osmotic stress probably does not mediate increased hydrogen peroxide influx.

TLF AND APOL1 IN HUMAN BIOLOGY

As apolipoprotein complexes involved in innate immunity, the TLFs have roles beyond killing trypanosomes. In the human body, ApoL1 provides protection against HIV and variants of ApoL1 are linked to increased kidney disease risk. Under certain laboratory conditions, ApoL1 has been shown to induce cell death in human cells, though the mechanisms of toxicity are elusive and complex. My studies of trypanosome lysis due to ApoL1 may also give insight into the mechanisms of ApoL1-associated pathology in humans. The fourth chapter of this dissertation is a minireview comparing the plasma membrane models for ApoL1 lysis of trypanosomes and human kidney cells.

TLF and HDL Biogenesis

Understanding the biogenesis of the TLFs is important for understanding their diverse roles in human health. The biogenesis of HDL subspecies is a relatively new area of investigation (204). In fact, TLF-1 is one of the most well characterized sub-classes of HDLs, making TLF-` a great model for studying HDL biogenesis. There is no evidence for protein-protein interactions dictating the congregation of Hpr and ApoL1 in

the same class of HDL particles. Rather, biophysical interactions with the lipid bilayers seem to dictate the insertion of Hpr and ApoL1 into the same HDL particles (28, 29).

HDL particles arise from apolipoproteins secretion in the liver. Apolipoprotein A1 (ApoA1) are populated with a small number of lipids and free cholesterol molecules extracellularly with the aid of the membrane transporter ABCA1 (205). The resulting discoidal particles, termed pre-β HDLs, circulate in the serum, collecting free cholesterol from macrophages. Maturation to spherical HDL particles requires the esterification of the free cholesterol in the pre-β HDLs by lecithin-cholesterol acyltrasferase (LCAT), and increased lipidation via lipids transferred from very low density lipoprotein particles (VLDL). Eventually, mature HDLs return to the liver and transfer cholesterol to the hepatocytes via the hepatocyte receptor SR-BI.

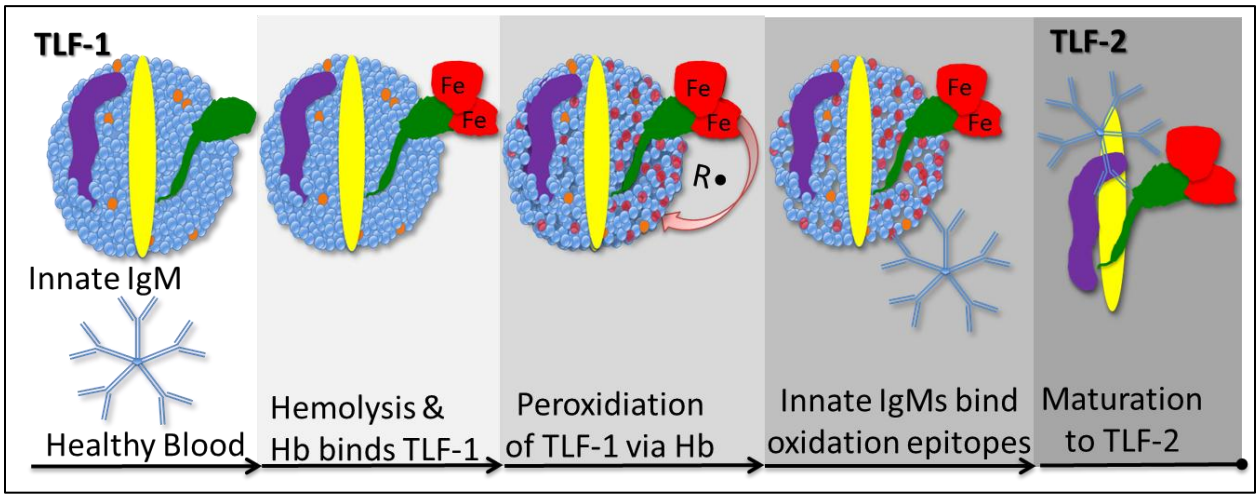

Figure 1.15**: Model for Biogenesis of TLF-2 from Peroxidized TLF-1**. In the human bloodstream hemolysis leads to Hb binding to Hpr on TLF-1. Over time, Hb catalyzes peroxidation of local TLF-1 lipids and proteins. Oxidation epitopes such as malondialdehyde are recognized by innate IgM molecules. Following IgM binding, the TLF-1 molecule loses lipid and matures into a mature TLF-2 molecule. Hpr is represented by the green cartoon, Hb by red cartoons (with Fe inside), apolipoprotein A1 by the yellow oval, ApoL1 by the purple cartoon, and IgM by the blue snowflake

shape, R● represents ROS peroxidation of the TLF-1 lipids (blue circles which turn red when peroxidized).

TLF-1 is an HDL, but TLF-2 is a poorly defined lipid-poor ApoA1 containing molecule. The relationship between the biogenesis of TLF-1 and the lipid-poor TLF-2 has not been defined. One possibility is that TLF-2 represents a unique form of pre-β HDL which serves as the precursor for TLF-1. However, the presence of IgM molecules in TLF-2 and not in TLF-1 is not consistent with the hypothesis that TLF-2 precedes TLF-1 because no mechanism for IgM removal (retaining particle integrity) is known. Therefore, I proposed a model where TLF-1 oxidation leads to the formation of TLF-2 in the bloodstream.

Figure 1.15 illustrates my proposed model for TLF-2 biogenesis from TLF-1. Firstly, hemolysis causes Hb dimers to bind to TLF-1. In the bloodstream, hemolysis releases free Hb dimers to bind to both Hp and Hpr (in TLF-1). While HpHb is rapidly cleared from the serum, HprHb is not cleared because it doesn't bind to the CD163 macrophage receptor (42). Consistent with the retention Hb-bound TLF-1 in the bloodstream, patients with chronic hemolysis (paroxysmal nocturnal hemoglobinuria and Tangier disease) have normal levels of Hpr and depleted levels of Hp in circulation (30, 206).

Preliminary data demonstrated that Hb can induce TLF-1 self-peroxidation under mild (neutral pH, low μM H_2O_2) conditions (Allen Witt, data not shown). Therefore, while circulating in the blood, Hpr-Hb induces TLF-1 lipid and protein peroxidation. Oxidative damage epitopes on TLF-1 such as malondialdehyde are then recognized by circulating innate IgMs. IgM molecules against oxidation-specific epitopes such as malondialdehyde are common soluble IgMs, many of which are developed *in utero* to

non-pathogenic self-targets; for this reason many oxidation-specific IgMs have germline-derived variable sequences (207, 208). One well-studied commercially available mouse IgM, E06, binds specifically to oxidized HDL and LDL (209). Some studies suggest that IgM-binding to oxidized LDL (or HDL) is anti-inflammatory and that IgM-coated oxidized LDL are not cleared via macrophages (210). The LDL data may explain how the TLF-2 pool accumulates without being quickly cleared from the circulation. Finally, through peroxidative damage and interaction with cells and serum factors, the TLF-Hb-IgM complex loses its lipid and cholesterol components, maturing into a steady-state pool of TLF-2.

ApoL1 Variants Associated with Kidney Disease

In 2010, a group published in the journal *Science* that kidney disease risk is increased in African Americans carrying variant alleles of ApoL1 (211). That publication grabbed the attention of researchers outside of the trypanosome community, and led to investigations into the role of ApoL1 in human diseases, including various kidney conditions, heart disease, and HIV infection (see Figure 1.16). Consequently, the number of papers published on ApoL1 have ballooned in the five few years since the genomic link to kidney disease was published (see Figure 1.17). The effects of ApoL1 on variants on various cell types in humans are only beginning to be understood, with less mechanistic understanding than for the effects of ApoL1 on trypanosomes.

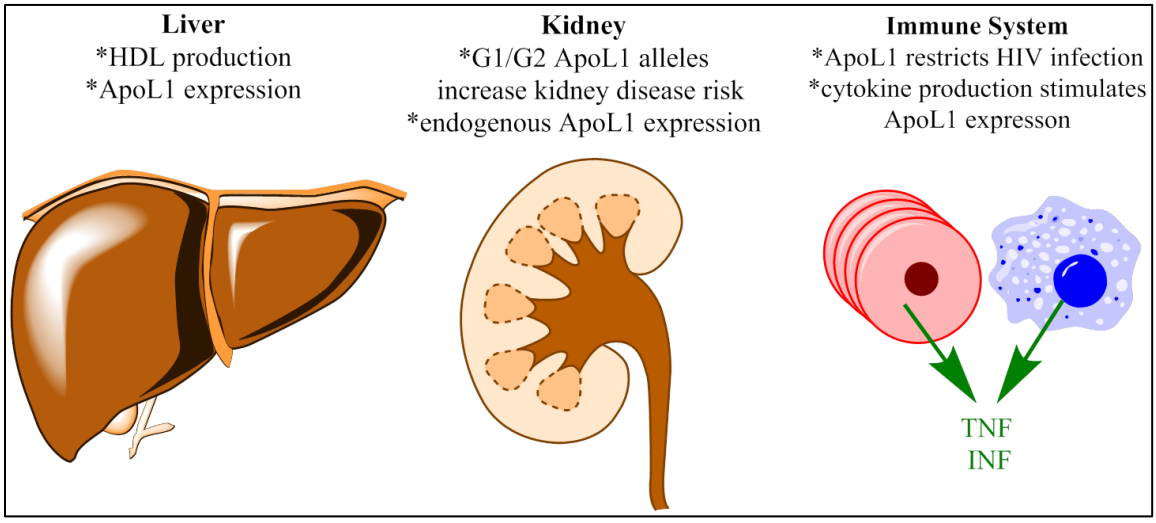

Figure 1.16: **Human Tissues Associated with TLF-1/ApoL1 Activity**. TNF: tumor necrosis factor. INF: interferons (may be α, β, or γ).

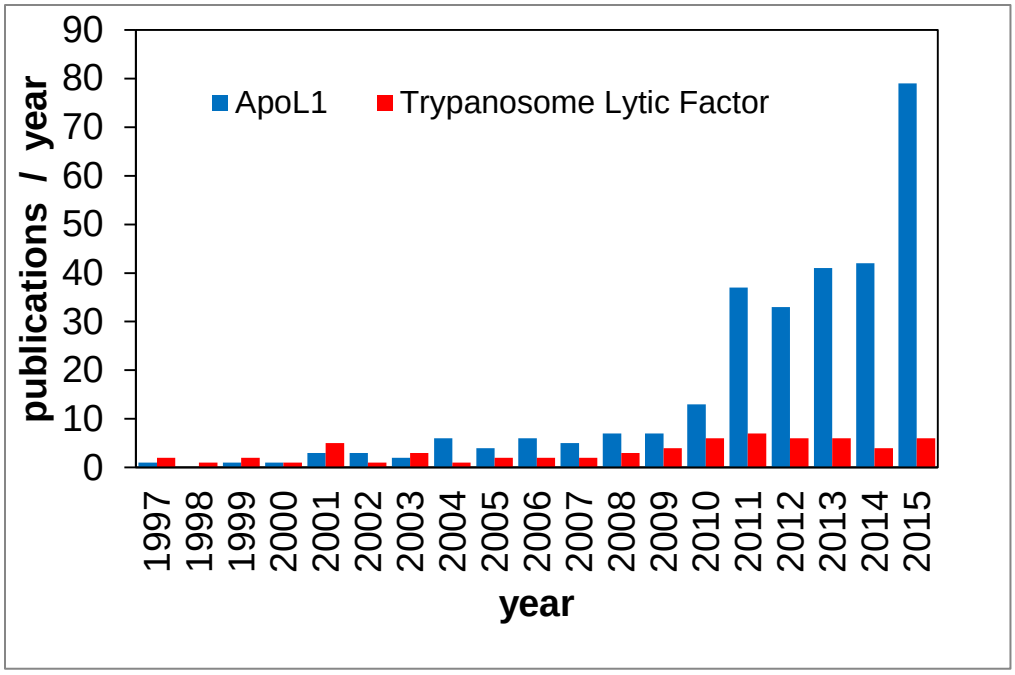

Figure 1.17: **ApoL1 Publications in PubMed.** This graph depicts the number of publications using the term “Trypanosome Lytic Factor” (red bars) or the term “ApoL1” (blue bars) in the title or abstract.

Kidney disease risk is higher among those of African ancestry partially because of common polymorphisms in the ApoL1 gene. The G1 allele encodes for ApoL1 with two amino acid substitutions in the C-terminal SRA-binding domain of ApoL1. The G2 allele is a 6 nucleotide (2 amino acid) deletion also in the SRA-binding domain of ApoL1. Due to their proximity in the same gene, the G1 and G2 mutations are always found on separate chromosomes. These two alleles are the only ApoL1 alleles consistently linked statistically with kidney disease (212). In a population-wide study, non-diabetic African Americans had nearly a 4-fold greater risk of chronic kidney disease if they carried two ApoL1 variant alleles (213). Interestingly, while ApoL1 mutations are deleterious, ApoL1 null people exist, and a small study of individuals with 1-2 null alleles for ApoL1 did not show an increased risk of kidney disease suggesting

that the presence of mutant ApoL1, not the absence of functioning ApoL1 is responsible for increased kidney disease risk (214).

A causative role for ApoL1 in disease pathology and progression is not well established. In fact, ApoL1 mutations could represent genetic markers obscuring more functionally important genes which may have hitchhiked in the same human populations. The presence of ApoL1 risk variants are associated with global changes in HDL profiles, increasing indirect risk factors for kidney diseases (215). The expression patterns of ApoL1 may also change in those with variant alleles or those with kidney disease. In kidneys with G0 (normal) ApoL1, most protein is localized in the kidney podocytes, however in people with risk alleles, ApoL1 seems to expand into epithelial and muscle tissue (216, 217).

For people expressing G1/G2 alleles, the lifetime risk of kidney disease is low. ApoL1-associated pathology probably requires a “second hit” from an infection such as HIV or pathogen which causes increased ApoL1 expression (218-220). Supporting this idea, 7 patients who received interferon treatment (for unrelated conditions) and later developed end-stage kidney disease (focal segmental glomerulosclerosis, FSGS) had two ApoL1 risk alleles (219). Interferons up-regulate ApoL1 expression in multiple organs including the liver (219, 221, 222).

It is unclear whether circulating HDL-associated ApoL1 or ApoL1 endogenously expressed in kidney cells is responsible for kidney disease. There are several lines of evidence that favor ApoL1 expression in the kidney as the source of disease. First, the lifetime of a kidney transplant is significantly shorter if the donated kidney carries 2 ApoL1 risk alleles (223-225). Secondly, a genetic study showed no correlation between

circulating ApoL1 levels and chronic kidney disease in African Americans (226). Thirdly, in a mouse model of ApoL1-induced liver necrosis, deletion of the signal peptide for ApoL1 excretion did not prevent necrosis, indicating that endogenously expressed ApoL1 may be responsible for tissue damage (227).

Within the kidney, ApoL1 variants may be excreted and cause damage to neighboring cells in a paracrine manner. One study measured ApoL1 protein levels in human kidneys that was higher than expected due to intracellular synthesis (216). Cultured podocytes internalize exogenous HDL-free ApoL1 media (216). HDL particles are reportedly too large to cross the kidney's glomerular filtration barrier, so the authors argued that a proportion of ApoL1 circulates independent of HDL particles and that HDL-free ApoL1 is internalized by podocytes (216).

Mechanism of ApoL1-Induced Damage to Human Cells

Chapter four of this dissertation is a short mini-review comparing the plasma membrane models for ApoL1 lysis of both human kidney cells and trypanosomes. Here, different models for ApoL1 variant-induced human cell death will be discussed in more detail (see Figure 1.18). The mechanism of ApoL1 variant-induced cell death in mammalian cells is understood less than in *T. b. brucei*. There is no consensus about the mode of ApoL1 uptake, the origin of ApoL1-induced damage, or whether programmed cell death occurs.

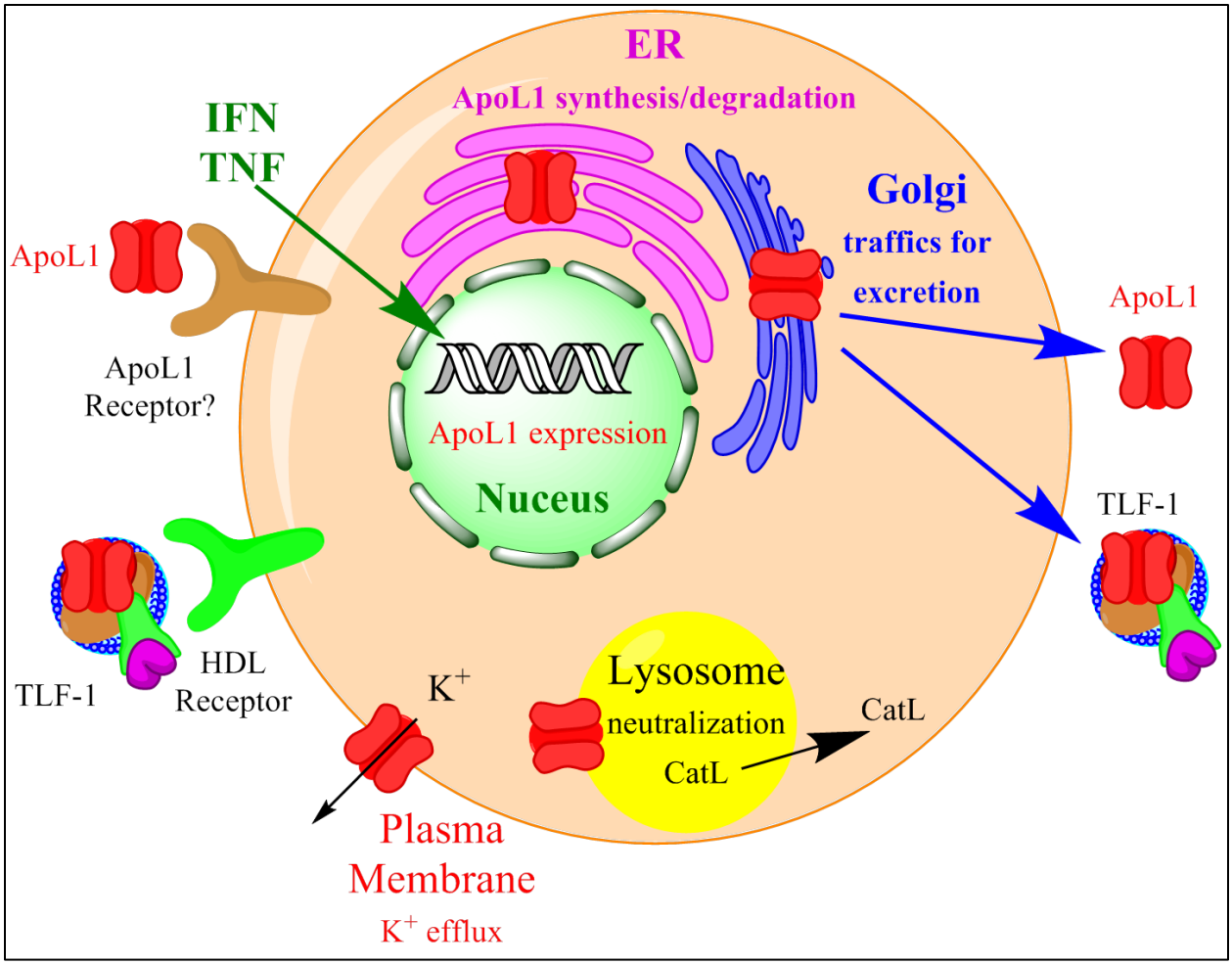

Figure 1.18: **Various proposed mechanisms of ApoL1 variant toxicity to human cells.** ApoL1 enters the cell either through endogenous expression stimulated by interferons (IFN) or tumor necrosis factor (TNF), or through uptake mediated by HDL receptors or other uncharacterized ApoL1 receptors. Over-expressed ApoL1 and ApoL1 variants may accumulate in the endoplasmic reticulum (ER) or the golgi during excretion. Internal ApoL1 may traffic to the lysosome where it is proposed to mediate neutralization of lysosomal pH, and lysosomal permeabilization leading to release of cathepsin L and downstream cell death signaling. Internal ApoL1 variants may alternatively traffic to the plasma membrane where they may mediate efflux of K+ and downstream stress signaling. G1 and G2 alleles of ApoL1 are associated with toxicity, while G0 ApoL1-associated toxicity is rarely observed.

Following the trypanosome literature, lysosomal phenotypes were sought and observed in ApoL1-treated kidney cells. The G1 and G2 alleles of ApoL1, and to a lesser extent the normal G0 allele, induced lysosomal damage membrane breakdown in

podocytes and vascular smooth muscle cells (228, 229). ApoL1-induced lysosomal damage was measured by release of the lysosomal dye Lucifer yellow and cathepsin L into the cytoplasm, and quenching of lysotracker dye fluorescence, indicating loss of lysosomal acidity (228, 229). Their proposed model was that under inflammatory conditions vascular smooth muscle cells express high levels of ApoL1. Secreted ApoL1 is subsequently taken up by neighboring podocytes, causing lysosomal damage, necrosis, and kidney disease (229). In contrast to the lysosomal damage caused by ApoL1 in podocytes, in human embryonic kidney (HEK) cells and *Xenopus* oocytes ApoL1-induced cytotoxicity was not rescued by addition of the pH neutralizing agent chloroquine or other lysosomal disruptors (19, 230).

Autophagy is the most published type of programmed cell death initiated by ApoL1 in human cell lines (222, 231, 232). It is unclear whether autophagy is initiated by signaling via the BH3 cell death domain sandwiched within its pore-forming domain, or as a result of ion channel formation (19, 222, 228). One study showed that deletion of the BH3 domain prevented ApoL1-induced autophagy in various cancer cell lines, but the BH3 domain deletion may have disrupted ApoL1 structure and pore-formation ability (232). In an HEK cell line, the BH3 domain of ApoL1 was required for cell damage, but the signal peptide for excretion was dispensable (233). In colorectal cancer cell lines, ApoL1 addition caused LC3-II recruitment to autophagic vacuoles (232). The addition of the autophagy inhibitors 3-methyl adenine and wortmannin prevented ApoL1-indcued autophagic cell death (232). Similarly, mouse fibroblast lines where Atg5 or Atg8 were knocked out did not experience ApoL1 toxicity (232). ApoL1-induced autophagic cell death is not observed by all researchers. For instance, in ApoL1-expressing HEK cells

and *Xenopus* oocytes cell death was not via classical autophagic cell death (19, 230, 234).

Apoptosis or related cell death pathways may be initiated by ApoL1. In G1 ApoL1 variant expressing hepatocytes, one group found increased annexin-V staining in dead cells, suggesting that cell death may be apoptotic (231). In their study, caspase I inhibition also prevented ApoL1-induced cell death, implicating pyroptosis as another potential cell-death pathway induced by ApoL1 (231).

The complexity of kidney disease development in humans makes it difficult to design appropriate cell culture experiments to investigate pathogenesis. For instance, immortalized podocyte cells express lower ApoL1 levels than endogenous human kidney cells (216). One study showed that while transgenic mice expressing ApoL1 efficiently excreted ApoL1 into HDL particles, several cultured primary and immortalized cell lines inefficiently excreted ApoL1 (231). They found that ApoL1 accumulated in the ER was subsequently degraded in the proteasome, and it is not clear whether this aberrant build-up of protein was responsible for the observed toxicity in cell culture (231).

It is not known whether differently processed forms of ApoL1 play a role of pathology. Different transcriptional or post-transcriptional forms of ApoL are commonly observed and their number and abundance increase in the context of overexpression (219, 230, 235). The different sized bands observed on Western blots are often dismissed as artifacts. One study found that only splice variants of ApoL1 containing N-terminal regions encoded by exon 4 induced autophagy in HEK cells (230). Thus, differences in cell death phenotypes observed in human and trypanosomes cell lines

may be linked to differences in the splice variant of ApoL1 which is expressed. Also, the leucine zipper motif in SRA-binding domain of ApoL1 may have direct roles in gene modulation which have never been investigated.

For investigations of external ApoL1 addition, recombinant ApoL1 is difficult to express and purify due to toxicity to the overexpressing cell, lack of efficient excretion, and low solubility when not HDL-associated. Moreover, the way that recombinant ApoL1 is applied to cells may affect its uptake. In some studies, ApoL1 is introduced in serum-containing media or in the supernatant of ApoL1 over-expressing cells, which allows ApoL1 association with HDLs, as opposed to addition of de-lipidated ApoL1 (216, 228). In human blood, most circulating ApoL1 is found in Hpr-containing TLF particles, which are not routinely purified for use in human toxicity studies.

A recent publication invoked a model where ApoL1 variants induce osmotic stress at the plasma membrane, reminiscent of the osmotic model for trypanosome lysis (234). Their work was done in HEK cells overexpressing ApoL1. In HEK cells, the export of potassium rather than the import of sodium was required for cell death, suggesting that ApoL1 channels act as a potassium importer, disrupting ionic gradients at the plasma membrane. Only HEK cells overexpressing the G1 or G2 variants of ApoL1, but not the G0 allele, experienced cell swelling, stress-activated kinase signaling, and cell lysis. Other studies support ApoL1-induced osmotic swelling in human cell lines. In podocytes, ApoL1-induced cytoplasmic swelling which was rescued by the chlorine channel inhibitor DIDS (228, 229). The osmotic stress model of lysis for kidney cells are compared to the plasma membrane model of trypanosome lysis in a review article as the 4th chapter of this dissertation.

In conclusion, recent studies from human genetics and cellular assays have yielded insights into diverse ApoL1-associated immune functions. However, there are far more questions than answers, and new results often complicate the biological story rather than clarify the roles of ApoL1 in humans. There is a paucity of mechanistic biochemical basis for ApoL1 toxicity. It is unclear how and where in the cells ApoL1 forms an ion channel and how the majority of ApoL1 expressing cells protect themselves from damage. In the long-term context of kidney disease, ApoL1 variants may shift immune signaling through genetic mechanisms unrelated to ApoL1 ion channel formation. The structural differences between G1/G2 variants and their effects on protein function have not been adequately addressed (236). It also unknown how circulating ApoL1 levels shift in response to different disease states. As interest in ApoL1 research continues to expand, fascinating answers to many of these questions should emerge.

Other Roles for ApoL1 in Human Innate Immunity

Other roles for ApoL1 in innate immunity are just beginning to be recognized though few mechanistic details have been worked out. People carrying two ApoL1 risk alleles have an approximately 2-fold increased risk for heart disease and stroke (237). But not all the associations are negative. G1 and G2 ApoL1 alleles are associated with a lower risk of atherosclerosis and type two diabetes in African Americans compared to those with normal G0 ApoL1 (238).

In addition to killing *T. b. brucei,* TLFs may restrict the growth of other human pathogens. The disease Leishmaniasis is caused by a group of kinetoplastids

(*Leishmania sp.*) which are somewhat susceptible to TLF-1 lysis. Unlike *T. b. brucei, Leishmania* parasites reside in macrophages. Within the acidic environment of the macrophage phagosome, ApoL1 is postulated to form pores in the outer membrane of the parasite without a requirement for TLF-1 endocytosis (239).

ApoL1 is an anti-viral restriction factor induced in response to innate immune signals (240). Interferon (α, β, or γ) and certain toll-like receptor agonists (TLR3 and TLF4) upregulate ApoL1 expression in both podocytes and endothelial cells (219, 221, 228). Up-regulation of ApoL1 mRNA was associated with the binding of TLF3-stimulated transcription factors IFN-regulator factor 1 and 2 (IFN1, IFN2) (219). In addition to interferons, the inflammatory cytokine tumor necrosis factor alpha (TNFα) has been shown to induce ApoL1 expression (222). The mechanism of ApoL1-associated viral restriction has not been extensively investigated. One paper found that ApoL1 promotes the degradation of HIV proteins in lysosomes, and that ApoL1 increases excretion of the HIV accessory protein Vif (221).

CONCLUSION

TLF-1 is an HDL particle unique to primates which is able to efficiently prevent infection by *T. b. brucei* parasites. TLF-1 rapidly lyses *T. b. brucei*, while human-infective *T. b. rhodesiense* and *T. b. gambiense* have evolved resistance to human serum. The mechanism of lysis remains controversial, but requires TLF-1 endocytosis into the parasite, and ion channel formation by the lipoprotein ApoL1.

Chapters two and three of this work build a model ApoL1-induced osmotic lysis of *T. b. brucei.* Chapter two, entitled, “Trypanosome Lytic Factor-1 Initiates Oxidation-stimulated Osmotic Lysis of *Trypanosoma brucei brucei*” is a published manuscript in

the *Journal of Biological Chemistry* (47). The paper gives evidence against the lysosomal model for Hpr-Hb initiating peroxidative damage. Rather, thiol oxidation associated with ApoL1 may exacerbate and osmotic swelling of *T. b. brucei*. Chapter three, entitled "ApoL1 induces a loss of plasma membrane potential leading to osmotic lysis of *Trypanosoma brucei brucei"* expands on the plasma membrane model for ApoL1-induced lysis, showing that TLF-1 causes a rapid loss of plasma membrane potential which leads to cell swelling and lysis.

Chapter four sums up the conclusions from previous chapters with a short review article comparing the mechanisms of lysis between trypanosomes and human kidney cells. The review is a hypothesis piece entitled, "ApoL1 toxicity to humans and trypanosomes: could ApoL1-induced osmotic stress at the plasma membrane initiate cell death?" The thesis will conclude with a short overview of the mechanism of TLF-1 induced lysis of *T. b. brucei* based on my work. Overall, my research has contributed mechanistic insights into vulnerable aspects of *T. brucei* biology which the human immune system evolved to attack.

CHAPTER 2

TRYPANOSOME LYTIC FACTOR-1 INITIATES OXIDATION-STIMULATED OSMOTIC LYSIS OF *TRYPANOSOMA BRUCEI BRUCEI*[1]

[1] Greene, A.S., and Hajduk, S.L. 2016. Journal of Biological Chemistry. 291:3063-3075. Reprinted here with permission of the publisher.

ABSTRACT

Human innate immunity against the veterinary pathogen *Trypanosoma brucei brucei* is conferred by trypanosome lytic factors (TLFs), against which human-infective *T. b. gambiense* and *T. b. rhodesiense* have evolved resistance. TLF-1 is a subclass of high density lipoprotein particles defined by two primate specific apolipoproteins: the ion-channel forming toxin apolipoproteinL1 (ApoL1), and the hemoglobin (Hb) scavenger haptoglobin related protein (Hpr). The role of oxidative stress in the TLF-1 lytic mechanism has been controversial. Here we show that oxidative processes are involved in TLF-1 killing of *T. b. brucei*. The lipophilic antioxidant DPPD protected TLF-1 treated *T. b. brucei* from lysis. Conversely, lysis of TLF-1 treated *T. b. brucei* was increased by addition of peroxides or thiol-conjugating agents. Previously, the Hpr-Hb complex was postulated to be a source of free radicals during TLF-1 lysis. However, we found that the Fe-containing heme of the Hpr-Hb complex was not involved in TLF-1 lysis. Furthermore, neither high concentrations of transferrin nor knockout of cytosolic lipid peroxidases prevented TLF-1 lysis. Instead, purified ApoL1 was sufficient to induce lysis, and ApoL1 lysis was inhibited by the antioxidant DPPD. Swelling of TLF-1 treated *T. b. brucei* was reminiscent of swelling under hypotonic stress. Moreover, TLF-1 treated *T. b. brucei* became rapidly susceptible to hypotonic lysis. *T. b. brucei* cells exposed to peroxides or thiol-binding agents were also sensitized to hypotonic lysis in the absence of TLF-1. We postulate that ApoL1 initiates osmotic stress at the plasma membrane which sensitizes *T. b. brucei* to oxidation-stimulated osmotic lysis.

INTRODUCTION

Humans and higher primates are unable to be infected by the veterinary pathogen *T. b. brucei* because of a novel form of innate immunity mediated by trypanosome lytic factors (TLFs). Related parasites, *T. b. gambiense* and *T. b. rhodesiense,* have evolved resistance to the TLFs and cause the deadly disease human African trypanosomiasis. TLF-1 is a subclass of HDL particles defined by two primate specific apolipoproteins, apolipoproteinL1 (ApoL1) and haptoglobin related protein (Hpr). ApoliproteinL1 is an ion pore-forming protein which inserts into anionic membranes at low pH (15, 29). Haptoglobin related protein has over 95% sequence identity to human haptoglobin (Hp), a non-HDL associated acute phase serum protein (42). The primary function of Hp is to bind free Hb, preventing heme-induced oxidative damage. Like Hp, Hpr binds to Hb dimers with high affinity (42). However, while the HpHb complex is cleared from the bloodstream via the macrophage CD163 receptor, Hpr-Hb in TLF-1 is not removed from circulation by CD163 because of four amino acid substitutions in the Hp-CD163 binding site (26, 42).

A haptoglobin-hemoglobin receptor (HpHbR) located within the flagellar pocket of *T. b. brucei* binds to both HpHb and HprHb, facilitating high-affinity endocytosis of Hb-bound TLF-1 into the parasite (33, 40). Following binding to the HpHbR, TLF-1 and Hb traffic through the endolysosomal pathway. Within an acidic compartment, ApoL1 inserts into the vesicle membrane (15, 29).

Until recently, it was thought that ApoL1 inserted into the lysosomal membrane forming a chloride channel (15). However, a recent *in vitro* study of ApoL1 found a strong preference for cations (16). Surprisingly, they discovered that ApoL1 is an acid gated channel which is not active at the low pH values found in the trypanosome

lysosome (16). They proposed that after endocytosis, ApoL1 traffics through recycling endosomes to the flagellar pocket and plasma membrane, where it causes osmotic swelling of *T. b. brucei* (16). In contrast, another recent study showed that ApoL1 traffics to the mitochondrial membrane of *T. b. brucei*, inducing apoptosis-like cell death (18). Thus, the primary target organelle for ApoL1-induced lysis remains to be elucidated.

The mechanism of *T. b. brucei* cell death due to TLF-1 is disputed. An observed phenotype of TLF-1 lysis is swelling of the plasma membrane of *T. b. brucei* into a rounded “kite-shape” as shown in this paper (61, 96, 177). In contrast, one group has reported predominant lysosomal swelling induced by ApoL1 under certain conditions (15, 56). In contrast with osmotic swelling of the lysosome, TLF-1 has been shown to induce lysosomal membrane permeability to dextrans, suggesting that the lysosomal membrane breaks down following TLF-1 treatment (18, 43, 44). In fact, recently published data indicate that neither lysosomal swelling nor lysosomal membrane permeability is responsible for TLF-1 induced lysis (18).

There is plentiful evidence for TLF-1 inducing osmotic stress at the *T. b. brucei* plasma membrane. For instance, high concentrations of sucrose prevent TLF-1 lysis by preventing the influx of water into cells (57, 61). Similar to cells under hypotonic stress, TLF-1 incubation induces an efflux of potassium ions and an uptake of calcium ions in *T. b. brucei* (61). In support of ApoL1 forming a sodium channel at the plasma membrane, TLF-1 lysis of *T. b. brucei* is decreased in a sodium-free buffer (57).

The role of oxidative processes in the mechanism of TLF-1 lysis is also controversial. In favor of an oxidative mechanism of TLF-1 induced lysis, increased

lipid peroxides were observed in TLF-1 treated versus control cells (48). Also, addition of exogenous catalase or the antioxidant DPPD decreased lysis due to TLF-1 (13, 48). Within the lysosome, the Hpr-Hb complex has been proposed to act as the TLF-1 peroxidase, initiating oxidative damage to the lysosomal membrane (13, 43, 48). In contrast, another group found no evidence for peroxide formation during TLF-1 lysis (50). The research presented here addresses the origin and role of oxidative stress in TLF-1 induced trypanosome lysis. We show that Hpr-Hb mediated lysosomal lipid peroxidation is not required for killing. Rather, we propose that oxidation of free thiols in *T. b. brucei* treated with TLF-1 leads to osmotic de-regulation and osmotic lysis.

RESULTS

Thiol oxidation is involved in TLF-1 lysis

Consistent with older reports, we observed a role of oxidative stress in TLF-1 lysis (12,13,14). As shown previously, pre-loading *T. b. brucei* with the lipophilic antioxidant DPPD ameliorated TLF-induced lysis (Figure 2.1A) (48). To confirm a role for DPPD in decreasing oxidative stress to *T. b. brucei,* reactive oxygen species (ROS) in DPPD-treated cells was monitored using a fluorescent indicator DCF-DA. As expected, *T. b. brucei* treated with H_2O_2 experienced an initial increase in ROS, and DPPD addition significantly ameliorated the peroxide-induced increase in ROS (Figure 2.1B). We next investigated whether addition of peroxides to the TLF-1 treated *T. b. brucei* stimulated lysis. Consistent with a role for oxidation in TLF-1 lysis, a sub-lethal concentration of tert-butyl-hydroperoxide (+OOH) significantly increased TLF-1 lysis of *T. b. brucei* (Figure 2.1C). We next inhibited the peroxide metabolism of *T. b. brucei* using diethylmaleate (DEM) (150). Like peroxides, sub-lethal concentrations of DEM

dramatically sensitized the cells to TLF-1 killing (Figure 2.1D). These results indicate that TLF-1 induces oxidative stress to *T. b. brucei*, which may be ameliorated by antioxidants or exacerbated by pro-oxidants.

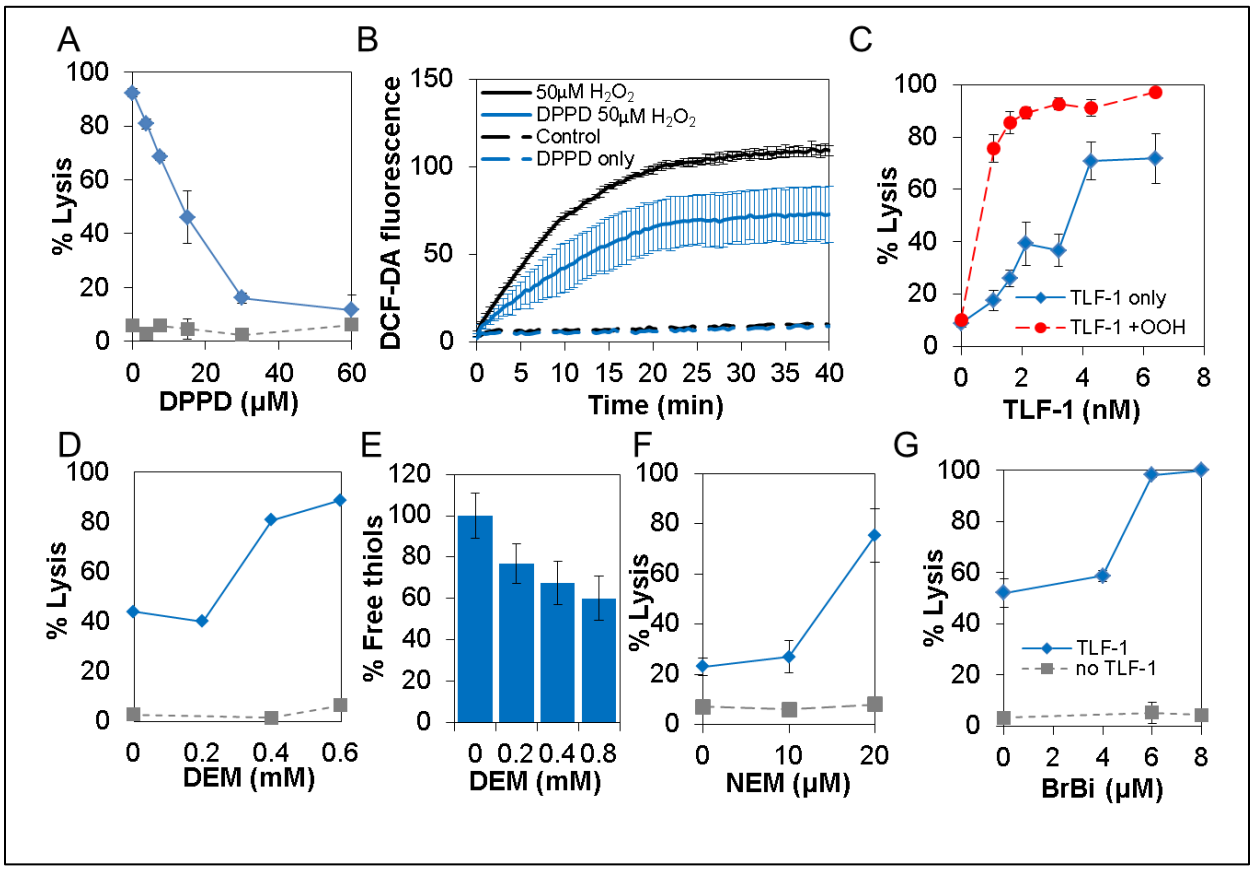

Figure 2.1: **Oxidative stress is involved in TLF-1 induced lysis**. (**A**) TLF-1 lysis assay (8.8 nM), 2 h at 37˚C following pre-incubation with DPPD (blue diamonds) for 30 min at 37˚C. No TLF-1 (grey squares). (**B**) Kinetics of ROS production measured in *T. b. brucei* pre-treated for 30 min with 30μM DPPD (blue), or nothing (black). In the indicated samples, 50 μM H_2O_2 (solid lines) or 5μL H_2O (dashed lines) was added at 0 min (solid lines). N = 4 for peroxide-treated samples with standard deviation bars, while untreated samples are in duplicate with no error bars shown. (**C**) TLF-1 lysis assay at concentrations shown on the x-axis, 2 h at 37˚C. TLF-1 treatment only (blue diamonds). TLF-1 treatment with concurrent addition of 40 μM tertbutyl hydroperoxide (+OOH) (red circles). (**D**) TLF-1 lysis assay (8.8 nM), 2 h at 37˚C with concurrent addition of diethyl maleate (DEM) (blue diamonds). No TLF-1 (grey squares). (**E**) Thiol determination assay. DEM at the indicated concentrations was pre-incubated with *T. b. brucei* for 110 min at 37˚C before thiol determination on flow cytometry. (**F**) TLF-1 lysis assay (3 nM) for 2 h at 37˚C with the indicated concentrations NEM added 1hr after TLF-1 addition (blue diamonds). No TLF-1 (grey squares). (**G**) TLF-1 lysis assay (1.7 nM) for 2 h at 37˚C with the indicated concentrations BrBi added 1hr after TLF-1 addition (blue

diamonds). No TLF-1 (grey squares). Error bars for lysis assays show standard deviations of three or four counts from one representative lysis assay.

In addition to inhibiting trypanothione-based hydrogen peroxide metabolism, DEM binds to free thiols in cells (150). A fluorescent BrBi assay was used to quantify free thiols in trypanosomes (241). DEM competed with BrBi for thiol binding, depleting total cellular free thiols by about 30% at a 0.4 mM concentration (Figure 1E). Thus, the effects of DEM may reflect thiol binding activity rather than direct effects on hydrogen peroxide metabolism.

Free thiols are some of the first targets of peroxide-induced oxidation in cells (242). To investigate the role of thiol oxidation in TLF-1 lysis, the promiscuous free thiol binding molecules BrBi and NEM were tested on *T. b. brucei* treated with TLF-1. TLF-1 lysis of *T. b. brucei* was increased by BrBi or NEM addition (Figure 2.1F and G). In the absence of TLF-1 neither BrBi nor NEM were toxic to cells (Figure 2.1F and G).

Hpr-Hb is not the peroxidase involved in TLF lysis

The Hpr-Hb complex was previously suggested to be the source of peroxides during TLF-1 lysis (13). To evaluate the role of Hpr-Hb as a peroxidase involved in TLF-1 lysis, we first determined whether Hb catalyzed peroxidation of endogenous TLF-1 lipids *in vitro* (Figure 2.2A). We measured the lipid peroxidation bi-product malondialdehyde (MDA) in TLF-1 samples incubated at low pH in the presence of H_2O_2 at 37˚C. In order to investigate the role of the heme iron in this reaction, Hb was denatured, the heme removed, and the resulting apoglobin was reconstituted with zinc protoporphyrin IX to form Zn^{2+}-globin (Zn-globin), or reconstituted with heme to form

Fe^{3+}globin (methemoglobin). Only iron-containing globins (Fe^{3+}-globin, reduced Fe^{2+}-globin, and Hb), but not reconstituted Zn-globin or apo-globin, induced TLF-1 lipid peroxidation (Figure 2.2A).

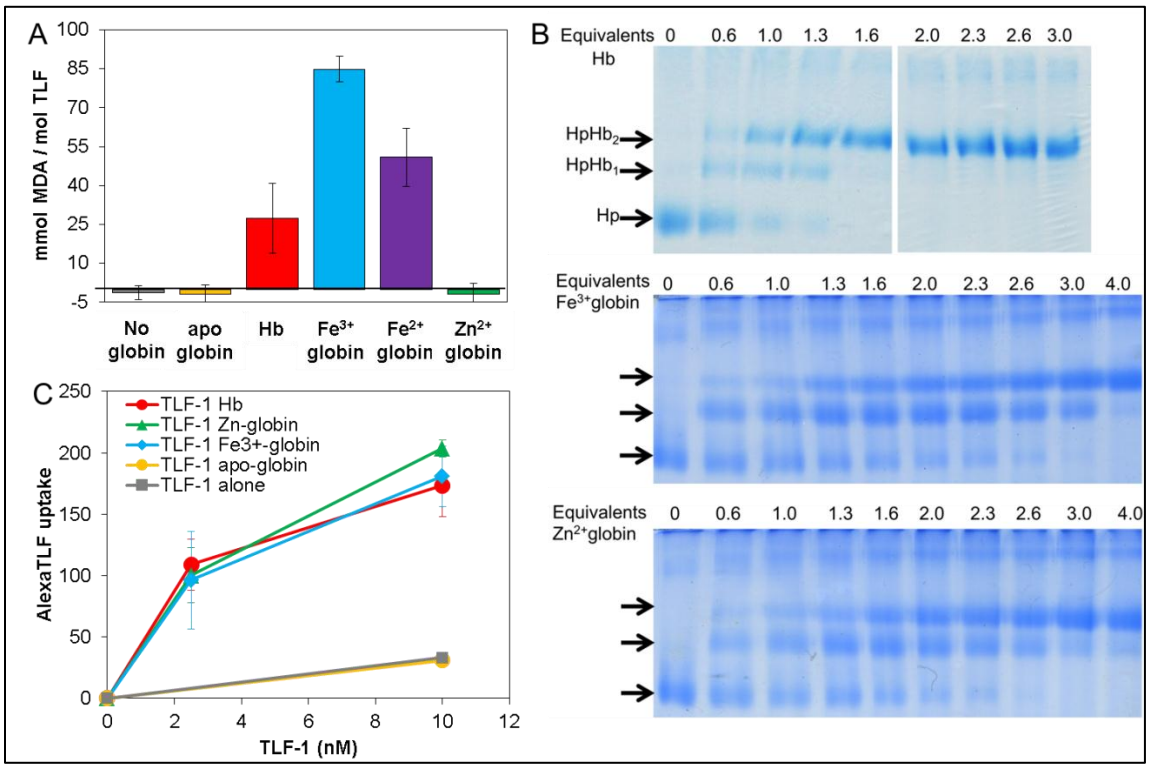

Figure 2.2: **Hemoglobin causes peroxidation of TLF-1 lipids**. (**A**) *In vitro* TLF lipid peroxidation assay. TLF-1 (125 nM) was incubated for 30 min with native Hb, or Fe^{3+}, Fe^{2+} Zn^{2+}, or apo-globin in pH 4.8 buffer with 70 μM H_2O_2. All globins except Hb were prepared from acid-acetone precipitation of globin and reconstitution with free porphyrins. Malondialdehyde production was measured by the TBARS assay. Average and standard deviation error bars are from 2 samples each from 2 independent experiments. (**B**), Native PAGE gel mobility shift assay for globin binding to Hp1-1. Representative gel. Human Hp1-1 was incubated with increasing mole equivalents of Hb, Fe^{3+}, or Zn^{2+}-globins. Brightness and contrast adjusted on each gel in Microsoft Power Point. Hb samples run on two separate gels. (**C**) Measurement of TLF-1 uptake by flow cytometry. 20 min uptake assay at 37˚C in serum free media with the indicated globin. Average of 3 independent experiments with standard deviation error bars. N = 2 for TLF-1 and apo-globin. One of the 3 replicas labeled as Hb is actually reconstituted Fe^{2+}globin.

The reconstituted Zn-globin was not as stable as the native Hb, necessitating fresh reconstitution for each set of experiments. However, binding of freshly

reconstituted Zn-globin and Fe-globin to haptoglobin1-1 (Hp) was observed by blue native PAGE, indicating that most of the Zn-globin was in the native conformation (Figure 2B). Furthermore, *T. b. brucei* efficiently bound and endocytosed Alexa488-labeled TLF-1 with Hb, or Zn-globin, or Fe-globin, through HpHbR-dependent uptake (Figure 2.2C). As expected, globin-free TLF-1 was not efficiently endoctyosed due to lack of HpHbR binding. Similarly, porphyrin-free globin was not bound and endocytosed by *T. b. brucei*. Although porphyrin free globin monomers will bind to haptoglobin, the Hp1-1 apo-globin complex is less structured than the HpHb complex, which may explain its lack of binding and uptake in the parasite (243).

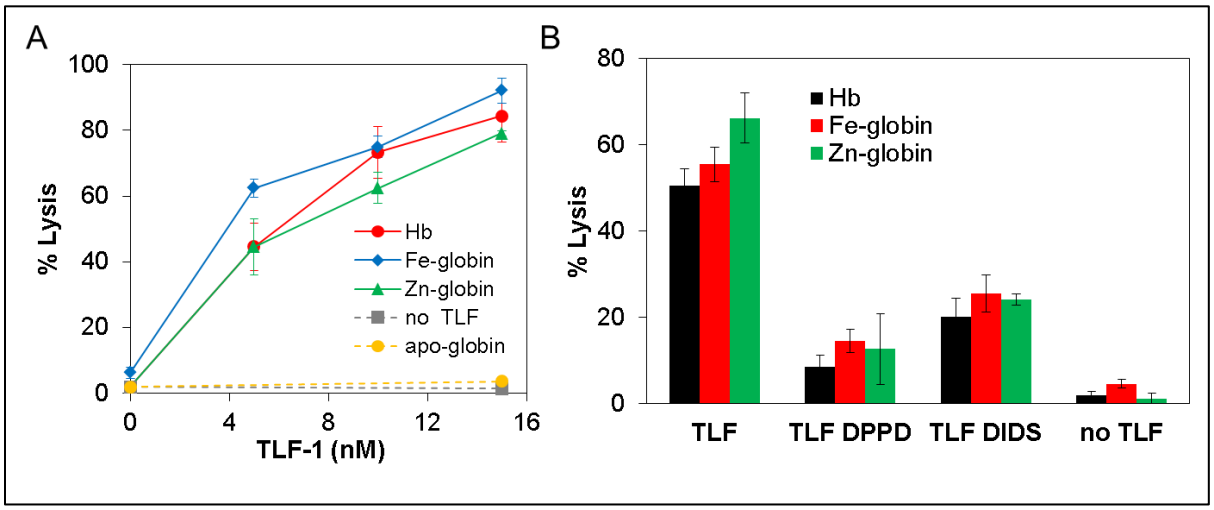

Figure 2.3: **Hb-mediated peroxidation is not required for TLF-1 lysis of *T. b. brucei***. (**A**) TLF-1 lysis assay for 2 h at 37˚C in serum-free media with 100 mole equivalents of either Hb (red circles), Zn^{2+}globin (green triangles), Fe^{3+}globin (blue diamonds), apo-globin (yellow circles), or no hemoglobin (grey squares). No differences between Hb and Zn-globin or Fe-globin had a p-value less than 0.01. (**B**) TLF-1 lysis assay (2.5 nM) for 2 h at 37˚C in serum-free media with TLF-1 (10 nM) and 100 equivalents of the Hb (red circles), Zn^{2+}globin (green triangles), Fe^{3+}globin (blue diamonds). *T. b. brucei* were pre-incubated for 1 h with either DPPD (30 μM) prior to TLF-1 addition. DIDS (300 μM) was added concurrently with TLF-1. Error bars show standard deviation of three counts from one representative lysis assay.

TLF-1 lysis assays *in vivo* showed no difference in lysis based on the oxidative capacity of the globin. Zn-globin and Hb-bound TLF-1 killed the trypanosomes equally effectively (Figure 2.3A). Furthermore, the antioxidant DPPD rescued TLF-1 lysis with either iron or Zn-globin, suggesting that hemoglobin is not the source for peroxide stress (Figure 2.3B). The chlorine channel inhibitor DIDS, which inhibits lysis of TLF-1 treated *T. b. brucei*, also saved cells from lysis regardless of the type of globin added (Figure 2.3B) (15).

Lysosomal lipid peroxides are not the source of oxidative stress in TLF killing

The role of lysosomal lipid peroxidation in the TLF-1 lytic mechanism was next investigated. In addition to Hb uptake, transferrin also delivers iron to the lysosome and is a major source of oxidative stress in bloodstream form trypanosomes (160). To determine whether transferrin iron uptake played a role in TLF-1 lysis, we pre-incubated cells in serum-free media with either 100 μM transferrin or apo-transferrin, followed by a 2 h TLF-1 lysis assay. There was no difference in lysis between the three samples indicating that iron delivery to the lysosome is not important for TLF-1 lysis (Figure 2.4A).

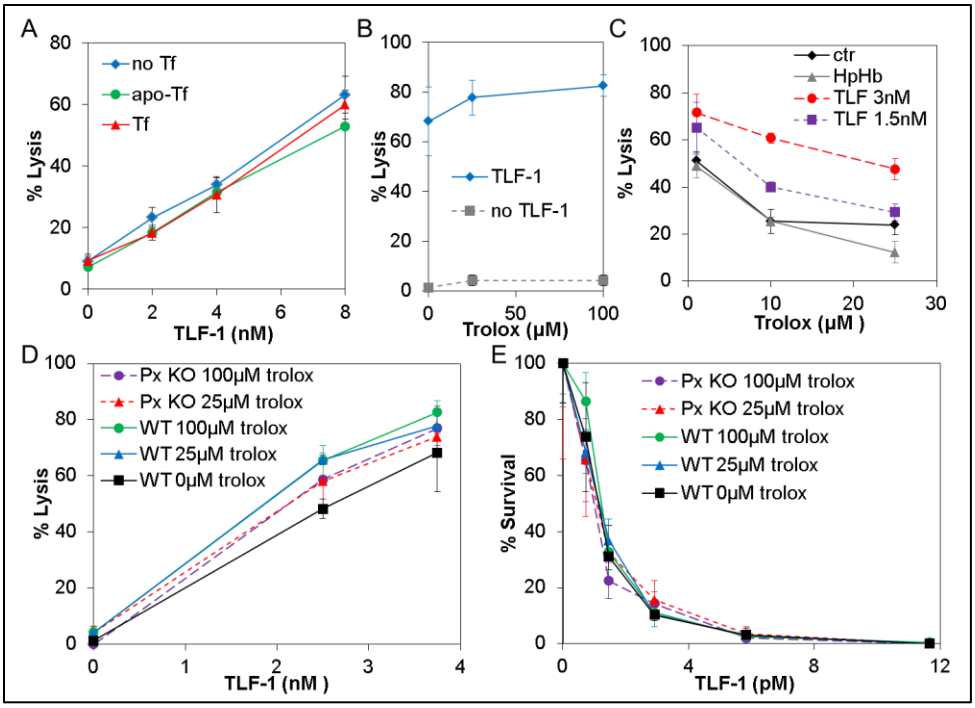

Figure 2.4: **Lysosomal lipid peroxidation is not required for TLF-1 lysis of *T. b. brucei***. (**A**) TLF-1 lysis assay for 2 h at 37˚C in serum-free media, after pre-incubation for 1.5 h with holotransferrin (100 μM FeTf, red triangles), apotransferrin (100 μM apo-Tf, green circles) or serum-free media alone (blue diamonds). (**B)** TLF-1 lysis assay in WT cells (3.75 nM) for 2 h at 37˚C, with trolox added concurrently with TLF-1. (**C**) TLF-1 lysis assay for 2 h at 37˚C with *T. b. brucei* Px KO cells. Cells were washed from 100 μM trolox and resuspended in media with the indicated trolox concentration. Lysis was determined with 1.5 nM TLF-1 (purple squares), 3 nM TLF-1 (red circles), no TLF-1 (black circles), or 1.5 μM Hp1-1 with 50 equivalents Hb (grey triangles). (**D**) TLF-1 lysis assay for 2 h at 37˚C with WT and Px KO cells. Cells were washed from 100 μM trolox, and resuspended in media with no trolox and WT cells (black squares), 25 μM trolox and WT cells (blue triangles), 100 μM trolox and WT cells (green circles), 25 μM trolox and Px KO cells (red triangles), or 100 μM trolox and Px KO cells (purple circles). *E,* Survival assay with WT and Px KO *T. b. brucei*. Legend inset. All error bars show standard deviation of three counts from one representative lysis assay.

Bloodstream form *T. b. brucei* express two cytosolic tryparedoxin peroxidases which detoxify lipid hydroperoxides arising from the lysosome (159, 160). We asked whether *T. b. brucei* with both cytosolic peroxidases knocked out (Px KO) were more sensitive to TLF-1 lysis. The lethal phenotype of the Px KO cells is rescued by addition of an antioxidant, trolox, without which the cells die within 1 h at 37˚C (159, 160). The

antioxidant trolox, a water soluble vitamin E derivative, did not inhibit TLF-1 lysis of wild-type *T. b. brucei* at concentrations up to 100 μM (Figure 2.4B). This result contrasts with the lipophilic antioxidant DPPD which prevented TLF-1 lysis (compare Figure 2.4B and Figure 2.1A). The two antioxidants have different mechanisms and lipid solubility, perhaps partitioning into different regions of the cell, accounting for differences in their ability to modulate TLF-1 activity (244, 245).

When trolox was titrated down to levels allowing approximately 50% spontaneous cell death of the Px KO cells, TLF-1 addition did not cause a synergistic increase in lysis, indicating that the Px enzymes are not important for metabolizing TLF-1 induced lipid peroxides (Figure 2.4C). Furthermore, in lysis assays where sufficient trolox was added to rescue maintain viability of the Px KO cells, there was no difference in TLF-1 lysis between Px KO cells and wild-type trypanosomes (Figure 2.4D). There was no difference in survival of the Px KO cells compared to wild-type *T. b. brucei* treated with TLF-1 in an overnight lysis assay (Figure 2.4E). Thus, lysosomal lipid peroxidation is not the source of oxidative stress during TLF-1 lysis.

ApoL1 initiates lysis involving oxidative stress

We next asked whether the TLF-1 protein ApoL1 induced the oxidative stress involved in TLF-1 lysis. ApoL1 was purified from the native TLF-1 particles as described previously, and was tested for lytic activity in the presence of antioxidants and pro-oxidants (21). To prevent high-affinity uptake of trace amounts of TLF-1 possibly contaminating the purified ApoL1 preparation, assays were conducted in a HpHbR KO line of *T. b. brucei* (39). The HpHbR receptor is not involved in purified ApoL1 uptake,

and therefore HpHbR KO cells are equally susceptible to ApoL1 lysis as wild-type *T. b. brucei*. Both ApoL1 and TLF-1 treated HpHbR KO cells responded to addition of the antioxidant DPPD and the pro-oxidants DEM and +OOH (Figure 2.5). Higher concentrations of TLF-1 were needed to kill the HpHbR KO cells than wild-type *T. b. bruce*i. However, HpHbR KO cell lines responded to antioxidants and pro-oxidants in a similar manner to wild-type *T. b. brucei*. Thus, ApoL1-induced *T. b. brucei* lysis involves oxidation even when the TLF-1 or ApoL1 uptake is much slower due to the lack of receptor-mediated uptake.

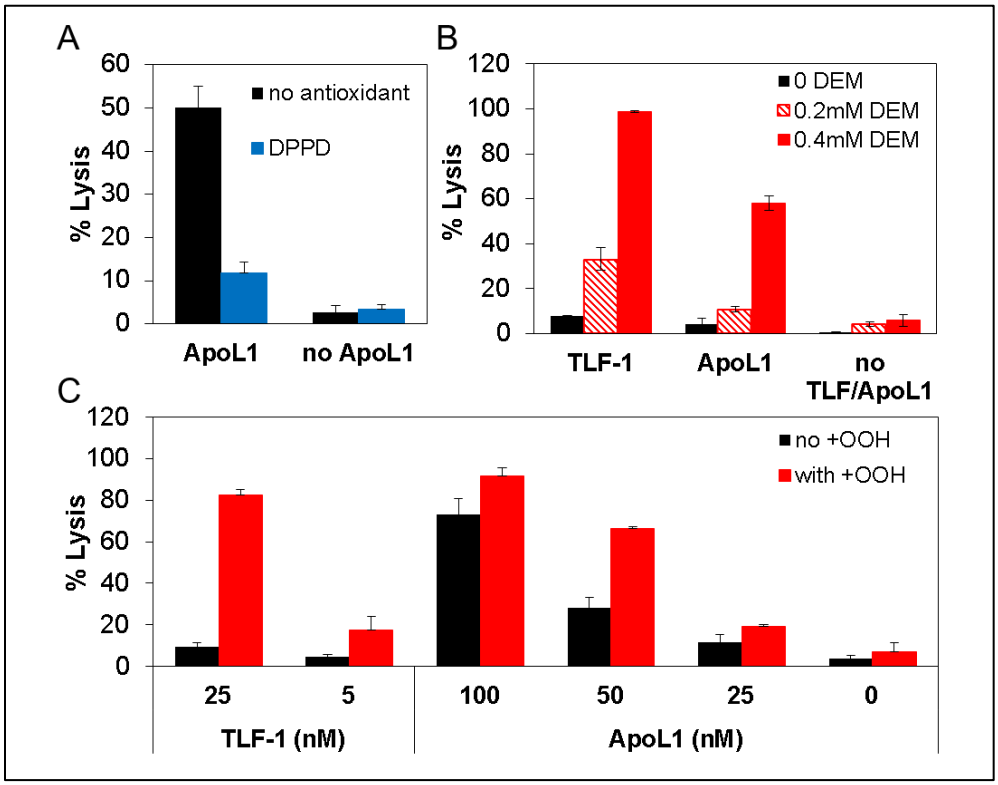

Figure 2.5: **ApoL1 initiates lysis stimulated by oxidation**. (**A**) ApoL1 lysis assay for 6 h at 37˚C in HpHbR KO *T. b. brucei* following pre-incubation for 1 h with 30 µM DPPD. (**B**) Lysis assay for 5 h 37˚C in HpHbR KO *T. b. brucei* with TLF-1 and ApoL1 both approximately 50 nM; DEM added 1 h after start of lysis for 0.2 mM DEM or 0.4 mM DEM. (**C**) Lysis assay for 4 h at 37˚C in HpHbR KO *T. b. brucei* with or without 40 µM +OOH added 1 h after the start of the assay. All error bars show standard deviation of three counts from one representative lysis assay.

Kinetics of sensitivity to peroxides

Hydrogen peroxide was next used to assess the time point during TLF-1 lysis that *T. b. brucei* become sensitive to oxidation. Unlike +OOH, H_2O_2 is metabolized by *T. b. brucei* within several minutes (150). The lifetime of ROS produced by peroxides extends longer than the H_2O_2 molecular itself. In Figure 1B, the level of ROS plateaus about 15-20 minutes after H_2O_2 addition. Due to its rapid metabolism, H_2O_2 was utilized as a time-sensitive pro-oxidant which only causes oxidative stress to cells for a limited window of time after its addition. TLF-1 lysis was only increased by H_2O_2 if added after the cells had been incubated with TLF-1 for 20 min (Figure 6A).

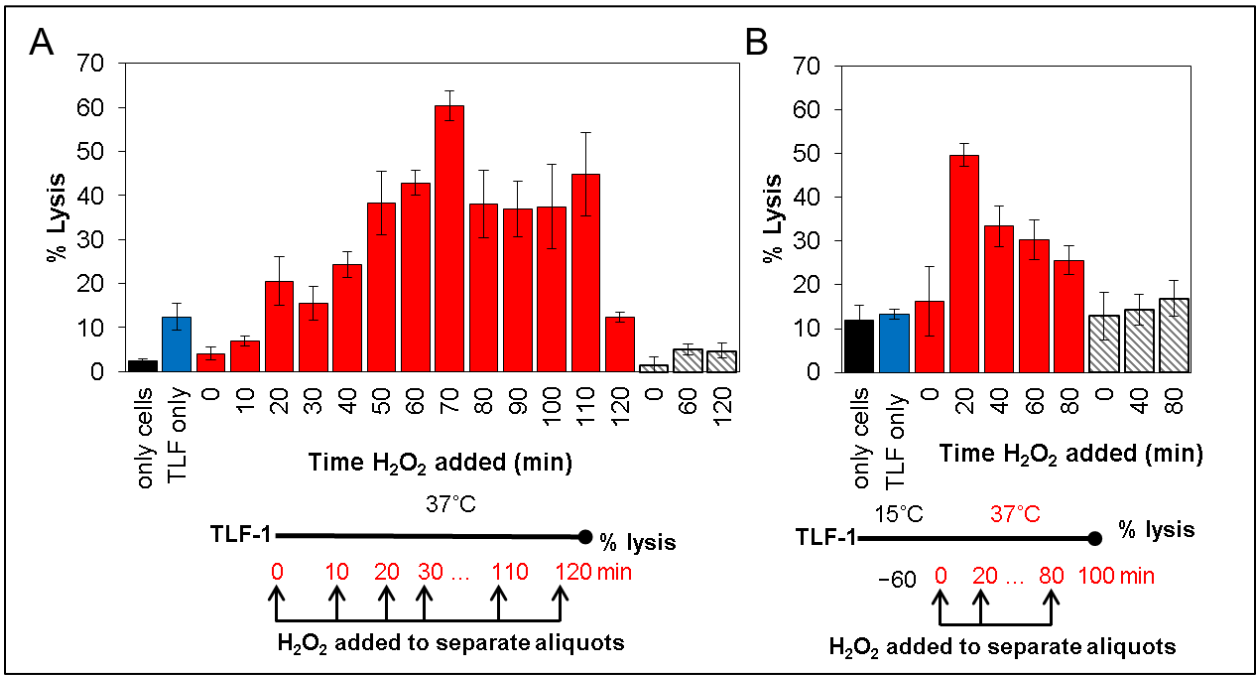

Figure 2.6: **TLF-1 trafficking from the endosomes precedes peroxide sensitivity.** (**A**) TLF-1 Lysis assay (0.4 nM) for 2 h at 37˚C. H_2O_2 (40 µM) added to aliquots every 10 min from the start of the assay (0 min) until 120 min. See diagram below figure for experimental set-up. (**B**) TLF-1 (4 nM) was pre-loaded into the endosomes at 15˚C for 1 h, washed at 4˚C, and shifted to 37˚C at 0 min as shown in the diagram below the figure. H_2O_2 (40 µM) was added once to each aliquot of TLF-1 treated *T. b. brucei* at the indicated times, and lysis was recorded after 100 min at 37˚C. All error bars show standard deviation of three counts from one representative lysis assay.

We next investigated whether TLF-1 internalization and activation preceded sensitivity to oxidative stress. Blocking endosomal fusion by low temperature (15˚C) has been shown to prevent TLF-1 lysis in a reversible manner (246). Parasite endosomes were loaded with TLF-1 at 15˚C, the free TLF-1 was washed away, the temperature shifted to 37˚C, and then H_2O_2 was added in 20 min intervals (Figure 2.6B). Immediately after the temperature block was released, hydrogen peroxide had no effect on lysis. However, 20-minutes after the temperature block was released, H_2O_2 dramatically increased cell lysis. The temperature block may prevent ApoL1 trafficking from the endosome to its site of action (15, 16, 18).

TLF-1 treatment does not cause global oxidative damage to *T. b. brucei*

Does TLF-1 addition lead to oxidative damage and ROS accumulation in *T. b. brucei*? Surprisingly, no accumulation of ROS was measured in TLF-1 treated cells versus control cells (Figure 2.7A, dashed lines). We hypothesized that TLF-1 treatment might impair the oxidative stress response in *T. b. brucei*. When H_2O_2 was spiked into TLF-1 treated cells at different time-points, however, control and TLF-1 treated *T. b. brucei* both accumulated ROS at the similar rates (Figure 2.7A, solid lines). Thus, although peroxides stimulate TLF-1 lysis of *T. b. brucei*, TLF-1 does not lyse the parasites by inducing extensive oxidative damage.

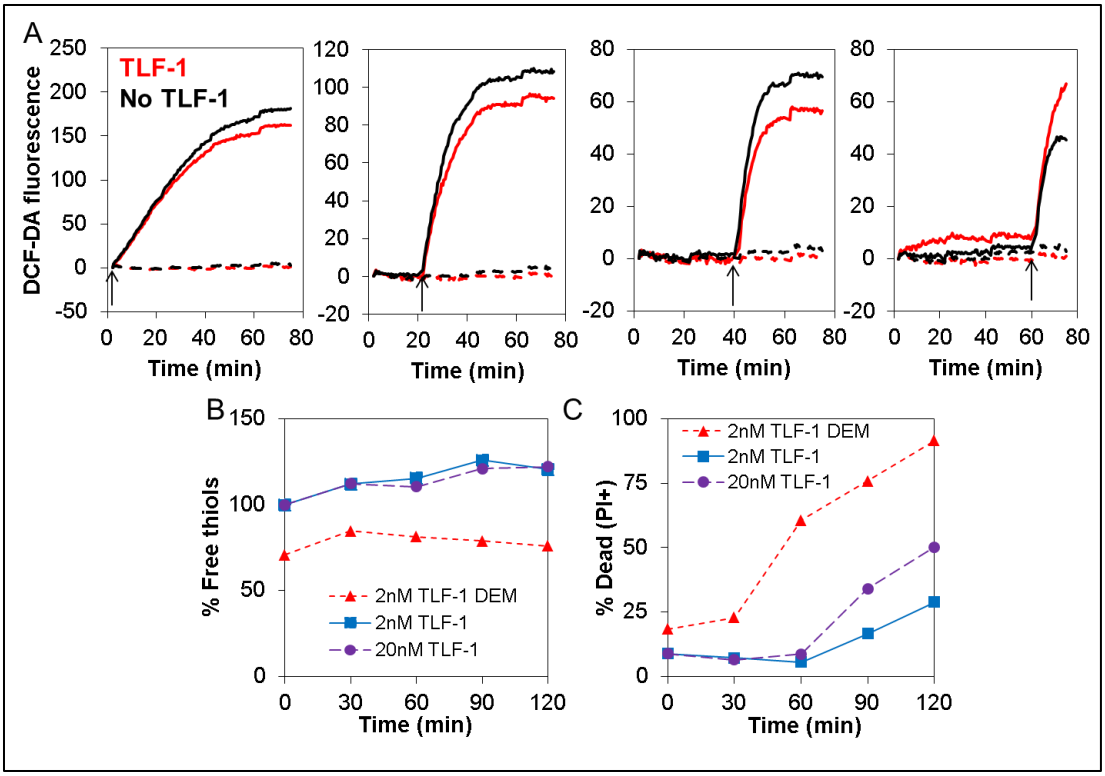

Figure 2.7: **TLF-1 treatment does not cause global oxidative damage to *T. b. brucei*.** (**A)** Kinetics of ROS production by cells treated with 10nM TLF-1 (no Hb) added at 0 min (red lines) or without TLF-1 (black lines). Each graph shows a different sample from the same experiment, with an arrow indicating the time(s) when 50 μM H_2O_2 were added to the wells. The dotted lines show TLF-1 and control samples without H_2O_2 added as a reference in each graph. Less than 20% lysis due to TLF-1 or H_2O_2 was measured at the endpoint of this assay though TLF-1 treated cells had begun to swell. (**B**) Thiol determination assay. At the start of the assay TLF-1 (2 or 20 nM) or DEM (0.6 mM) was added to cells at 37˚C. Flow cytometry analysis of free thiols was performed at the times shown on the x-axis. Representative assay (N=1). (**C**) Percent PI-positive cells of total cells counted by flow cytometry in panel "B".

Due to the implication of thiol oxidation in *T. b. brucei* treated with TLF-1, we next tested whether TLF-1 induced a global oxidation of cellular free thiols. Surprisingly, no decrease in free thiols was observed at different TLF-1 concentrations or time-points (Figure 2.7B). As expected, DEM-treated cells had lower total free thiols, but TLF-1 treatment did not further decrease the free thiol levels in DEM-treated cells. The slightly increased fluorescent signal observed during TLF-1 incubation was likely an artifact of

the cytoplasmic swelling of *T. b. brucei* exposed to TLF-1. In the flow cytometry assay for free thiols, dead cells were excluded based on propidium iodide (PI) uptake into the nucleus. Consistent with the lysis assays (Figure 2.1D), DEM dramatically accelerated cell lysis in TLF-1 treated cells compared to TLF-1 alone (Figure 2.7C).

TLF-1 causes osmotic stress to *T. b. brucei*

We next addressed whether TLF-1 and ApoL1 cause osmotic stress to the plasma membrane of *T. b. brucei* cells, as described previously (57, 61). *T. b. brucei* was treated with TLF-1, ApoL1, or a short-term hypotonic shock (in 60% diluted media for a few minutes), and live cells were imaged by Differential Interference Contrast (DIC) microscopy. TLF-1, ApoL1, and hypotonic treatment all caused cells to form a kite-shaped swollen morphology easily distinguishable from the normal cell morphology (Figure 2.8A). Osmotic swelling seems to be required for TLF-1 lysis, because when the assay media was made hypertonic with high concentrations of cell-impermeable sucrose, cells no longer lysed (Figure 2.8B). Importantly, sucrose rescued TLF-1 induced lysis even when added half-way through the 2 h lysis assay, after cell swelling had initiated. Hypertonic sucrose may prevent TLF-1 lysis of *T. b. brucei* by preventing the ultimate influx of water which directly leads to cell death.

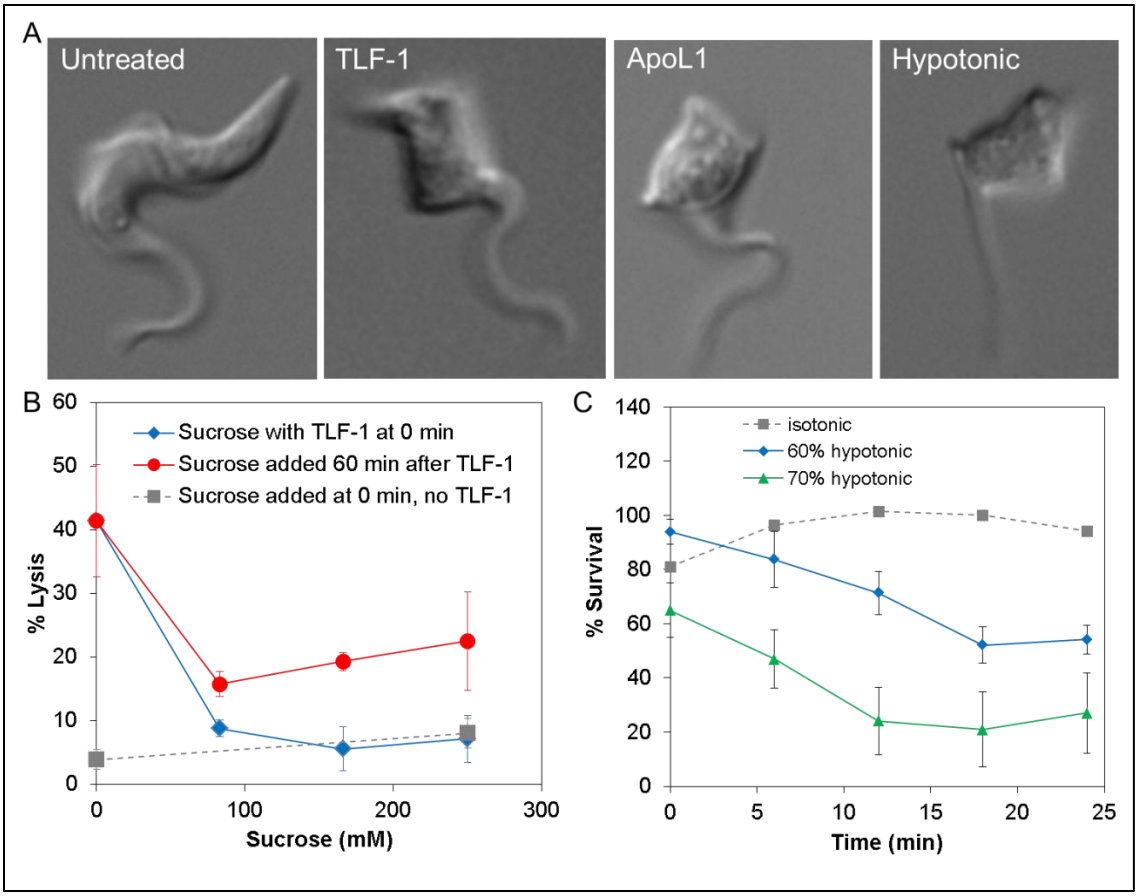

Figure 2.8: **TLF-1 causes osmotic stress to *T. b. brucei*.** (A) DIC images of *T. b. brucei* treated at 37˚C in culture media with either 10nM TLF-1 (with Hb) for 75 min, 100nM ApoL1 (in HpHbR KO cells) for 5 h, or 60% diluted hypotonic media for less than 5 minutes. (**B**) 2 h lysis assay. Addition of sucrose to the isotonic growth media saves *T. b. brucei* from TLF-1 lysis if added concurrently with TLF-1 or 1 h into the assay. (**C**) Hypotonic assay (5 min). Aliquots of cells incubated with 8nM TLF for the time indicated on the x-axis were placed under hypotonic shock for 5 minutes and then counted. N=1 for TLF-1 treated *T. b. brucei* in isotonic buffer, and 60% and 70% hypotonic shock shows the average of 3 independent assays. Error bars show standard deviation.

Although hypertonic rescue of lysis has been demonstrated before, no one has ever published the effect of hypotonic conditions on TLF-1 lysis of *T. b. brucei*. Therefore, a hypotonic shock assay was developed. Cells were incubated in hypotonic media (culture media diluted with water). Normally, when exposed to hypotonic shock, cells undergo regulatory volume decrease (RVD), recovering cell volume and motility

within 10 min (247). In this assay, most untreated cells (shown in Figure 2.7C as the 0 min time points) recovered from 60% or 70% hypotonic shock for 5 min (111 mosM and 82 mosM, see methods section for the unit conversion). But after only 12 min of incubation with TLF-1, *T. b. brucei* become hyper-sensitive to hypotonic shock (Figure 2.8C). Thus, even before visible cell swelling or death due to TLF-1, ApoL1 induces osmotic stress at the plasma membrane.

Hypotonic shock confers susceptibility to oxidation-induced osmotic lysis

We tested whether peroxides mediated the response of *T. b. brucei* to hypotonic stress, similar to how peroxides modulated the response of *T. b. brucei* to ApoL1-induced osmotic stress. In the absence of peroxides, most *T. b. brucei* cells recovered from 5 minutes of 0-70% hypotonic shock. In contrast, cells exposed to 4 to 20 μM H_2O_2 lost their ability to volume regulate, and osmotic lysis occurred (Figure 2.9A). The observed lysis was not due to extensive oxidative stress within the cells, because ROS production in *T. b. brucei* following H_2O_2 addition was not higher in hypotonic than in isotonic media (Figure 2.9B).

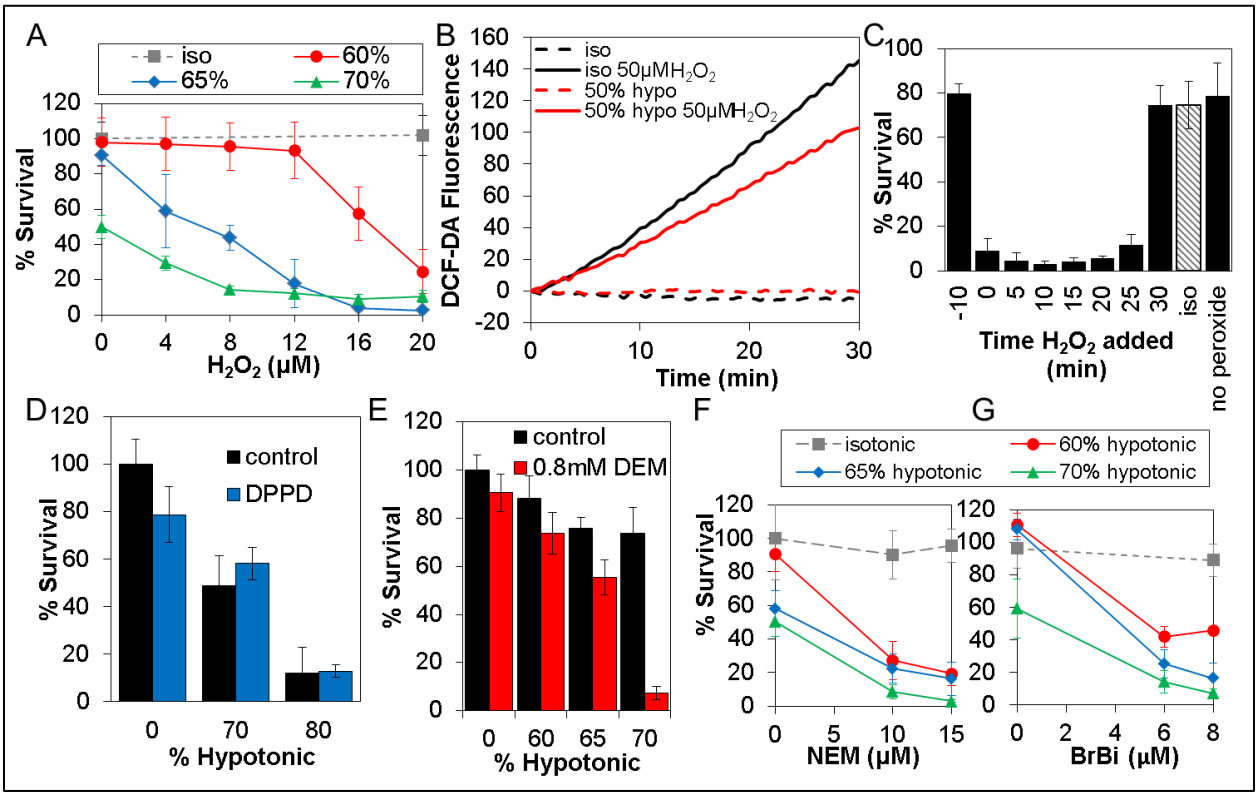

Figure 2.9: **Oxidation induces osmotic lysis of *T. b. brucei***. (**A**) Hypotonic assay (5 min) with indicated concentrations H_2O_2 added concurrently with hypotonic shock into 60% hypotonic media (red circles), 65% hypotonic media (blue diamonds), 70% hypotonic media (green triangles), or isotonic media (grey squares). Error bars show standard deviation from 6 counts from 3 assays. (**B**) Kinetics of ROS production measured by DCF-DA fluorescence in *T. b. brucei* diluted into either 50% DMEM (black lines) or water (red lines), with (solid lines) or without (dashed lines) concurrent addition of 50 μM H_2O_2. (**C**) Hypotonic assay (5 min) on *T. b. brucei* pre-incubated for 1 h at

37˚C with DMSO (0.5%), or 60 μM DPPD. Control cells had no added DPPD. Error bars show the standard deviation of 6 counts from 3 assays. (**D**) Hypotonic assay (5 min) with 0.8 mM DEM (red bars) pre-incubated with *T. b. brucei* for 30 min. No DEM (black bars). Error bars show standard deviation from 6 counts from 3 assays. (**E**) Hypotonic assay (5 min) on cells pre-incubated for 30 min at 37˚C with NEM. Legend indicates % hypotonic media. Error bars show standard deviation from 6 counts from 3 assays. (**F**) Hypotonic assay (5 min) on cells pre-incubated for 30 min at 37˚C with BrBi. Legend indicates % hypotonic media. Error bars show standard deviation from 6 counts from 3 assays. Isotonic controls are 70% PBS rather than 100% media. (**G**) Hypotonic assay for 30 min in 50% hypotonic buffer. H_2O_2 (10 μM) was added at the beginning of the assay (0min) and in 5 min intervals subsequently (black bars). Peroxide addition at 0 min in isotonic buffer is shown as a grey striped bar. Error bars show standard deviation for 4 counts from 2 assays.

Following hypotonic shock, cells initially swell with water, and then rapidly return to normal volume through activation of volume regulatory channels in the plasma membrane. To probe whether *T. b. brucei* were most sensitive to peroxides during initial cell swelling, a longer-term 30 min 50% hypotonic stress assay was performed. Hydrogen peroxide (10 μM) was spiked into the cells in hypotonic media every 5 min for the duration of the 30 min assay (Figure 2.9C). At all the time points where H_2O_2 was incubated with cells for at least 5 min in hypotonic buffer, H_2O_2 dramatically induced osmotic lysis. At the 30 min time-point when cells were immediately quenched into isotonic buffer for immediate counting, the peroxide had no effect on the cells. Moreover, if peroxides were added prior to hypotonic shock, there was no effect on the cells. Thus, H_2O_2 only affects cells undergoing osmotic stress concurrently with peroxide addition.

In contrast to the peroxide effect, the antioxidant DPPD did not make *T. b. brucei* more resistant to osmotic lysis (Figure 2.9D). The thiol-binding inhibitor DEM, like H_2O_2, stimulated osmotic lysis, though in this case pre-incubation of the *T. b. brucei* cells was required for DEM uptake (Figure 2.9E). Similarly, the promiscuous free thiol

binding molecules BrBi and NEM stimulated osmotic lysis of *T. b. brucei* (Figure 2.9F-G).

DISCUSSION

The results in this paper provide an integrated model for oxidative stress and osmotic swelling during TLF lysis of *T. b. brucei.* Earlier work suggested that the Hpr-Hb complex initiated the peroxides involved in TLF-1 lysis (48). However, using zinc-substituted globin, we showed that the iron in Hb is dispensable for TLF-1 lysis (Figure 3). In addition, none of our data supports lysosomal damage due to ApoL1 in *T. b. brucei* (15). Rather, our data is consistent with the model that after Hpr-Hb mediated TLF-1 internalization, ApoL1 alone initiates *T. b. brucei* lysis (Figure 2.5) (248). Moreover, our results support the recent model that ApoL1 induces cell swelling by channel formation in the plasma membrane of *T. b. brucei* (16). We propose that ApoL1-induced ionic disruption of plasma membrane of *T. b. brucei* leads to oxidation-stimulated osmotic lysis.

Our data suggests that oxidation of sensitive thiol groups in osmotically stressed *T. b. brucei* leads to increased cell swelling and lysis. Over time, ApoL1 from TLF-1 induces osmotic stress to *T. b. brucei* by disrupting ion gradients at the plasma membrane. Therefore, TLF-1 induced osmotic stress may be modelled by hypotonic stress. *T. b. brucei* treated with either TLF-1 or hypotonic media are extremely sensitive to lysis in the presence of peroxides or thiol-binding agents (Figure 2.9). It appears when thiol oxidation occurs in the context of osmotic stress, the cells become unable to undergo RVD, inducing uncontrolled cell swelling and death. In the case of TLF-1 treatment, *T. b. brucei* were not sensitive to hydrogen peroxide until about 20 min after

TLF-1 addition (Figure 2.6). The kinetics suggest that TLF-1-induced osmotic stress develops over time, perhaps as more ApoL1 molecules traffic out of the endosomes, and that osmotic stress precedes peroxide sensitivity.

We found that TLF-1 lysis is not due to overwhelming the cell with oxidative stress, in agreement with a previous study (Figure 2.7) (50). In other cell types, hypotonic shock leads to ROS production (249-251). In *T. b. brucei,* however, osmotic regulation may be disrupted by peroxides produced at endogenous levels, or levels of peroxides below the limits of detection in our assays. Alternatively, thiol oxidation by a non-peroxide oxidizing agent may induce osmotic swelling during TLF-1 lysis The exact origin and chemical nature of the oxidations in *T. b. brucei* treated with TLF-1 remain unknown. The commonly cited candidates for the source of ROS production in mammalian cells are the mitochondria and NADPH oxidase. Bloodstream form trypanosomes, however, do not contain NADPH oxidase or an active electron transport chain in the mitochondria.

We propose that local oxidation of a small number of cellular thiol(s) involved in osmotic volume regulation leads to uncontrolled cell swelling and lysis due to TLF-1. Three diverse thiol binding molecules (DEM, NEM, and BrBi) increased TLF-1 lysis and stimulated hypotonic lysis (Figure 2.1 and Figure 2.9). Because total free thiols do not decrease during TLF-1 lysis, global redox imbalance does not appear to be necessary for induction of osmotic lysis of *T. b. brucei.*

The specific target(s) which are oxidized in osmotically stressed trypanosomes are unknown, but some candidates can be selected from the literature. A multi-functional intracellular ATPase in trypanosomes, TbVCP, is sensitive to NEM inhibition

(252). In bloodstream form *T. b. brucei,* NEM caused depolarization of the plasma membrane potential, presumably through inhibition of H^+-ATPases (183). In addition to ATPases, phosphatases often contain redox-active cysteine residues that are sensitive to oxidation (253). In a related parasite, *Trypanosoma rangeli,* H_2O_2 was shown to inhibit the activity of phosphatases in the outer membrane, and thiol reducing agents reversed phosphatase inhibition (254). In various organisms, ROS have been shown to activate ion channels and aquaporins (255-258). More directly, aquaporins can transport peroxides and therefore may contribute to trypanosome peroxide uptake, especially in cells under osmotic stress (203). In erythrocytes and vascular smooth muscle cells, KCl co-transport is activated by oxidizing agents, sulfhydryl reagents, or hypotonic stress, but the oxidized proteins in the signaling cascades are unknown (259).

Like *T. b. brucei*, in the insect parasite *Crithidia* N-ethyl-maleate (NEM) inhibited RVD and amino acid efflux after hypotonic stress (192). Similarly, in rat neonatal cardiomyocytes, endogenously produced reactive oxygen species inactivate RVD during hypotonic conditions (250). In rabbit hearts, the proposed signaling cascade linking osmotic swelling and ROS production involves peroxides activating swelling-activated chloride channels (260). In rat pheochromocytoma cells (PC12), either hypotonic shock or 100μM H_2O_2 activated an outward rectifying chloride channel, and incubation in media with a high D-mannitol concentration prevented channel activation (258). Like D-mannitol in rat cells, high sucrose concentrations prevent TLF-1 lysis in *T. brucei* (Figure 2.8B and reference 10). Moreover, ROS activation of chloride channels may occur during TLF-1 lysis of *T. b brucei.* Incubating TLF-1 or ApoL1-treated cells with the chloride channel inhibitor DIDS prevents lysis (Figure 2.3B) (15).

The synergy between oxidative stress and osmotic lysis of trypanosomes might be exploited for drug development. Combination therapy with drugs which have synergistic mechanisms is a goal for anti-parasitic drug development, but the current clinically available drugs show no synergy in field studies (261). The nifurtimox/efluonithine combination therapy used to treat central nervous system *T. b. gambiense* infection shows no mechanistic synergy, but is used to reduce costs and slow the development of resistant parasites (133, 262). Exploiting the synergy between oxidative and osmotic stress may be possible utilizing existing drugs. Thiol-modulating drugs like the clinically used anti-trypanosomal drug melarsoprol may synergize with ionophores like salinomycin, which kills trypanosomes via cytoplasmic swelling, resembling TLF-1 lysis (127, 129, 263).

Various models for TLF-1 induced lysis of *T. b. brucei* have been proposed. Historically, the localization of TLF-1 and ApoL1 in the lysosome led to a model where lysosomal damage caused cell lysis. In the current work, however, oxidative damage to the lysosome was not observed as a result of TLF-1 treatment (15). Moreover, a recent study observed that ApoL1-induced damage to the lysosome is not sufficient to induce lysis (18). While it is indisputable that a high proportion of TLF-1 and ApoL1 traffics to the lysosome, the lysosome may represent the parasite's way of detoxifying TLF-1 rather than the site of trypanolytic activity.

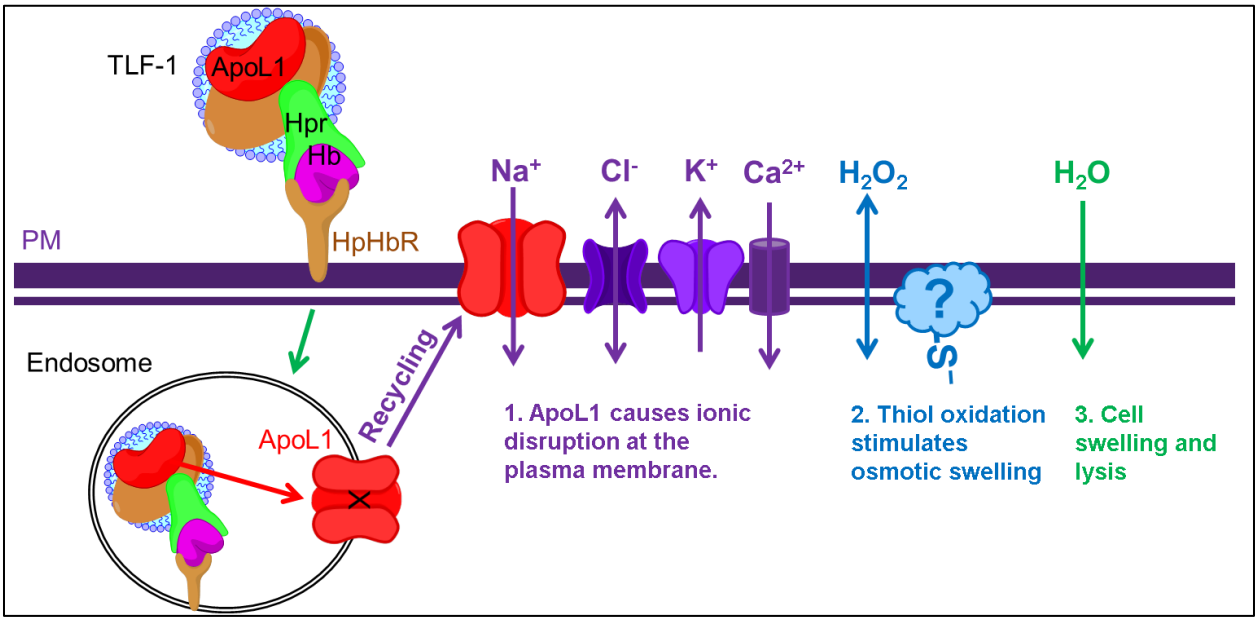

Figure 2.10: **Model for oxidation-stimulated osmotic lysis of *T. b. brucei* via ApoL1 trafficking to the plasma membrane.** TLF-1 is endocytosed via the HpHbR in the flagellar pocket of *T. b. brucei.* Inside an acidic endosomal vesicle, ApoL1 inserts into the membrane. The sodium channel activity of ApoL1 is inhibited in acidic conditions, thus an "x" is drawn over the channel. The series of steps leading to trypanosome lysis are indicated in the figure. First, after recycling to the plasma membrane (PM) ApoL1 causes early ionic disruption and osmotic stress to *T. b. brucei* at the plasma membrane (shown in purple). Next, peroxide-induced oxidation of cellular thiols stimulates osmotic de-regulation (shown in blue). Finally, lytic cell death is caused by excessive influx of water through the plasma membrane of *T. b. brucei* (shown in green).

Our model for TLF-1 lysis involves ApoL1 trafficking to the flagellar pocket of *T. b. brucei,* causing ionic imbalance at the plasma membrane (Figure 2.10). Supporting this model, cellular swelling due to osmotic imbalance is a hallmark of TLF-1 induced lysis (Figure 8) (57, 61). There are notable similarities at both the morphological and biochemical level between *T. b. brucei* swelling due to TLF-1 and swelling due to hypotonic stress. The observed cytoplasmic volume increase observed in TLF-1 treated *T. b. brucei* resembles cell swelling due to hypotonic shock, although RVD after hypotonic shock facilitates recovery of cell volume after a short time (61, 195). Both TLF-1 treatment and hypotonic shock are associated with potassium ion efflux and calcium ion influx in *T. b. brucei* (61, 199, 201).

Another recently published study suggests that ApoL1 causes apoptosis-like cell death by trafficking to the mitochondria (18). It is important to note that in bloodstream form trypanosomes, apoptosis has many divergent features due to the lack of a ROS-producing electron transport chain in the mitochondria, no cytochrome c, and no annotated caspases. Osmotic swelling of *T. b. brucei* during TLF-1 incubation was not specifically addressed in the apoptotic model (18). Importantly, apoptosis is canonically associated with volume decrease, not volume increase due to water influx. For instance, in *T. cruzi*, volume decrease is associated with apoptotic cell death induced by serum complement (264). Nevertheless, many common features exist between osmotic stress and apoptosis in trypanosomatids, suggesting that the osmotic response and cell death pathways are interconnected. Hypotonic stress leads to an influx of calcium, and increased cytosolic calcium is an inducer of apoptosis (199, 265). Calcium influx occurs following TLF-1 addition to *T. b. brucei,* and calcium is important for the lytic activity of

human serum (61, 62). Future studies should elucidate whether ApoL1-induced effects to the plasma membrane induce mitochondrial effects, or vice versa.

In conclusion, in this study we resolved several important questions surrounding the mechanism which the human innate immune factor TLF-1 utilizes to kill *T. b. brucei*. First, oxidative stress is important to TLF-1 lysis, but does not arise from Hpr-Hb in the lysosome. Second, oxidation of cellular thiols causes de-regulation of ApoL1-induced osmotic swelling, exacerbating lysis. Our discoveries advance the understanding of cell death pathways in *T. b. brucei,* which may facilitate the development of better drugs for the deadly disease human African trypanosomiasis.

EXPERIMENTAL PROCEDURES

Trypanosome growth and preparation for assays

Bloodstream form *T. b. brucei* Lister 427(MiTat 1.2) cells were grown in cell culture media make from HMI-9 with 10% fetal bovine serum (Sigma-Aldrich) and 10% Serum-Plus (Sigma-Aldrich). Cytosolic tryparedoxin peroxidase I and II double knock out *T. b. brucei* 449 cells, strain Lister 427 (Px KO) were generously donated by Luise Krauth-Siegel (Heidelburg University, Germany), (159, 160). The Px KO cells were grown in the presence of 100 μM trolox antioxidant. The HpHbR knockout *T. b. brucei* (Lister 427MiTat 1.2) cell line has also been described previously (39). Unless otherwise noted, all trypanosomes assays were performed in culture media with mid-log phase cells grown at 37˚C with 5% CO_2.

TLF-1 and ApoL1 purification

TLF-1_and ApoL1 were purified as described previously (21). Briefly, TLF-1 was purified from human HDLs from single donors. HDLs were eluted from an anti-Hpr column, dialyzed into phosphate buffered saline solution with EDTA (PBSE), and concentrated by Centricon filtration with a 100 kDa cut-off size (Millipore). For ApoL1 purification, purified TLF-1 was solubilized in CHAPS, eluted from an anti-ApoL1 column, dialyzed into PBSE, and concentrated. SDS-PAGE gels and Western blots against Hpr and ApoL1 confirmed the identity and purity of TLF-1 and ApoL1 preparations.

TLF-1 and ApoL1 lysis assays and survival assays

Most lysis assays were performed as previously reported with 1 x 10^7 trypanosomes/ml in serum-containing cell culture media (43). Unless otherwise specified, all TLF-1 assays were conducted following pre-incubation of TLF-1 on ice with an excess of Hb. For assays with reconstituted globins, cells were washed and re-suspended in serum-free media composed of HMI9 with 1% by weight glucose and 1% by weight bovine serum albumin (BSA). Before addition to the trypanosomes, 100 mole equivalents of globin were pre-incubated with TLF-1 on ice for several minutes. For ApoL1 assays, time-courses were longer than 2 h as indicated in the figure legends.

Reagents used in lysis assays were purchased from Sigma-Aldrich: Human hemoglobin A (Hb), *N*,*N*′-Diphenyl-*p*-phenylenediamine (DPPD), Diethyl maleate (DEM), monobromobimane (BrBi), and *N*-Ethylmaleimide (NEM). DIC microscopy of live trypanosomes incubated with ApoL1, TLF-1, or hypotonic media were performed using a Zeiss Axio Observer inverted microscope.

For survival assays, TLF-1 was added to 1 ml cells at a density of 1 x 10^5 cells/ml in triplicate wells of a 6-well plate. Cells grew to mid-log phase during a 20 h incubation in the cell culture incubator. At the endpoint, cells were counted and graphed as percent of untreated cell number.

DCF-DA kinetic measurements of reactive oxygen species (ROS)

DCF-DA was used to measure ROS in trypanosomes treated with H_2O_2 (266). 50 μM 2′,7′-Dichlorofluorescein diacetate was incubated with *T. b. brucei* cells (2 x 10^7 cells/mL) for 30 min at 37˚C before washing 3 times with HyClone® HyQ DMEM/High Modified media (without phenol red) with 10% FBS and re-suspended at 1 x 10^7 cells/mL with 200 μL per well in a 96 well plate. The fluorescence was monitored in kinetic mode using an excitation of 485 nm (band width 20 nm) and an emission of 528 nm (band width 20nm). The initial values for each sample at 0 min were set to 0 fluorescence units. For Figure 2.1B, antioxidants were pre-incubated with the cells for 30 min at 37˚C before adding H_2O_2 at 0 min. For Figure 2.9B, 100 μL 2 x 10^7 cells/mL were added to the wells and 100 μL of DMEM with 10% serum (isotonic) or H_2O (hypotonic) added at time 0 with or without concurrent addition of 50 μM H_2O_2.

Porphyrin substituted globins

Hemoglobin was denatured in acid-acetone and re-constituted with iron or zinc protoporphyrin IX as described previously (267). First, 4 mg of Hb was dissolved in 200 μl deionized water. A 20 μl aliquot of Hb was reserved for control experiments, and 180 μl was added to 14 ml acid acetone (40 mM HCl in acetone) and incubated for 10 min in

the -80˚C freezer. Globin was precipitated by centrifuging for 5 min at 4˚C and 3200 g. Acetone-heme supernatant was removed, and the globin pellet re-dissolved in 180 µl de-ionized water, suspended in 15 ml acid acetone, and incubated 10 min at −80˚C. Globin was re-pelleted and washed a second time before re-suspending the pellet in 1mL de-ionized water and dialyzed three times. The first dialysis was in 0.1% $NaHCO_3$ and 0.2 mM DTT buffer for at least 3 h at room temperature. The second dialysis was 50 mM KPi pH 7.5 buffer overnight at 4˚C. The third dialysis was 100 mM Boric Acid pH 9.5 for at least 3h at 4˚C. Globins were re-constituted with at least 4 equivalents protoporphyrin IX (Fe^{3+} or Zn^{2+}) which were mixed gradually into the globin solution. Contaminating aggregated porphyrins were pelleted by centrifuging at 4˚C. Free porphyrins were removed from the supernatant by elution by gravity through a Sephadex G-50 column. To make re-constituted reduced Fe^{2+}-globin, sodium dithionite was placed at the top of the G50 column for reduction during purification. Globin-containing fractions were concentrated on a Centricon® filter (10 kDa cutoff) and the protein concentration was determined by a Bradford Assay. Reconstituted globins were used within 24 h of synthesis.

MDA peroxidation assays

MDA was measured by the thiobarbituric acid reactive substances (TBARS) assay as previously reported using reagents from the Zeptometrix MDA assay kit (48, 50). TLF-1 (125 nM) was incubated with equimolar globin dimer in 25 µl total PBS for 5 minutes at room temperature. To this mixture, 175 µl citric acid buffer at pH 4.8 containing 70 µM H_2O_2 was added and incubated at 37˚C in a benchtop thermomixer set to 300 rpm for

30 min. The reaction was quenched with 30 μM SDS solution, then 770 μl thiobarbituric acid (TBA) solution was added and the mixture was incubated for 1 h at 95˚C. Fluorescence readings were taken on a PerkinElmer Life Sciences LS55 spectrofluorometer (excitation 530 nm, emission 550 nm, slit widths 3 and 10 nm, respectively). MDA (malondialdehyde) equivalents were determined from a linear MDA standard curve. Negligible fluorescence from samples with only globin and no TLF-1 were background subtracted from the TLF-1 plus globin samples.

Blue Native PAGE assay

Blue Native PAGE was utilized to observe reconstituted globin binding to human Hp1-1 (268). Non-reducing native gel contained 3 layers: 16% polyacrylamide in the bottom layer, 10% in the middle layer (where the HpHb complex migrated), and a 4% stacking gel. Measured equivalents of globin in PBS were incubated with 5 nmol human Hp1-1 per well (Sigma) at room temperature for 5-10 min before mixing with loading buffer before loading the gel and running at 150 V. After the solvent front had moved into the second layer of the gel, the central cathode buffer was replaced with imidazole anode buffer for better contrast. Gel was fixed with methanol (40% v/v) and acetic acid (10% v/v), stained with colloidal coomassie dye, and de-stained in 8% acidic acid.

AlexaTLF uptake assay

Alexa488-labeled TLF-1 (AlexaTLF) was prepared from TLF-1 using the Alexa 488 protein/antibody labeling kit (Invitrogen), and dialyzed against PBSE (39). For uptake assays, AlexaTLF and the indicated globin (100 equivalents) were incubated

with 300 µl of 1 x 10^7 cells/ml for 20 min in serum-free media at 37˚C, washed twice in ice-cold serum-free media, and analyzed by flow cytometry with a 488 nm laser and 530/30 nm BP filter on a Beckman Coulter Cyan instrument. FlowJo software was used for data analysis. Dead cells were excluded from the analysis through gating by light scatter, and the mean fluorescence of histogram peaks was calculated as previously described (39).

Osmotic Sensitivity Assays

T. b. brucei were pelleted and re-suspended in fresh media at 2x10^7 cells/ml. At the 0 min time-point, 40 µl cells were added to 160 µl of a mixture of cell culture media and distilled water for the final percent by volume hypotonic dilution reported (% v/v water/media solution).

To calculate the conversion of "% hypotonic" to osmolarity, the osmolarity of a series of six media and water dilutions was measured with an Advanced Instruments 3D3 osmometer. These data were used to construct a linear standard curve with the following equation (R-squared vale = 0.999):

mosM = −2.94 x (% hypotonic) + 290.7

The measured isotonic osmolarity of 290.7 mosM was near the 300 mosM expected for eukaryotic cells.

For 30 min assays, cells and osmotic mixtures were incubated for 30 min on a benchtop thermomixer at 37˚C, mixing at 300 rpm for 5 or 30 min. Cells were quenched with 300 µl isotonic media and counted immediately on a hemocytometer in duplicate.

Thiol determination assays

Thiol determination was by flow cytometry using monobromobimane (BrBi), similar to assays previously described (269, 270). For the measurement of loss of free thiols with DEM, 2.5 x 10^6 cells/ml in serum-containing media were pre-incubated with DEM for 110 min at 37˚C. Then, 70 μM BrBi and 30 μM propidium iodide (PI) were added to the cells on ice for 10 min before flow cytometry analysis on a Beckman Coulter Cyan instrument with a 405 laser excitation and a 450/50 BP filter for bromobimane fluorescence and 485/42 BP filter for PI. FlowJo software was utilized for data analysis. Cells positive for propidium iodide were excluded from thiol analysis, and cell thiols were determined as a percentage of control cell fluorescence after background subtraction of unstained cell fluorescence. For the thiol analysis during TLF-1 treatement, BrBi at 50μM was added to TLF-1 treated cells for 10 min at 37˚C before quenching into 5 μM propidium iodide on ice 1 min before flow analysis. Again, PI-positive dead cells were excluded from the thiol analysis and BrBi fluorescence was normalized to untreated cell fluorescence.

CHAPTER 3

APOLIPOPROTIEN L1 INDUCES A LOSS OF PLASMA MEMBRANE POTENTIAL LEADING TO OSMOTIC LYSIS OF *TRYPANSOMA BRUCEI BRUCEI*[2]

[2] Greene, A.S., and Hajduk, S.L. To be submitted to Molecular Microbiology.

ABSTRACT

Human serum contains potent innate immune factors called trypanosome lytic factors (TLFs) which contain the cation-channel forming toxin apolipoprotein L1 (ApoL1). Following endocytosis into an acidified endosome, TLF-1 causes a rapid loss of plasma membrane potential (Ψ_{pm}) in *Trypanosoma brucei brucei*. The observed Ψ_{pm} loss occurs concurrently with mitochondrial membrane potential loss, suggesting multiple localizations for ApoL1 action. The observed Ψ_{pm} loss correlated with subsequent cell swelling and osmotic lysis. Swelling and Ψ_{pm} loss require flux of Na^+, K^+, and Cl^- ions through the plasma membrane, occur much slower in the absence of high-affinity receptor-mediated TLF-1 uptake, and are blocked by the *T. b. rhodesiense* serum resistance associated protein (SRA) binding to ApoL1. Our kinetic data support a model for ApoL1 disruption of ionic flux at the plasma membrane leading to swelling and osmotic lysis of *T. b. brucei* parasites.

INTRODUCTION

Human serum effectively kills the veterinary parasite *Trypanosoma brucei brucei,* while human-infective trypanosomes have evolved resistance to human innate immunity and cause Human African Trypanosomiasis (HAT). The anti-trypanosomal activity of serum comes from the primate-specific trypanosomes lytic factors (TLFs). TLF-1 is an HDL particle comprised of the proteins haptoglobin related protein (Hpr), apolipoprotein A-1 (ApoA1), apolipoprotein L-1 (ApoL1) (21). ApoL1 is believed to be the primary protein toxin present in the TLFs (14). TLF-1 enters the *T. b. brucei* via a high-affinity haptoglobin hemoglobin receptor (HpHbR) in the flagellar pocket of the parasite, the specialized region of the plasma membrane where endocytosis and exocytosis occurs

(33). After trafficking into an acidic endosome, ApoL1 inserts into the membrane of the endosome, forming an ion channel (15, 57). Although ApoL1 inserts into membranes under acidic conditions, the channel is acid-gated with optimal permeability to cations at neutral pH (16).

Human infective African trypanosomes have evolved effective resistance mechanisms to TLF-1. The human-infective species *Trypanosoma brucei gambiense* prevents TLF-1 endocytosis through mutations and down-regulation of the HpHbR, increases endo-lysosomal membrane stiffness via the *T. b. gambiense* specific glycoprotein TgsGP, and a lower endosomal pH and cysteine protease activity than *T. b. brucei* cells (39, 73, 75-77). Resistance in the other human infectious subspecies, *Trypanosoma brucei rhodesiense,* is conferred by the serum resistance associated (SRA) protein, which binds to the C-terminal domain of ApoL1, destabilizing its interaction with parasite membranes (14, 271). Parasite resistance mechanisms give limited insight into the mechanism of ApoL1-induced cell death because they block ApoL1 early in the lytic process. Therefore, understanding the downstream cell death mechanisms for TLF-treated trypanosomes may lead to novel drug targets for the human-infective *T. b. gambiense* and *T. b. rhodesiense*.

It is unclear in what cellular membranes ApoL1 exerts its lytic activity. Most studies assumed that ApoL1 was active in the lysosome of *T. b. brucei* because labeled ApoL1 and TLF-1 were primarily localized there, and because changes in lysosomal morphology are observed (15, 44). Recently, ApoL1 was shown to traffic via kinesin-positive (KIFC1) vesicles to the mitochondrion of *T. b. brucei* in addition to the lysosome (18). Because ApoL1 is an acid-gated channel with minimal activity in acidic vesicles,

we examined whether TLF-1 disrupts the ionic balance at the plasma membrane, causing osmotic lysis of *T. b. brucei* (16). Trypanosomes have rapid endocytic and recycling systems to allow clearance of host immunoglobulins from the parasite membrane (272). Therefore, a portion of endocytosed ApoL1 may recycle to the flagellar pocket and plasma membrane (16, 92). Consistent with the plasma membrane model of cell death, TLF-1 treatment leads to osmotic swelling of *T. b. brucei* (47, 61, 246).

The most prominent cell death phenotype in TLF-1 treated trypanosomes is cell swelling (9). Osmotic swelling appears to be critical for TLF-1 to cause cell death. Lysis may be prevented by the addition of hypertonic concentrations of membrane-impermeable dextrans or sucrose (47, 61). In addition to morphology, TLF-1 induced swelling shares hallmarks osmotic stress, including K^+ efflux, Na^+ influx, Cl^- influx, and water influx (57, 61). TLF-1 induced osmotic lysis requires this ionic flux through the plasma membrane. Replacing Na^+ or K^+ or Cl^- ions with larger, membrane-impermeable ions blocks ApoL1 from causing trypanosome cell death (57). Moreover, the chloride channel inhibitor DIDS inhibits TLF-1 activity by blocking Cl^- flux through the plasma membrane (15). Antioxidants also ameliorate TLF-1 induced lysis, perhaps by preventing oxidation-stimulated osmotic stress to *T. b. brucei* (47). For instance, the antioxidant DPPD saves prevents ApoL1 or TLF-1 from killing *T. b. brucei* (36, 47, 48).

This paper demonstrates that TLF-1 and ApoL1 induce a rapid loss of plasma membrane potential (Ψ_{pm}) in *T. b. brucei*. The observed ionic disruption at the plasma membrane is required for cell swelling and resulting lysis of the parasites. While ApoL1 is found in various cellular localizations including the lysosome and mitochondrion, an

ApoL1-induced disruption of ion gradients at the plasma membrane likely plays a major role in the mechanism of trypanosome lysis.

RESULTS

TLF-1 causes an early loss of plasma membrane potential in *T. b. brucei*

We developed a kinetic assay using flow cytometry to evaluate changes in the plasma membrane potential of *T. b. brucei* treated with TLF-1. Fluorescence from the membrane potential dye bisoxonol was assessed in living *T. b. brucei* using complete, serum-containing media to ensure that TLF-1 retained full activity (171). In serum-containing media, the exact concentrations of ions was not known for precise calculations of membrane potential, so the data was normalized to the bisoxonol fluorescence after incubation of *T. b. brucei* cells with the Na^+/K^+ ionophore gramicidin

D.

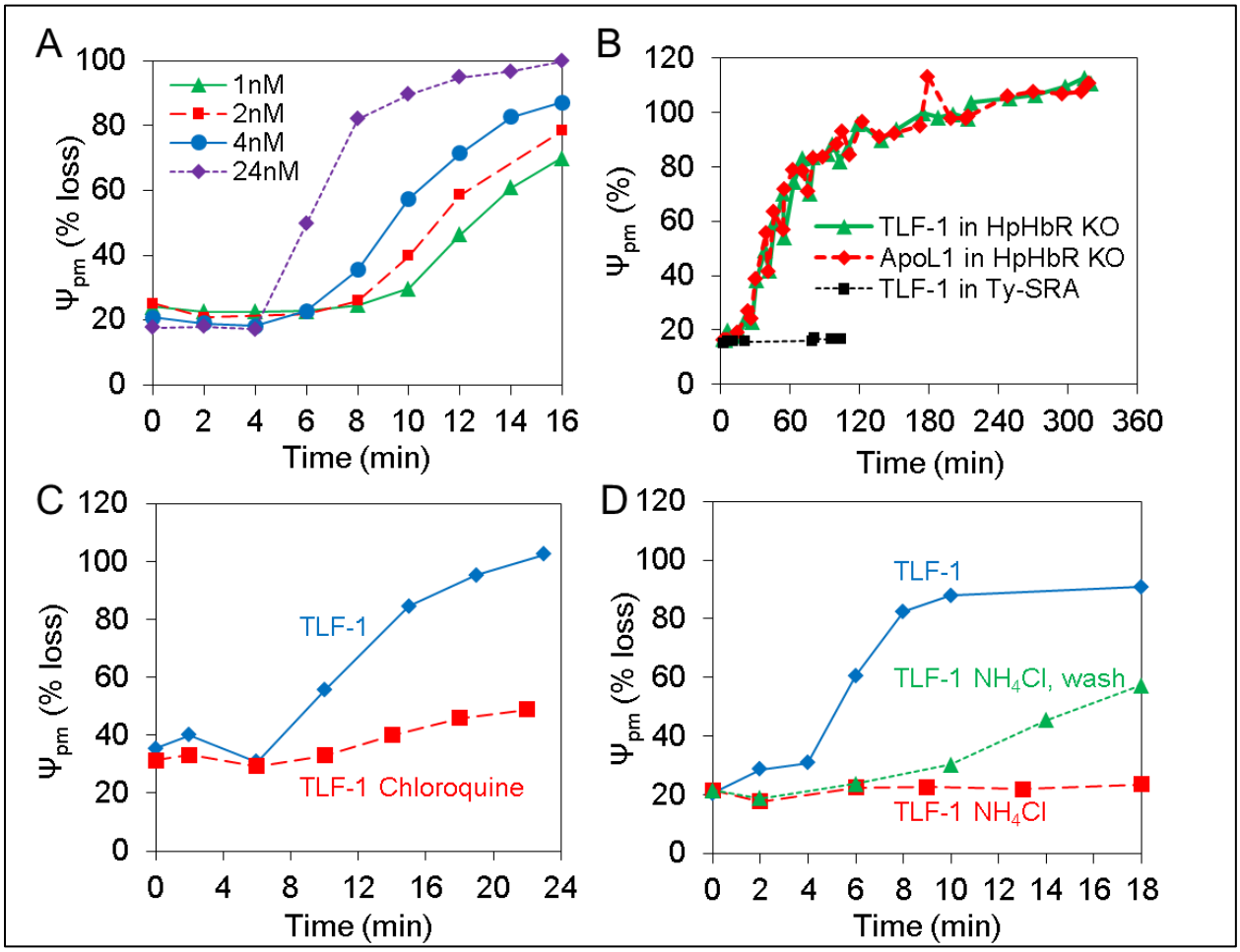

Figure 3.1: **ApoL1 induces loss of plasma membrane potential**. (**A**) TLF-1 dependent Ψ_{pm} loss. TLF-1 was added at the concentrations indicated in the legend (1-24nM) at time 0 min, and flow cytometry was run at the times indicated. N=1, representative data. (**B**) Ψ_{pm} loss in HpHbR KO and Ty-SRA *T. b. brucei.* HpHbKO *T. b. brucei* were treated with either 50nM TLF-1 (green triangles) or 50nM ApoL1 (red diamonds, dashed line). Ty-SRA *T. b. brucei* were treated with 20nM TLF-1 (black squares, dotted line). N=1. (**C**) TLF-1 dependent Ψ_{pm} loss is prevented by chloroquine. *T. b. brucei* were pre-incubated for 20 min with 50μM chloroquine at 37˚C before adding TLF-1 (20nM) at time 0 min (red squares). TLF-1 only, blue diamonds. N=1. (**D**) TLF-1 dependent Ψ_{pm} loss is prevented by NH_4^+. 25mM NH_4Cl was pre-incubated with cells for 20min at 37˚C before adding TLF-1 (20nM) at time 0 (red squares). TLF-1 only (blue triangles). Some *T. b. brucei* treated with both TLF-1 and NH_4Cl were washed at 4˚C and then shifted to 37˚C at time 0min (green triangles). All cells were quenched for the cytometry assay into buffer containing 25mM NH_4Cl. The change in membrane potential due to 25mM NH_4Cl alone was negligible (<5%) compared to the change due to TLF-1 or gramD. N=1.

Addition of TLF-1 to *T. b. brucei* induced a rapid loss of Ψ_{pm} observed as early as six minutes after TLF-1 addition (Figure 3.1A). *T. b. brucei* without TLF-1 treatment (time 0) showed bisoxonol fluorescence corresponding to their steady state membrane potential (Figure 3.1A). The rate of Ψ_{pm} loss correlated to the TLF-1 concentration. After 20 minutes of TLF-1 incubation, bisoxonol fluorescence in all samples reached maximum levels equivalent to complete loss of Ψ_{pm} due to ionophore addition (Figure 3.1A).

The HpHbR facilitates rapid and efficient endocytosis is the TLF-1/Hb complex in *T. b. brucei*, but the role of receptor-mediated uptake of TLF-1 in ApoL1 localization and activity has never been investigated. Previously, our lab created a *T. b. brucei* cell line with both alleles of the HpHbR gene knocked out (39). To investigate the role of receptor binding in TLF-1 induced Ψ_{pm} loss, high concentrations of TLF-1 (50nM) were incubated with HpHbR knockout cells. Fluid phase endocytosis in this cell line was sufficient to allow slow TLF-1 uptake, so despite the lack of HpHbR-mediated trafficking, the Ψ_{pm} dissipated over time (Figure 3.1B). Due to the slower kinetics of ApoL1 uptake, however, the loss of Ψ_{pm} occurred over hours rather than minutes (Figure 3.1B). The fact TLF-1 causes Ψ_{pm} loss in HpHbR knockout cells suggests that direct tethering to the membrane via the HpHbR receptor is not necessary for ApoL1 to disrupt of the plasma membrane potential in *T. b. brucei*.

To determine whether ApoL1 within TLF-1 is the source of Ψ_{pm} loss, *T. b. brucei* was treated with purified native ApoL1. Since *T. b. brucei* does not have a high-affinity ApoL1 receptor, Ψ_{pm} loss from purified ApoL1 was expected to resemble intact TLF-1 lysis in HpHbR knockout cells. For these experiments, ApoL1 was purified from human

plasma by antibody affinity chromatography and was shown to be free of Hpr contamination by Western blot (Supplemental Figure 3.1A) (21). ApoL1-induced Ψ_{pm} loss was measured in HpHbR KO cells to ensure that high-affinity uptake of contaminating TLF-1 would not contribute to Ψ_{pm} loss. However, ApoL1 lysis of both wild-type and HpHbR KO cells was approximately equal, suggesting that our ApoL1 preparations were free of TLF-1 (Supplemental Figure 3.1B). Purified ApoL1 exhibited nearly identical kinetics of Ψ_{pm} loss compared to the intact TLF-1 particle in HpHbR KO cells (Figure 3.1B).

Fluid phase endocytosis of TLF-1 in HpHbR KO *T. b. brucei* caused Ψ_{pm} loss to occur at different times in different cells, perhaps due to variable rates of TLF-1 endocytosis and trafficking within the trypanosome population. Histograms show two populations of cells, some of which lost their membrane potential due to ApoL1 uptake and trafficking, while others maintained control levels of fluorescence indicating that no ApoL1 had disrupted the plasma membrane (Supplemental Figure 3.2A). Rapid high-affinity uptake of TLF-1 via the HpHbR in wild-type *T. b. brucei* causes rapid Ψ_{pm} loss in the entire population of cells (Supplemental Figure 3.2B).

The SRA protein protects *T. b. rhodesiense* from human serum lysis by binding to the C-terminal domain of ApoL1 (14). SRA binding prevents ApoL1 from forming a stable transmembrane channel and facilitates lysosomal degradation of ApoL1 (16, 68). We tested whether Ty-SRA expressing *T. b. brucei* prevented TLF-1 induced Ψ_{pm} loss. When treated with high concentrations of TLF-1 (20nM), no Ψ_{pm} changes occurred in SRA-expressing *T. b. brucei* cells (Figure 3.1B).

ApoL1 inserts into membranes under acidic conditions (29). Therefore, we hypothesized that for TLF-1 to cause a loss of Ψ_{pm}, the endocytic system must remain acidified. Both chloroquine and ammonium chloride neutralize the acidic endosomes of *T. b. brucei* and prevent TLF-1 lysis (44). Both bases prevented Ψ_{pm} loss of *T. b. brucei* treated with TLF-1, presumably by preventing ApoL1 membrane insertion or trafficking to the plasma membrane (Figure 3.1C and D). We tested whether reversing acidification reversed the loss of Ψ_{pm}. After the ammonium chloride was washed away, some TLF-1 induced loss of Ψ_{pm} was observed, suggesting that a fraction of internalized ApoL1 remained active (Figure 3.1D).

We also investigated whether TLF-1 induced a loss of mitochondrial membrane potential (Ψ_{mito}). Recently, both ApoL1 and human serum caused an early loss of Ψ_{mito} in treated *T. b. brucei,* correlating with ApoL1 localization to the mitochondrial membrane (18). Because of overlapping in fluorescence spectra, direct comparison between the mitochondrial and plasma membrane potential of the same cells was not possible. Rather, cells were treated separately either with TMRM (tetramethylrhodamine, Ψ_{mito}) or bisoxonol (Ψ_{mito}) for flow cytometry analysis. A decrease in TMRM fluorescence corresponds to a loss of Ψ_{mito}, with the unstained control arbitrarily set to represent 100% loss of membrane potential. As previously shown with ApoL1, TLF-1 induced a rapid loss of Ψ_{mito} in *T. b. brucei,* completely dissipating the Ψ_{mito} within 15 min after TLF-1 incubation (Supplemental Figure 3.3A and C). In fact, TLF-1 induced loss of Ψ_{mito} surpassed the intermediate loss of Ψ_{mito} observed using the un-coupler CCCP (m-chlorophenylhydrazone) as a positive control (Supplemental Figure 3.3C). The TLF-1 induced loss of mitochondrial membrane

potential occurred with remarkably similar kinetics to the TLF-1 induced loss of plasma membrane potential (Supplemental Figure 3.3A and B). Therefore, it is impossible to attribute one membrane potential loss as the precursor or cause of the other. Rather, our data suggest that ApoL1 is active in multiple organelles including the plasma membrane and the mitochondrion.

ApoL1 lysis requires cation and chloride flux through the plasma membrane

Consistent with ApoL1 inducing ion flux at the plasma membrane, isotonic replacement of trypanosome buffers with large cations (tetramethyl ammonium, choline, and tetraethylammonium) has been shown to prevent TLF-1 lysis (57). We extended this list to include a large cation used for osmotic studies: N-methyl-D-glucamine (NMDG+) (171). *T. b. brucei* cells were loaded with TLF-1 in complete media by blocking their endosome-lysosome fusion by incubation at 15˚C (which does not harm the cells). The TLF-1 loaded *T. b. brucei* were washed into buffers with 120mM of either Na^+, $NMDG^+$, or K^+ (along with Cl^-, glucose, BSA, and HEPES buffer). Lysis was recorded after one hour. The cell impermeable cation NMDG+ prevented lysis (Figure 3.2A). However, TLF-1 was equally effective at lysing cells in the high K^+ buffer as in the Na^+ buffer (Figure 3.2A). These data suggest that the ApoL1 cation channel may transport either K^+ or Na^+ during lysis, and disruption of either major cation flux can induce lysis of *T. b. brucei*. Consistent with the lysis data, TLF-1 induces Ψ_{pm} loss in both Na^+ and K^+ buffers (Figure 3.2B). Similarly, Ψ_{mito} loss occurred in TLF-1 treated

cells in both Na^+ and K^+ buffers (Supplemental Figure 3.4C, D, and E).

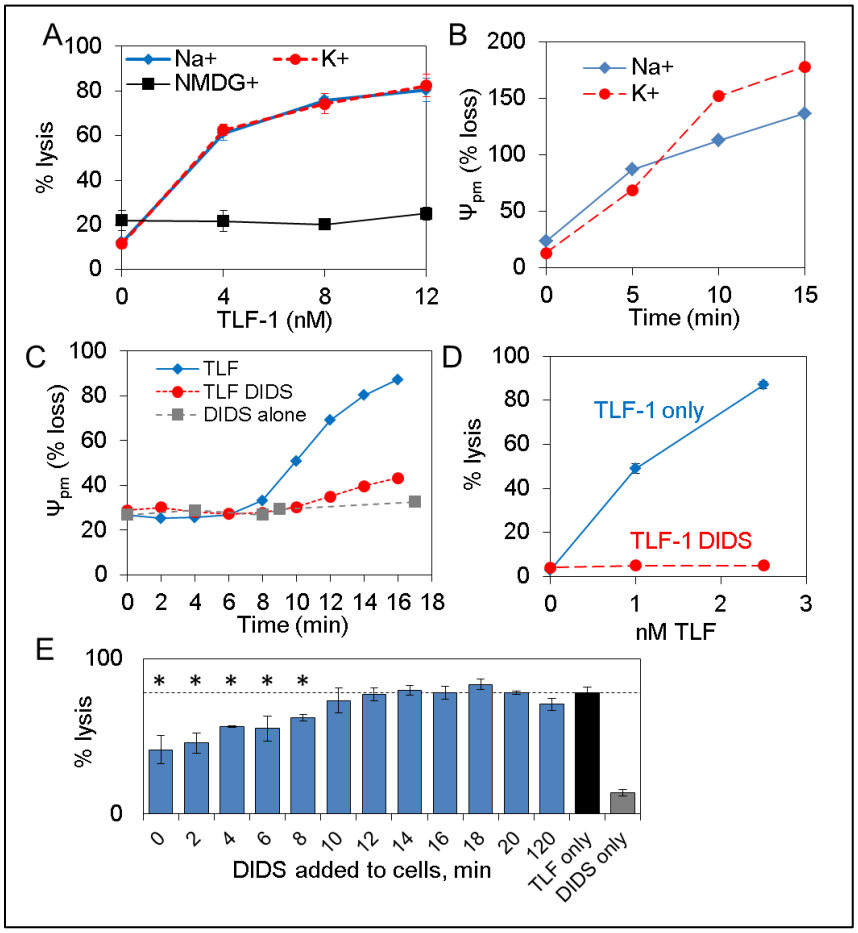

Figure 3.2: **Cation and Chloride Flux across the Plasma Membrane is Necessary for TLF-1 Lysis.** (**A**) TLF-1 Lysis requires cations. TLF-1 Lysis assay (2hr) for *T. b. brucei* in Na^+ buffer (blue diamonds), K^+ buffer (red circles, dashed line), or $NMDG^+$ buffer (black squares). *T. b. brucei* were pre-loaded with TLF-1 at 15˚C for one hour before washing into the indicated buffers and incubating at 37˚C for 1 hr before cells were placed on ice and counted. N=3 experimental replicates; error bars show standard deviation. (**B**) TLF-1 induces Ψ_{pm} loss in cells pre-incubated in Na^+ buffer (blue diamonds) or K^+ buffer (red circles, dashed line) for about 1 hr before flow cytometry analysis of Ψ_{pm}. N=1. (**C**) DIDS prevents TLF-1 induced Ψ_{pm} loss. TLF-1 (8nM, green triangles); 300μM DIDS added concurrently with TLF at time 0 (red diamonds, dashed line); DIDS alone (grey squares, dotted line). N=1, representative assay. (**D**) DIDS prevents TLF-1 lysis. TLF-1 lysis assay at 2hr for *T. b. brucei* treated with TLF-1 only (blue diamonds), or TLF-1 plus DIDS (300μM) incubated together at 37˚C for 2hr before counting cells. N = 3 experimental replicates; error bars show standard deviation. (**E**) DIDS only effective if added before Ψ_{pm} loss. DIDS (300μM) added to TLF-treated cells at different times after TLF-1 (12nM) addition. Lysis counts at 2hr. N=3 experimental replicates; error bars show standard deviation. *p-value <0.01 for DIDS treatment compared to TLF-1 only sample (2 tailed t-test).

We next investigated the role of chloride flux through the plasma membrane during TLF-1 lysis of *T. b. brucei.* Replacing chloride in the media with larger anions (gluconate) or adding the chloride channel inhibitor DIDS prevents lysis (14, 57). We found that DIDS prevents both ApoL1-induced Ψ_{pm} loss and cell death (Figure 3.2C and D). When followed for longer times, some loss of Ψ_{pm} occurred in cells treated with DIDS and TLF-1, but the Ψ_{pm} loss was attenuated by DIDS (Supplemental Figure 3.6A and B). Thus, DIDS may prevent TLF-1 lysis of *T. b. brucei* by preventing the ApoL1-induced loss of Ψ_{pm}.

In order to investigate the kinetics of chloride channel involvement, we incubated *T. b. brucei* with TLF-1 and added DIDS to aliquots of TLF-1 treated cells at different time-points. Dead cells were counted in all samples after two hours. DIDS was only effective at preventing lysis if added during the first 10 minutes of TLF-1 incubation (Figure 3.2E). Thus, chloride channel opening during the initial ionic disruption due to ApoL1 is critical for Ψ_{pm} loss and subsequent lysis.

Kinetics of osmotic swelling and cell lysis

TLF-1 and ApoL1 killing involves a series of morphologically distinct stages. After TLF-1 addition to *T. b. brucei* there is a lag phase of at least 20 minutes during which TLF-treated cells maintain normal morphology (61). Then cells begin to swell into visibly rounded kite-shapes, and eventually these rounded cells undergo osmotic lysis. These stages are visualized in fields of TLF-1 treated cells shown in Figure 3.3A.

In order to quantitate the osmotic cell swelling kinetically, we developed a flow cytometry-based assay. On flow cytometry, cell shape corresponds to changes in the

forward and side-scatter of the laser. TLF-1 treated *T. b. brucei* exhibit a similar shift in forward and side scatter compared to cells swollen in hypotonic buffer (Figure 3.3B). Cells were gated into a “normal,” “round,” and “dead” cell populations, and the percentage of the total cells in each gate were followed over time (Figure 3.3C). As a validation of this method, dead cells gated by light scatter alone overlapped almost completely with dead cells differentiated by propidium iodide uptake (Figure 3.3D). As an alternative to gating different populations of cells, the increase in the side scatter over time (proportional to the control) was used as a proxy for swelling of non-dead trypanosomes (Figure 3.3E).

The kinetics reveal that TLF-1 treated cells become swollen before dying (Figure 3C). The initial kinetics of cell rounding was similar between the different concentrations of TLF-1 tested. At a certain point, the percent rounded cells diminished as they died, though the non-dead cell population continued to swell (Figure 3.3C and E). The percentage of dead cells rose more rapidly in cells treated with higher concentrations of TLF-1 (Figure 3.3C). Although a distinct swollen population did not arise until later, an increase in side-scatter reveals that TLF-1 treated *T. b. brucei* begin swelling after 10-20 minutes of TLF-1 incubation (Figure 3.3E). In contrast, TLF-1 induced Ψ_{pm} loss plateaus after the first 20 min of lysis and precedes cell swelling.

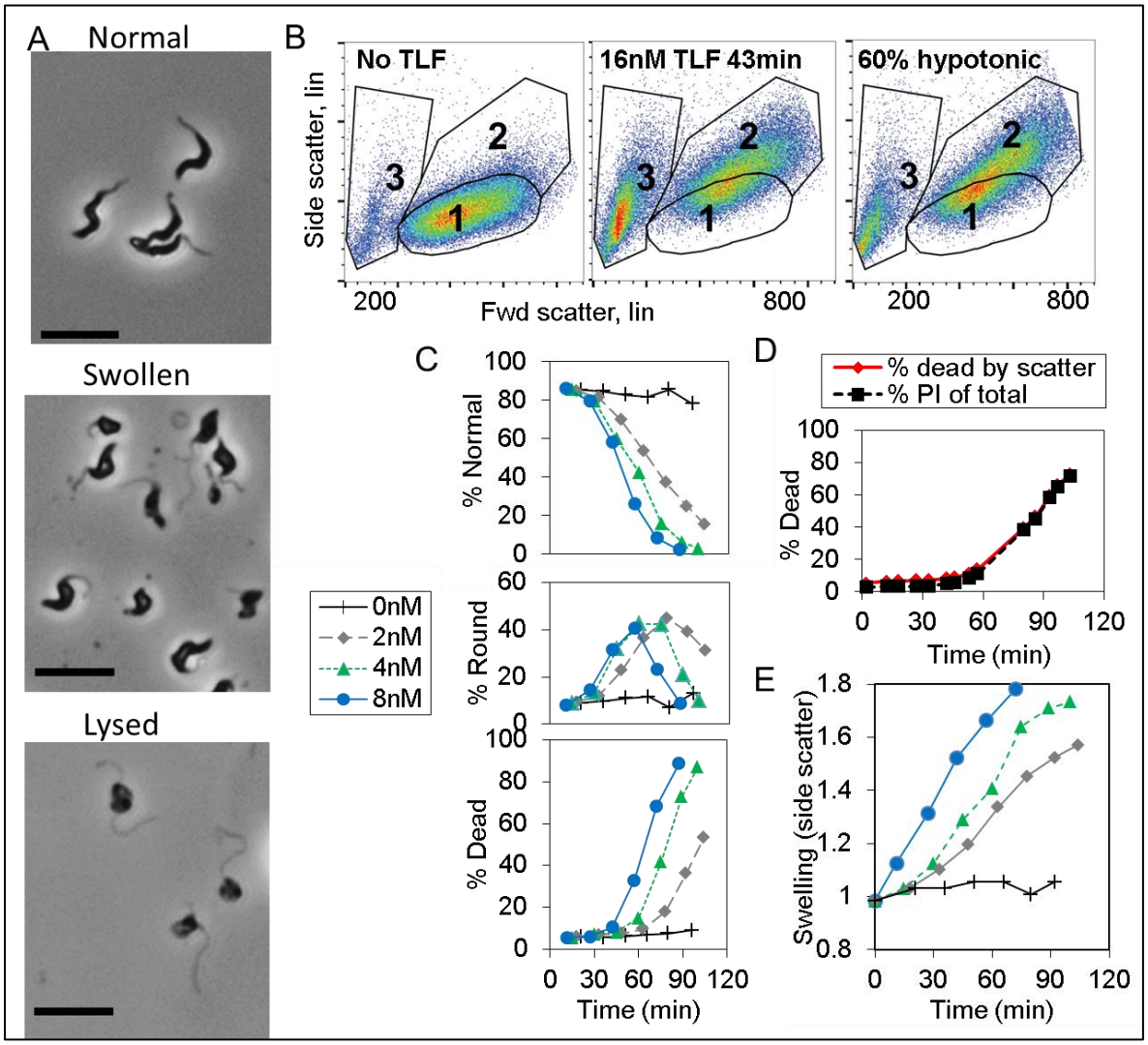

Figure 3.3: **Kinetic analysis of TLF-1 induced osmotic swelling**. (**A**) Phase contrast photos showing normal shaped, swollen, and lysed *T. b. brucei* after TLF-1 treatment. *T. b. brucei* were treated with 50nM TLF-1 for 30 min (top), 45 min (middle), 65 min (bottom). Bar length, 20µm. Representative photos. (**B**) Gating scheme for cell morphology based on light scatter. Top: no TLF-1 control. Middle: cells treated with 16nM TLF-1 for 43 min. Bottom: scatter plot of cells in 60% hypotonic diluted buffer, assayed immediately after hypotonic shock. Gate 1 indicates cells with normal morphology, gate 2 shows cells in the rounded morphology, and gate 3 shows cells gated as dead. Representative gating scheme. (**C**) Kinetics of swelling and death during TLF-1 treatment. Gated populations of normally shaped (left), round (center), and dead cells (right) as % of total cells counted. Refer to legend on the left for TLF-1 concentrations (0-8nM) added at 0 min. N=1, representative data. (**D**) Dead cells gated by side scatter represent the cell population permeable to propidium iodide. TLF-1 (3nM) was added at time 0 min. Cells gated by light scatter (red diamonds, dotted line)

or propidium iodide uptake (black squares, dotted line) N=1, representative data. (**E**) Swelling of the TLF-1 treated cells shown in panel C as measured by proportion of side scatter (excluding dead cells) treated with.TLF-1 (0-8nM). Refer to the legend to the left of panel C. N=1, representative data.

Slowing or preventing membrane potential loss prevents swelling and lysis

We utilized flow cytometry to observe the kinetics of cell swelling and lysis in cells where TLF-1 was blocked at various points in the lytic process. In all cases, if the Ψ_{pm} was dissipated, cell swelling and death followed. Firstly, preventing high affinity receptor-mediated uptake of by treating HpHbR KO cells with TLF-1 (50nM) or ApoL1 (50nM) dramatically slowed cell swelling and lysis (Figure 3.4A, B, and C). The HpHbR KO cell swelling data come from the same cells shown in Figure 3.1B, revealing that swelling and lysis occur with slower kinetics than Ψ_{pm} loss. Secondly, inhibiting ApoL1 in the endosomal system by treating Ty-SRA-expressing *T. b. brucei* with TLF-1 (20nM) prevented swelling and lysis (Supplemental Figure 3.5). Thirdly, preventing Ψ_{pm} loss in trans by blocking chloride channels with DIDS during TLF-1 treatment prevented cell swelling and lysis (Figure 3.4D and E). The Ψ_{pm} for the DIDS treated cells was shown in Figure 3.2C. DIDS alone did not increase cell swelling or death in the absence of TLF-1 (Figure 3.4E and Supplemental Figure 3.6C).

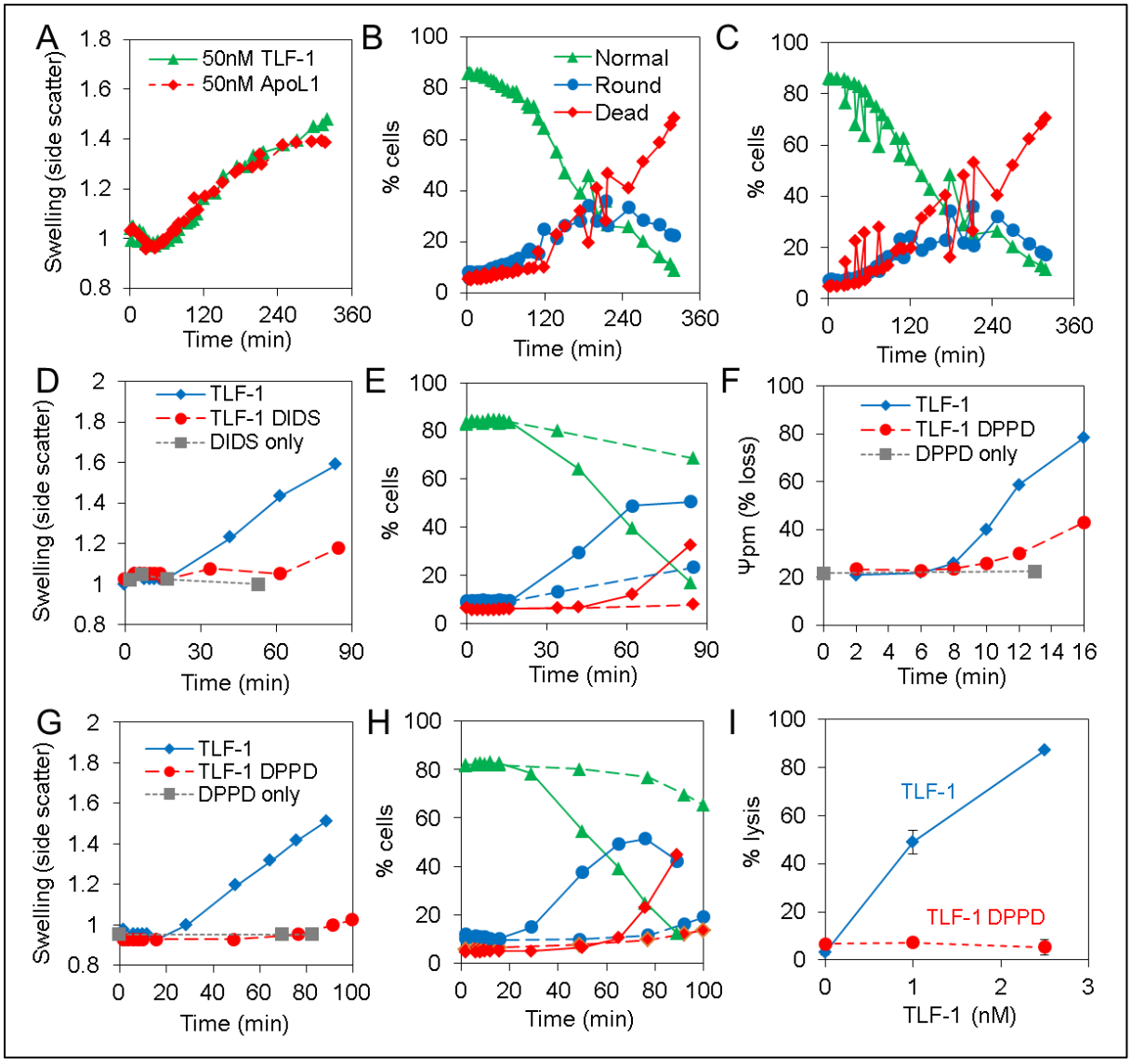

Figure 3.4: **Preventing TLF-1 from causing Ψpm loss prevents cell swelling and lysis**. (**A**) Slow cell swelling of HbHbR KO *T. b. brucei* treated with 50nM TLF-1 or 50nM ApoL1. These are identical cells to Figure 3.1B. (**B**) Cell morphology of TLF-1 treated HpHbR KO *T. b. brucei* shown in panel A. For all cell morphology graphs, cells gated as normal cells are green triangles, rounded cells are blue circles, and dead cells are red diamonds. (**C**) Cell morphology of ApoL1 treated HpHbR KO *T. b. brucei* from panel A. (**D**) Side scatter and (**E**) cell morphology analysis shows that DIDS prevents cell swelling. Co-addition of TLF-1 (8nM) and DIDS (300μM): red circles and dashed line; TLF-1 alone: blue diamonds; DIDS alone: grey squares, dotted line. This is a cell morphology analysis of the cells in Figure 3.2C. (**F**) The antioxidant DPPD prevents TLF-1 induced Ψ_{pm} loss. *T. b. brucei* were pretreated with 300μM DPPD for 1hr before adding 2nM TLF-1 (red circles, dashed line). TLF-1 alone: blue diamonds. DPPD alone: grey squares, dotted line. N=1 representative assay. (**G**) Side scatter and (**H**) cell morphology analysis of the DPPD and TLF-1 treated cells shown in panel F. (**I**) DPPD

prevents cells lysis. *T. b. brucei* were pretreated with 300μM DPPD for 1hr before adding TLF-1 (red circles, dashed line), or TLF-1 alone (blue diamonds). Cell counts taken after 2hr. Error bars show standard deviation of 3 experimental replicates.

Oxidative processes have been shown to be involved in the TLF-1 lysis with TLF-1 induced thiol oxidation causing osmotic stress in *T. b. brucei* (47). The lipophilic antioxidant DPPD prevents TLF-1 lysis of *T. b. brucei*, so we used DPPD to investigate whether oxidation occurs before or after ApoL1-induced Ψ_{pm} loss (47). Pre-incubating *T. b. brucei* with DPPD prevented TLF-1 from causing Ψ_{pm} loss, suggesting that oxidative processes contribute to ionic disruption early in the lytic process (Figure 3.4F, Supplemental Figure 3.7A and B). By blocking Ψ_{pm} loss, DPPD also prevented cell swelling and lysis (Figure 3.4G, H, and I). In the absence of TLF-1, DPPD addition did not cause cell swelling or lysis (Figure 3.4G, Supplemental Figure 3.7C).

DISCUSSION

The mechanism by which the human innate immune factor TLF-1 kills *T. b. brucei* parasites is controversial and not well characterized. In this paper we present evidence that ApoL1 perturbs ion flux at the plasma membrane of *T. b. brucei* causing a rapid loss of plasma membrane potential (Ψ_{pm}). The ApoL1-induced loss of Ψ_{pm} precedes and causes cell swelling and osmotic lysis.

Three major models for TLF-1 lysis involve damage to three different organelles where the ApoL1 channel has been experimentally localized or inferred to reside. The three postulated localizations of ApoL1 channel activity are the lysosome, the mitochondrion, and the plasma membrane (see Supplemental Figure 3.8). Historically, localization of TLF-1 and ApoL1 localization to the lysosome of *T. b. brucei* has been

linked to permeabiliztion of the lysosomal membrane and enlargement of the lysosome (15, 44, 56, 96). Lysosomal damage, however, occurred relatively late in the lytic process, and the morphological characteristics and timing of lysosomal damage varied between different labs and assay conditions. The discovery that ApoL1 is active at neutral pH and traffics to non-lysosomal organelles led to the hypothesis that the ApoL1 may recycle to the plasma membrane (16, 18). At the plasma membrane, ApoL1 induces a loss of plasma membrane potential and osmotic swelling leading to cell death (16, 47). Finally, ApoL1 trafficking to the mitochondrion is linked to mitochondrial membrane potential loss and apoptosis-like programmed cell death in *T. b. brucei* (18).

We chose to compare plasma membrane and mitochondrial damage in TLF-1 treated cells because the lysosomal model for ApoL1 killing has been primarily dismissed by recent data (18, 47). Comparing the kinetics of mitochondrial and plasma membrane phenotypes, we found that TLF-1 induces a loss of plasma membrane potential (Ψ_{mito}) in *T. b. brucei* with similar rapid kinetics to dissipation of the mitochondrial membrane potential (Ψ_{mito}). Because the two membrane potentials are both rapidly dissipated, osmotic stress and apoptosis-like cell death pathways may be concurrently activated during TLF-1 lysis. The interplay between apoptotic and osmotic stress responses may be important to interpreting observations of TLF-1 treated *T. b. brucei*. For instance, influx of Ca^{2+} into the cell, leads to mitochondrial Ca^{2+} influx which can lead apoptosis-like programmed cell death in *T. b. brucei* (17, 265). Therefore, ApoL1 at the plasma membrane may cause damage to the mitochondrion, and vice versa. Overall, however, the rapid kinetics of cell swelling and lysis seem more consistent with a primarily necrosis-like cell death via ApoL1 in the plasma membrane

rather than apoptosis-like programmed cell death via ApoL1 in a mitochondrial membrane (18).

ApoL1-induced loss of Ψ_{pm} is likely due to both K^+ and Na^+ flux through ApoL1 as well as the stress-induced movement of ions through endogenous plasma membrane transporters. The role of external ions in TLF-1 killing of *T. b. brucei* had been investigated previously. Early research showed that, similar to hypotonically stressed *T. b. brucei*, TLF-1 treatment caused an efflux of potassium and an influx of calcium in *T. b. brucei* (61). In agreement with previous work, we showed that replacement of K^+ and Na^+ in the lysis buffer with a larger cation ($NMDG^+$) prevented lysis by preventing cation influx (Figure 3.2A) (57). Unlike the previous study, we added $NMDG^+$ to cells that were pre-loaded with TLF-1 by a 15˚C endosomal trafficking block. This ensured that the large cation did not act by inhibiting endosomal or lysosomal activity, but directly by prevented cation flux through the plasma membrane.

We investigated the importance of ApoL1-induced Na^+ and K^+ fluxes during lysis in *T. b. brucei*. In HEK cells overexpressing ApoL1, K^+ ion efflux was determined to be critical for cell death (234). In the HEK cells, a high K^+ buffer prevented K^+ efflux and osmotic cell death associated with to ApoL1 at the plasma membrane (234). In contrast, in *T. b. brucei,* high K^+ buffer did not prevent TLF-1 induced lysis or the early events of plasma membrane and mitochondrial membrane potential loss (Figure 3.2 A and B and Supplemental Figure 3.4). Thus, it seems that the influx of cations, but not an efflux of K^+, is required for ApoL1-induced cell death in *T. b. brucei*.

The plasma membrane potential of most cell types is dissipated by placing the cells in high K^+ buffer because the Na^+/K^+ gradient across the membrane disappears.

In our experiments, however, bloodstream form *T. b. brucei* had normal Ψ_{pm} after incubation in high K^+ buffer for approximately one hour (Figure 3.2B). Some studies have observed no loss of Ψ_{pm} in *T. b. brucei* in high K^+ buffer (unless a K^+ ionophore is added), while another group showed a concentration-dependent loss of Ψ_{pm} due to K^+ addition (170, 171, 183, 184). The source of these discrepancies is unclear due to the paucity of studies on plasma membrane channels in trypanosomes. Unlike most previous work, in our experiments, the Ψ_{pm} was measured after incubating for an hour in high-K^+ buffer, possibly allowing *T. b. brucei* to activate compensatory mechanisms to restore their Ψ_{pm}. Overall, our data indicate that influx of Na^+ or K^+ cations through ApoL1 and endogenous channels is required for lysis, but efflux of K+ (which would not occur in high K^+ buffer) is not important. In a physiological context where external Na^+ ion concentration is high and K^+ ion concentration is low, ApoL1 likely mediates the influx of Na^+ down its concentration gradient.

Chlorine flux in TLF-1 treated cells has been shown to be critical for TLF-1 induced lysis of both *T. b. brucei* and kidney cells (14, 57, 229). The chloride channel inhibitor DIDS does not inhibit ApoL1 channel directly, and likely works in trans to prevent chloride flux through an endogenous parasites channel in the plasma membrane (or channels) (14). It is also possible that DIDS prevents TLF-1 lysis by acidifying the *T. b. brucei* cytosol, perhaps through off-target inhibition of pyruvate transporters (182, 186). Our work shows that DIDS-sensitive chloride channels are critical very early on in the lytic process, and that blocking chloride channels prevents ApoL1-mediated Ψ_{pm} loss (Figure 3.2C). In fact, blocking chloride channels after the Ψ_{pm} has been dissipated has no additional protective effect (Figure 3.2E). Either the

chloride channels only open during the initial ten minutes of *T. b. brucei* stress response, or beyond that initial window of time the Ψ_{pm} is completely dissipated and the cells have irreversibly committed to osmotic lysis.

Ionic disruption of the Ψ_{pm} in TLF-treated *T. b. brucei* causes osmotic swelling. Osmotic swelling of TLF-1 treated *T. b. brucei* has been observed in reports on TLF-1 mechanism, even when swelling is not central to the published model (12, 18, 43, 47). We quantified the extent and kinetics of cell swelling in TLF-1 treated *T. b. brucei* under various conditions. Our flow cytometry assay showed the *T. b. brucei* population beginning to swell within the first ten minutes of the lytic process, with swelling continuing until all swollen cells die (Figure 3.3).

Disrupting the lytic process at various stages slows or prevents the ApoL1-induced loss of Ψ_{pm}, swelling, and cell lysis. For instance, when high affinity uptake of TLF-1 is prevented using HpHbR knockout *T. b. brucei,* slow fluid phase uptake of TLF-1 leads to a loss of Ψ_{pm}, swelling, and lysis over hours rather than minutes. When ApoL1 is inhibited by SRA, cells show no TLF-1 induced responses. Blocking chloride channels with DIDS prevents ApoL1-induced Ψ_{pm} loss, swelling, and cell lysis, showing the importance of chloride flux to the lytic mechanism. Also downstream of ApoL1 membrane insertion, the antioxidant DPPD prevents Ψ_{pm} loss, cell swelling, and lysis. These data suggest that ApoL1 membrane insertion and plasma membrane trafficking quickly trigger osmotic stress response pathways including activation of endogenous chloride channels and protein oxidation (47).

In conclusion, we show that TLF-1 induces rapid changes at the plasma membrane of *T. b. brucei* leading to parasite swelling and lysis. Using flow cytometry,

genetic, and pharmacological manipulation, we developed a detailed kinetic profile of TLF-1 lysis (see Supplemental Table 3.1). In our model, ApoL1 from TLF-1 inserts into an endosomal membrane and a proportion of the ApoL1 recycles to the plasma membrane. Within the plasma membrane, ApoL1-induced influx of Na^+ disrupts ionic homeostasis, causing Ψ_{pm} loss, osmotic swelling, and eventual cell lysis. While ApoL1 may disperse to various parasite membranes, including vesicular trafficking compartments, the lysosome, the mitochondrion, and the plasma membrane, our data suggest that unregulated swelling via the plasma membrane is a core feature of TLF-1 induced cell death.

EXPERIMENTAL PROCEDURES

Trypanosome growth and preparation for assays

Bloodstream form *T. b. brucei* Lister 427(MiTat 1.2) were cultured *in vitro* as described previously (47). Unless otherwise indicated, trypanosomes assays were performed in culture media with mid-log phase cells.

Flow Cytometry Assays

T. b. brucei at a starting density of 0.5-1E6 cells/mL were pelleted and re-suspended in fresh media (full serum-containing media) at 1E7 cells/mL, and incubated on a 37˚C cell shaker, set to mix at 300rpm. At time zero, TLF-1 was mixed with the cells. At each time point, 75µL of the cell mixture was added to 300µL of a media-bisoxonol mixture for a final concentration of 0.5µM bisoxonol. Bis-(1,3-Diethylthiobarbituric Acid)Trimethine Oxonol (bisoxonol) was from Molecular Probes (Eugene, Oregon, USA). The cells were incubated with bisoxonol at room temperature for exactly 2 minutes. At exactly the 2 minute time-point the cells were analyzed by

Beckman-Coulter Cyan with an excitation of 488 with the 585/42 BP filter for emission. Data were analyzed with FlowJo software. Bisoxonol fluorescence was subtracted from the unstained cells fluorescence, and percentages were calculated of fluorescence of cells co-incubated with 0.8μM gramicidin D (Sigma-Aldrich) and bisoxonol for 2 minutes prior to cytometry analysis. For histograms in the supplemental data, log fluorescence values are plotted on the X-axis.

For Figure 3.2B, Supplemental Figure 3.3, and Supplemental Figure 3.4, the protocol was modified slightly to parallel the protocol for mitochondrial membrane potential. Rather than diluting the cells into bisoxonol-containing media, bisoxonol (0.5μM) was added to 300 μL of 2E6 cells/mL for 2 minutes at 37˚C before flow cytometry analysis. TMRM (tetramethylrhodamine methyl ester) was incubated with the cells at a 250nM concentration for 10 min at 37˚C before analysis on flow cytometry using an excitation wavelength of 488 and 585/42 BP filter for emission. Data were analyzed on FlowJo software. 0% membrane potential loss was set as the median fluorescence for control dyed samples with background fluorescence from unstained sample subtracted. Gramicidin D (0.8μM) or the un-coupler CCCP (50μM, carbonyl cyanide m-chlorophenyl hydrazine) was added concurrently with the TMRM dye as positive controls.

Cell morphology was analyzed concurrently with changes in the membrane potential. Cells shape characteristics were plotted on a forward vs side-scatter plot (with linear axis) with normal and dead cell gates drawn based on the unstained sample, and rounded cell gates drawn based on the cell population in TLF-treated samples. Percentages plotted are the percent in each gate of the total cells counted.

Propidium iodide (PI, from Sigma-Aldrich) was incubated with the cells at a 5μM concentration in media and on ice for about 1 minute before the start of the flow run. To assess cell swelling over time, the median side-scatter of cells was analyzed on FlowJo software, with cells gated as dead excluded from the analysis. Proportional side scatter values were plotted as the proportion of the median side-scatter of untreated controls.

TLF and ApoL1 purification

TLF and ApoL1 were purified as described previously (21). Briefly, purified human HDLs were eluted from an anti-Hpr column and dialyzed against PBS with EDTA (PBSE) for purified TLF. For ApoL1 purification, purified TLF was solubilized in CHAPS and eluted from an anti-ApoL1 column and dialyzed into PBSE. SDS-PAGE gels and Western blots against Hpr and ApoL1 confirmed the identity and purity of TLF and Apol1 preparations.

TLF-1 and ApoL1 lysis assays and cation replacement experiments

Lysis assays were performed as previously reported with 300 μL of 1E7 trypanosomes/mL in HMI9-based serum containing media, and TLF-1 pre-incubated briefly on ice with 50 equivalents of human hemoglobin A from Sigma-Aldrich (St. Luis, MO, USA) (47). For Figure 3.2A, TLF-1 was loaded into cells in complete serum-containing media at 15˚C for 1 h before washing the cells three times into defined buffers. All buffers contained 38mM glucose, 25mM HEPES, and 1% BSA, and were brought to pH 7.4. The Na^+-only buffer contained 120mM NaCl, the K+ buffer contained 120mM KCl, and the $NMDG^+$ (n-methyl-d-glucamine, from Sigma) contained 120mM with HCl added to adjust the pH to 7.4, and provide a chloride counter-ion. For membrane potential experiments with the different cation buffers, half of the normal

concentration of bisoxonol (250nM) and TMRM (125nM) were used for the flow cytometry assays because the lack of serum components in these buffers led to a higher background fluorescence from dye uptake.

SUPPLEMENTAL DATA

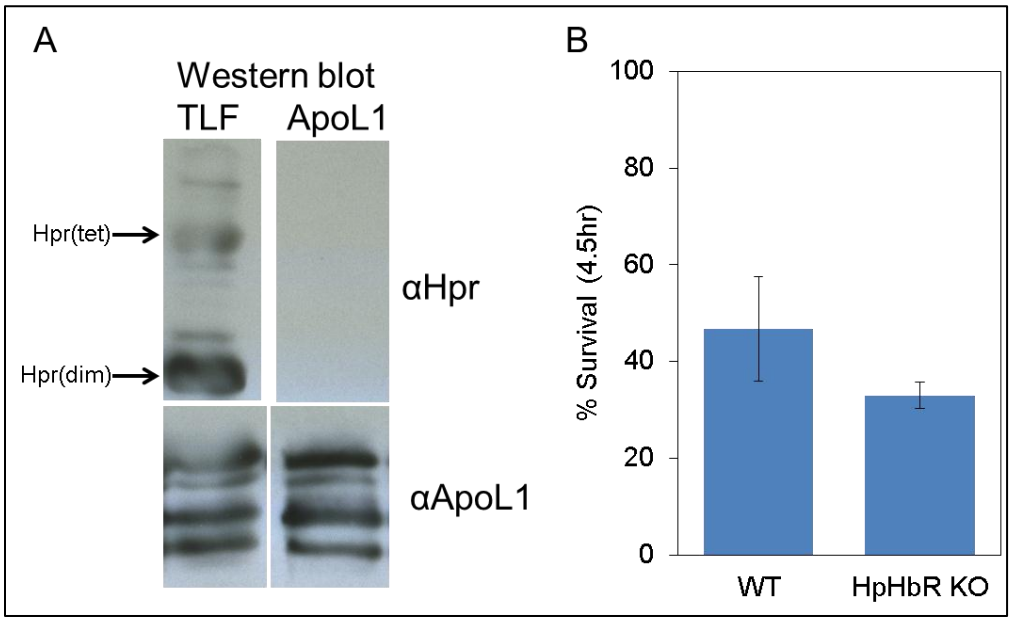

Supplemental Figure 3.1: **ApoL1 is Free from TLF-1 Contamination**. (**A**) ApoL1 and TLF-1 were loaded onto SDS-PAGE gels, blotted, and probed with anti-apoL1 and anti-Hpr antibodies. Twice as many apoL1 molecules were loaded as TLF-1. Hpr tetramer (tet) and Hpr dimer (dim) are isoforms which run at about 45 and 90kDa, respectively. There are four apolipoprotein L1 (ApoL1) isoforms around 40kDa visible by Western blot. (**B**) ApoL1 (50μL) was added to T. b. brucei cells and the surviving cells were counted and compared to PBS controls to yield the % surviving cells after 4.5hr. WT = wild type. HpHbR KO is in *T. b. brucei*.

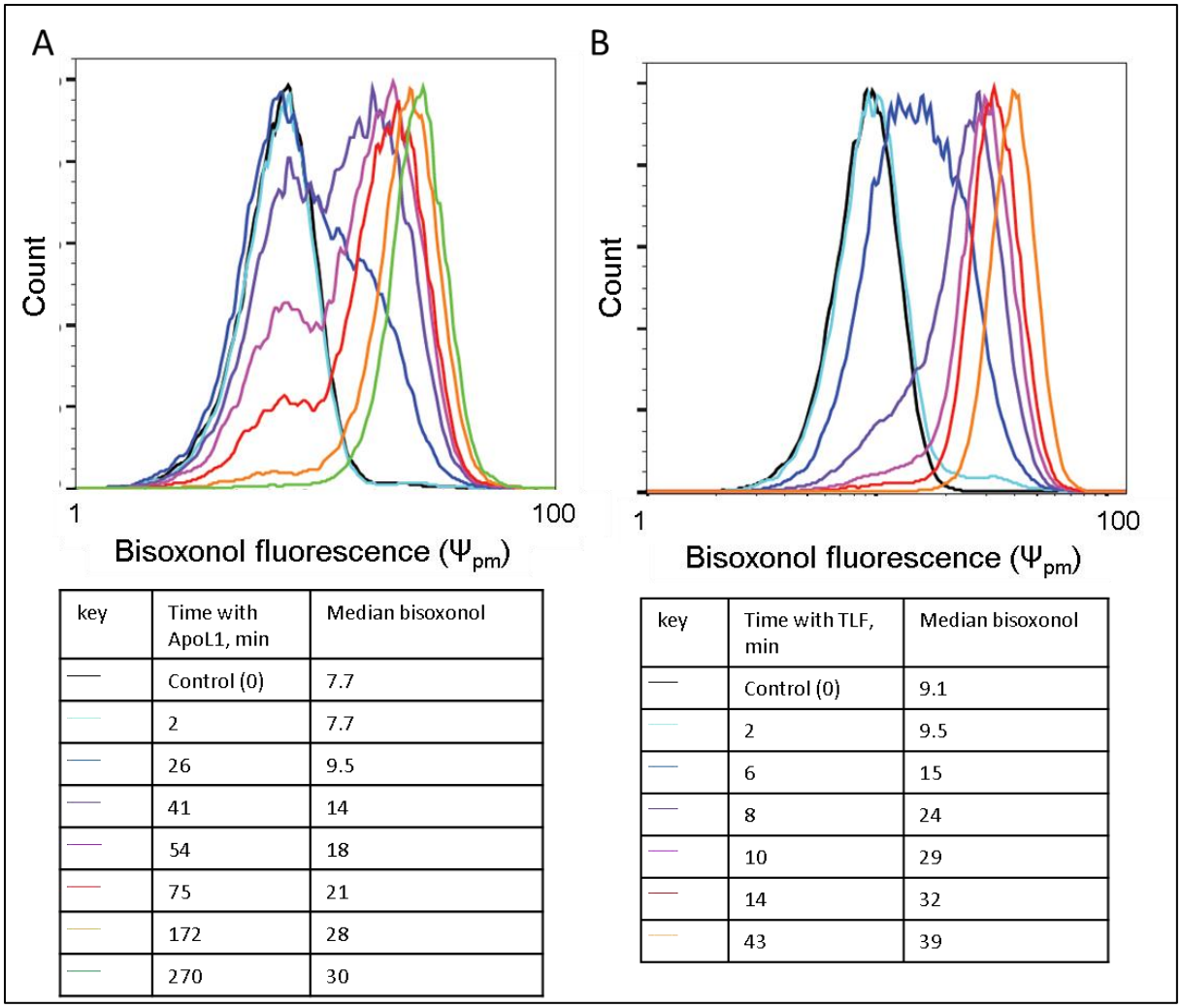

key	Time with ApoL1, min	Median bisoxonol
	Control (0)	7.7
	2	7.7
	26	9.5
	41	14
	54	18
	75	21
	172	28
	270	30

key	Time with TLF, min	Median bisoxonol
	Control (0)	9.1
	2	9.5
	6	15
	8	24
	10	29
	14	32
	43	39

Supplemental Figure 3.2: **Histograms of the Ψ_{pm} for cells** treated with either (**A**) 50nM ApoL1 in HpHbR knockout cells, or (**B**) 16nM TLF-1 in wild-type *T. b. brucei* cells. The data in panel B is plotted in the scatter plot of Figure 3.1B. The two peaks in ApoL1-treated cells suggest two populations of cells, some of which have taken up ApoL1 and lost their Ψ_{pm}, and others which have taken up no ApoL1 and not lost their Ψ_{pm}. In contrast, TLF-1 treated *T. b. brucei* almost simultaneously lose their Ψ_{pm} because of synchronized TLF-1 uptake via the HpHbR.

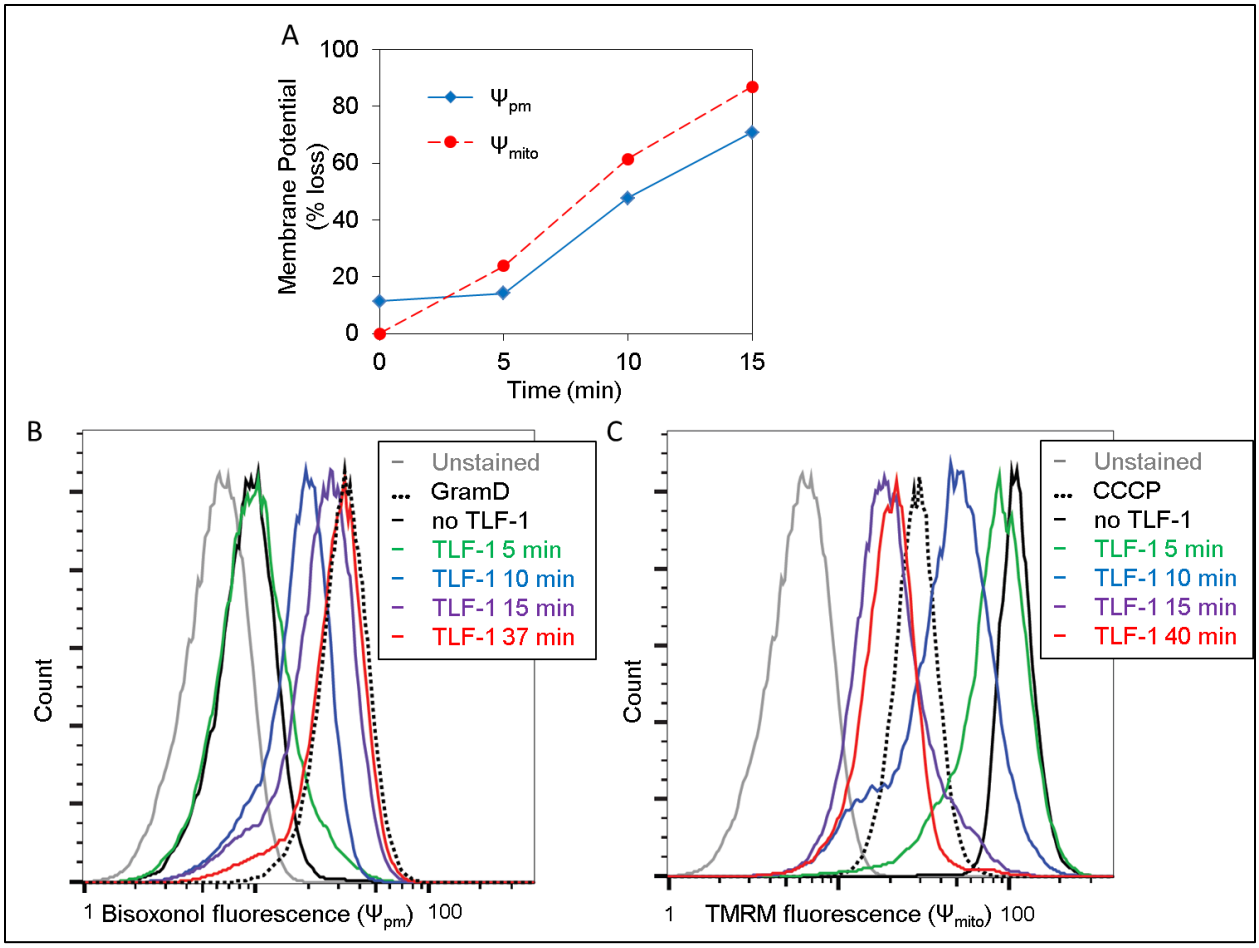

Supplemental Figure 3.3: **TLF-1 causes a rapid loss of both Ψ_{mito} and Ψ_{pm} potential**. (**A**) Ψ_{mito} and Ψ_{pm} potential % loss assessed by flow cytometry from the TMRM (Ψ_{mito}) or bisoxonol (Ψ_{pm}) fluorescence. TLF-1 (10nM) and Hb were added to cells at the indicated times before the flow cytometry run. N=1 representative experiment. (**B**) Histograms for the Ψ_{pm} data in from panel A, with the gramD (0.8 μM, 2 min) control shown. (**C**) Histogram for the Ψ_{mito} data from panel A, with the CCCP (50μM, 20min) control shown.

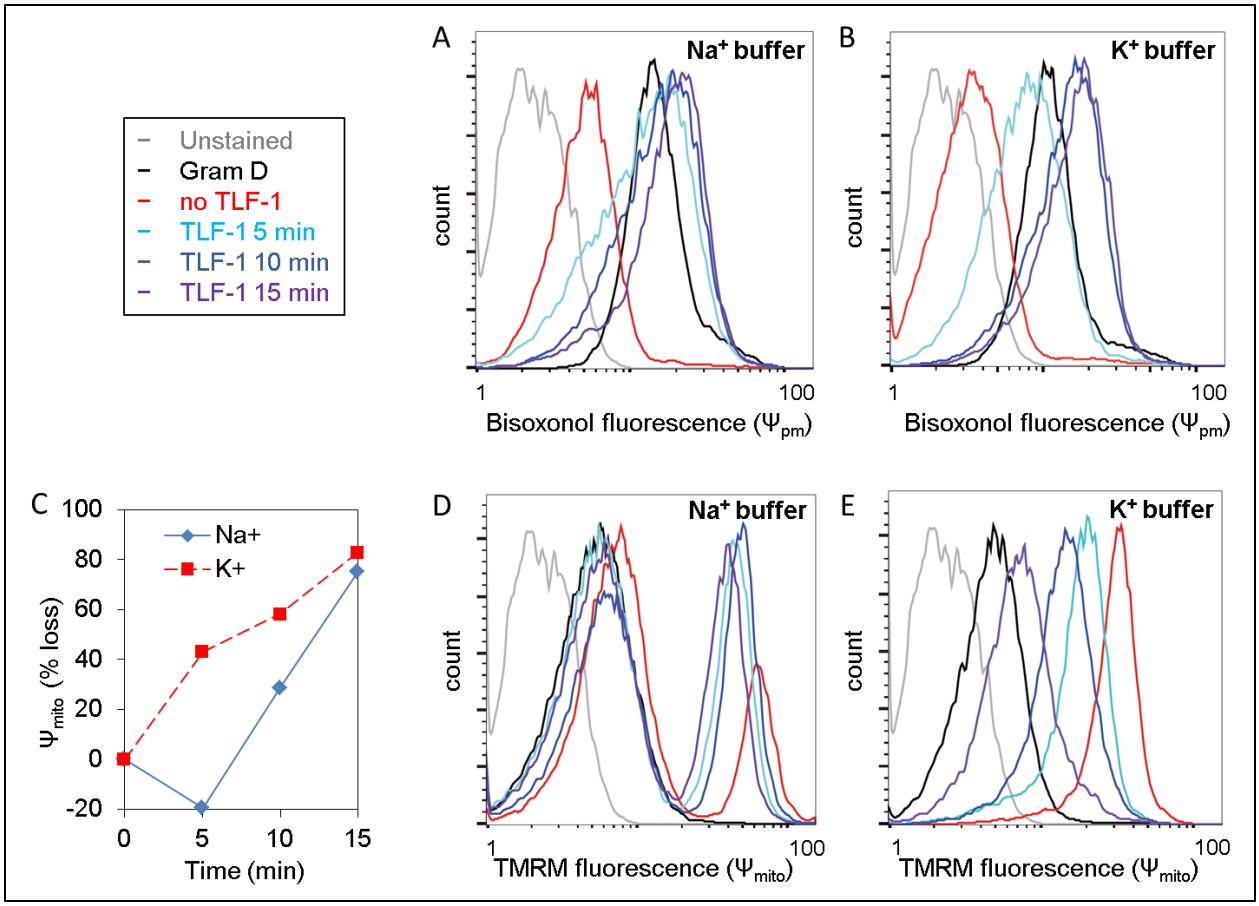

Supplemental Figure 3.4: **In both Na^+ and K^+-dominated buffers, TLF-1 induces a rapid loss of plasma membrane potential and mitochondrial membrane potential**. The Legend on the left refers to panels A, B, D, and E. Gram D (0.8µM) was added for 2min to the Ψ_{pm} experiments and for 10 min to the Ψ_{mito} experiments as a positive control for membrane potential loss. (**A**) Histogram for the plasma membrane potential data from Na^+ buffer plotted in Figure 3.2B and (**B**) Histogram for the plasma membrane potential data from K^+ buffer plotted in Figure 3.2B. (**C**) The percentage mitochondrial membrane potential loss in Na^+ and K^+ buffers plotted from the histogram data in panel (**D**) (Na^+ buffer) and panel (**E**) (K^+ buffer).

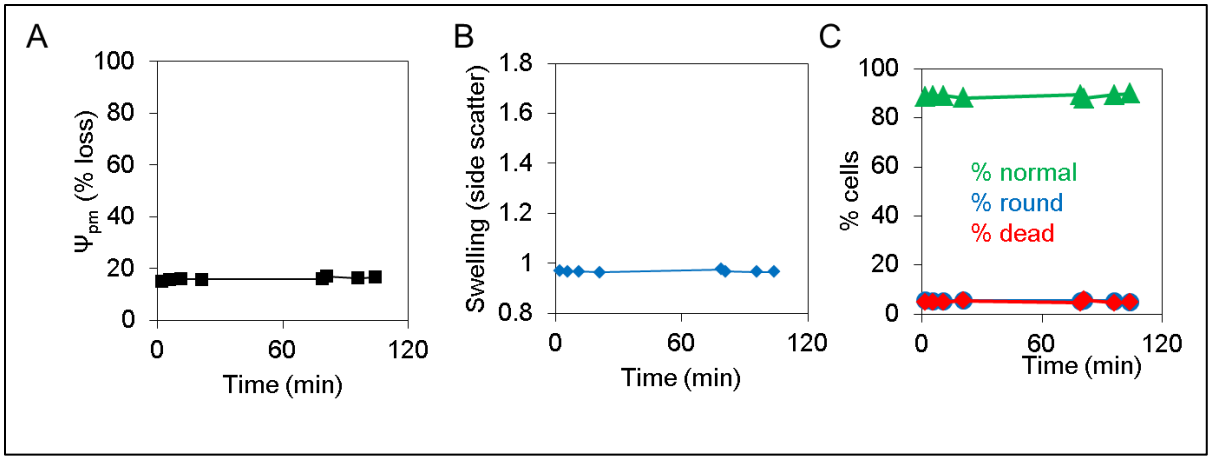

Supplemental Figure 3.5: **Expression of SRA prevents Ψ_{pm} loss, swelling, and lysis of *T. b. brucei.*** (**A**) SRA prevents Ψ_{pm} loss. Ty-SRA *T. b. brucei* were treated with 20nM TLF-1 and Hb for the indicated times before flow cytometry. Same data as in Figure 3.1B. (**B**) Cell swelling and (**C**) Cell morphology assay for the cells in panel A. Cells populating the normal gate are green triangles, round are blue circles, and dead are red triangles.

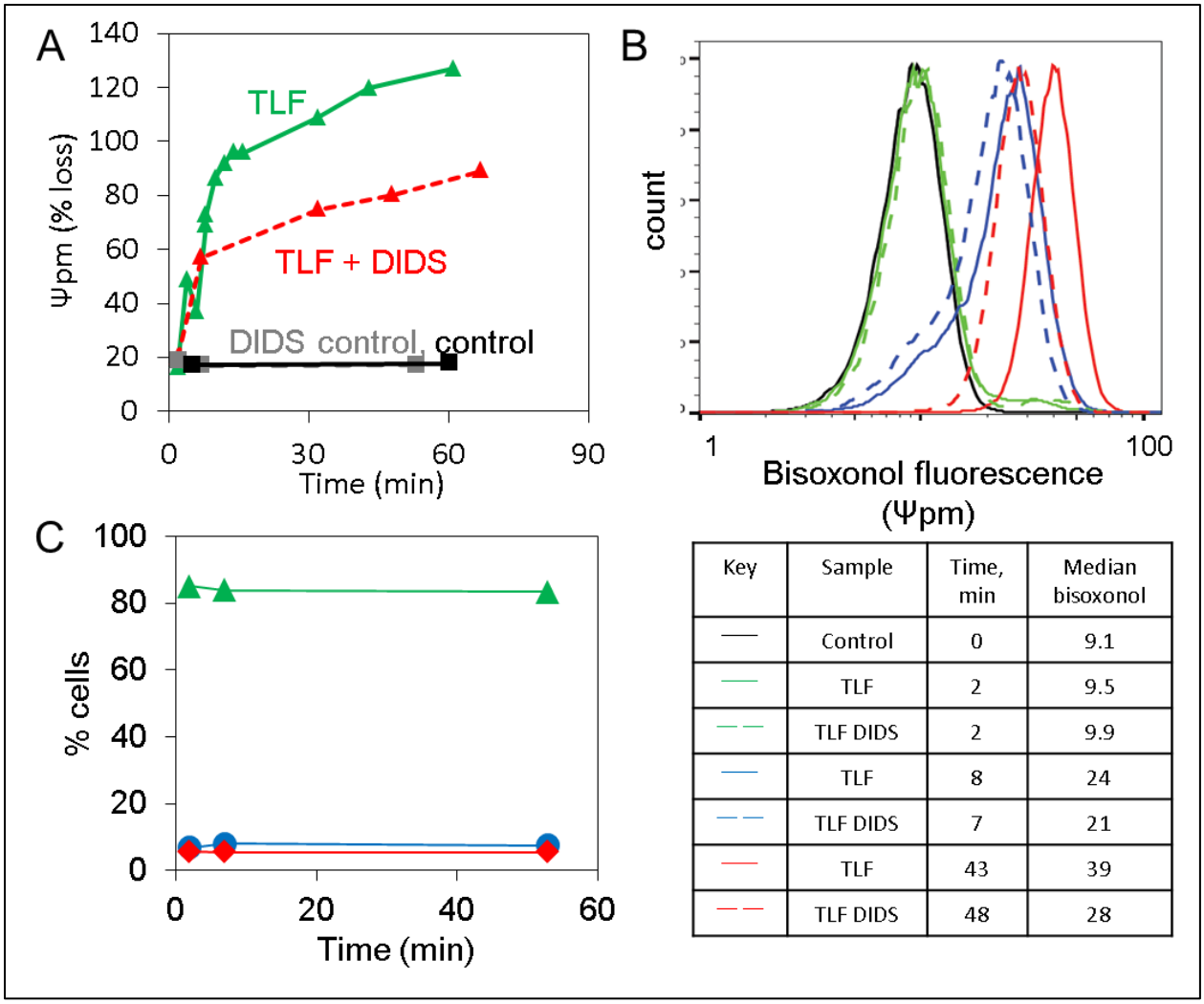

Key	Sample	Time, min	Median bisoxonol
	Control	0	9.1
	TLF	2	9.5
	TLF DIDS	2	9.9
	TLF	8	24
	TLF DIDS	7	21
	TLF	43	39
	TLF DIDS	48	28

Supplemental Figure 3.6: **DIDS Attenuates Ψ_{pm} loss** (**A**) Longer-term Ψ_{pm} measurements in cells incubated with 16nM TLF-1 (green triangles),TLF-1 with 300μM DIDS added concurrently (red triangles, dashed line). Controls are shown without TLF-1 (black squares) and with DIDS alone (grey squares, dashed line). (**B**) Histograms of membrane potential loss with 16nM TLF-1 (solid lines) and 16nM TLF + 300μM DIDS (dashed lines), as shown in the legend below the histogram. (**C**) Cell morphologies for cells treated with only DIDS. This data is the cell morphology data for the DID-only cells from Figure 3.4D. The cells gated as normal morphology are green triangles, rounded cells are blue circles, and dead cells are red diamonds.

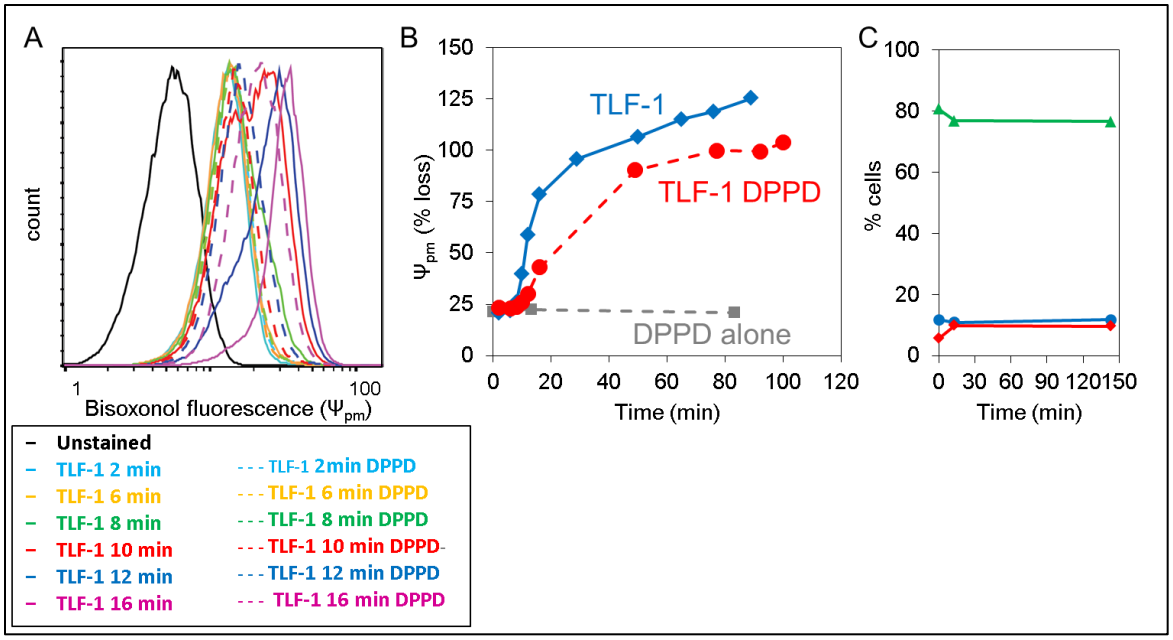

Supplemental Figure 3.7: **The antioxidant DPPD prevents plasma membrane potential loss in TLF-1 treated *T. b. brucei*.** (**A**) Histogram for the Ψ_{pm} data in Figure 3.4F. Dashed lines indicate DPPD treatment with TLF-1; solid lines are TLF-1 alone. See legend for time points. (**B**) Membrane potential data extending Figure 3.4F to longer time-points with the DPPD-only control included. *T. b. brucei* were pretreated with 300μM DPPD 1hr before adding TLF-1. 2nM TLF-1 and DPPD: red circles, dashed line. TLF-1 alone: blue diamonds. DPPD alone: grey squares, dashed line. (**C**) Cell morphology analysis for the DPPD treated sample without TLF-1. The data corresponds to the control sample in Figure 3.4G. Cells populating the normal gate are green triangles, round are blue circles, and dead are red triangles.

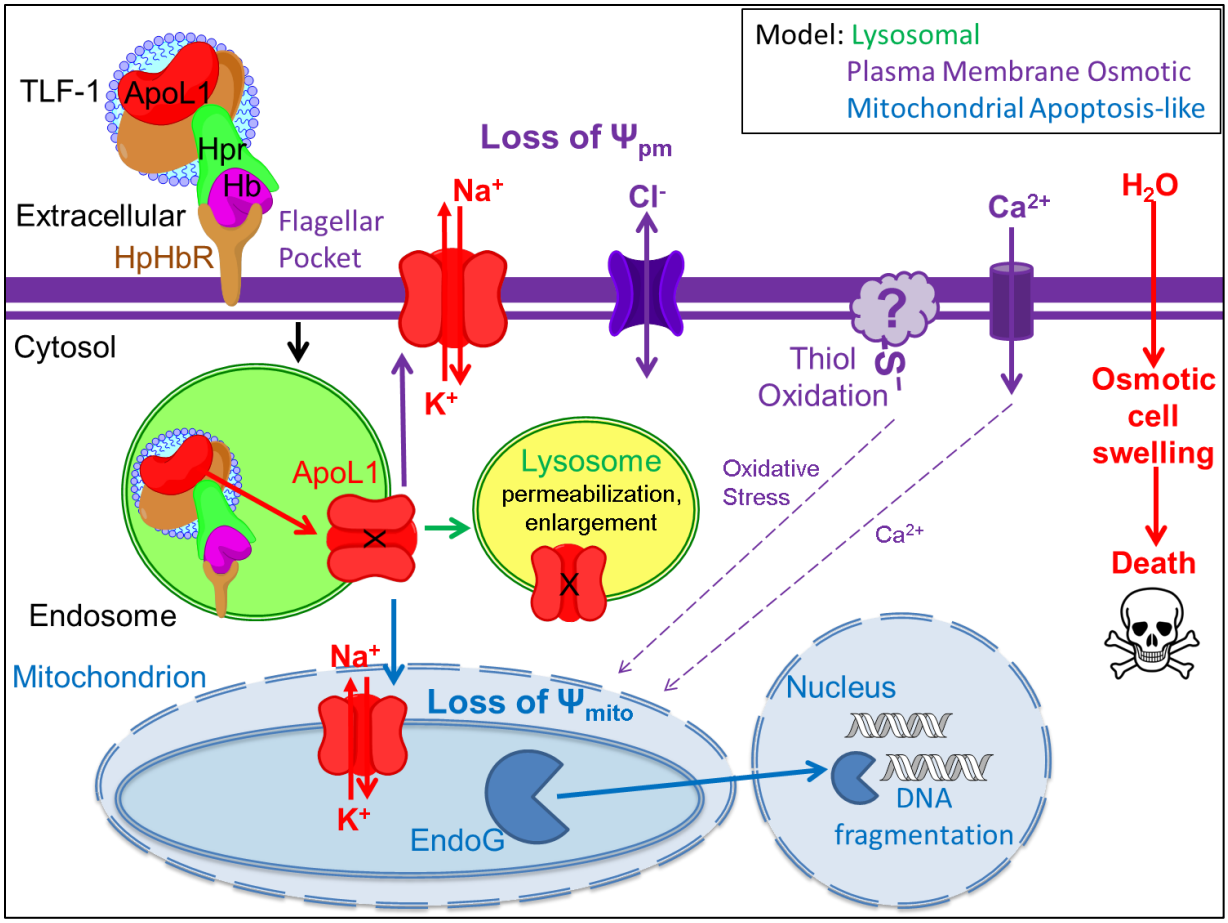

Supplemental Figure 3.8: **Three proposed ApoL1 localizations in *T. b. brucei*.** After endocytosis of TLF-1, ApoL1 may move to various compartments of the cell, including the lysosome (green), the mitochondrion (blue), and the plasma membrane (purple). Lysosomal ApoL1 may cause lysosomal permeabilization and increased lysosomal size. Mitochondrial ApoL1 has been associated with mitochondrial membrane potential loss and apoptosis-like phenotypes including the release of endonuclease G (endoG) and DNA fragmentation. ApoL1 forming a cation channel at the plasma membrane leads to influx of Na^+ and possibly an efflux of K^+. The ionic imbalance leads to activation of Cl^- channels and other endogenous plasma membrane channels. Oxidation of an osmo-regulatory protein(s) leads to a loss of volume regulatory capacity, leading to water influx, cell swelling, and lysis of *T. b. brucei*. Ca^{2+} influx and oxidative stress may both contribute to mitochondrial stress, suggesting overlapping effects from ApoL1 in the different compartments (see dashed purple lines and arrows).

Supplemental Table 3.1: **Timeline for TLF-1 induced lysis of *T. b. brucei***

Event	Time, min	Experimental Evidence

TLF-1 endocytosis via the HpHbR	0	HpHbR KO *T. b. brucei* have slower endocytosis, plasma membrane potential (Ψ_{pm}) loss, swelling, and lysis.
ApoL1 inserts into endosomal membrane	0-5	Neutralization of the endosomal system with chloroquine or NH_4^+ prevents Ψ_{pm} loss. SRA prevents Ψ_{pm} loss, swelling and lysis.
ApoL1 traffics to the plasma membrane and mediates cation influx	1-5	Replacing Na^+ or K^+ ions in the lysis buffer with the large cation $NMDG^+$ prevents lysis.
Cl^- channels open	1-5	DIDS prevents Ψ_{pm} loss, swelling, and lysis only when added during initial 10 min after TLF-1.
Plasma membrane potential (Ψ_{pm}) loss	4-20	The kinetics of plasma membrane potential loss depends on TLF-1 concentration.
Mitochondrial membrane potential (Ψ_{mito}) loss	4-20	ApoL1 in the mitochondrial membrane or secondary effects from ApoL1 at the plasma membrane may cause loss of $\Psi_{mito.}$ and may initiate apoptosis-like programmed cell death.
Oxidation leads to osmotic sensitivity	1-20	DPPD prevents membrane potential loss in TLF-1 treated *T. b. brucei.*
Influx of water and cytosol swelling	10+	Microscopy and side-scatter on flow cytometry show swelling cell population as early as 10 min after TLF-1 addition. Swelling is slowed or prevented by every reagent which inhibits TLF-1 induced Ψ_{pm} loss.
Osmotic cell lysis	30+	Swollen cells die. Their cell membranes become permeable to propidium iodide.

CHAPTER 4

APOL1 TOXICITY TO HUMANS AND TRYPANOSOMES: COULD APOL1-INDUCED OSMOTIC STRESS AT THE PLASMA MEMBRANE INITIATE CELL DEATH?[3]

[3] Greene, A.S. and Hajduk, S.L. Review to be submitted to Biochemistry

ABSTRACT

The human innate immune protein ApoL1 is toxic for veterinary trypanosome species as well as human cells overexpressing variant ApoL1 alleles (G1 and G2). ApoL1 G1 and G2 alleles offer protection against the sleeping sickness parasite *T. b. rhodesiense* but increase kidney disease risk in people of African ancestry. Recent work on both parasites and human kidney cells suggest that ApoL1-induced osmotic swelling of either *Trypanosome brucei brucei* cells or human embryonic kidney (HEK) cells is important to the lytic mechanism. Research in both parasites and humans is has yielded varying phenotypes of cell death and different models for ApoL1-induced lysis. We discuss how a model with ApoL1-induced ionic disruption at the plasma membrane is consistent with published data in both human kidney cells and trypanosomes, and how osmotic stress may serve as an initiator for downstream cell death pathways. Finally, we highlight important questions about the ApoL1 lysis mechanism, such as definitive linking of ApoL1 cellular localization and activity, and a structural understanding how the G1 and G2 mutations alter the biological activity of ApoL1.

REVIEW ARTICLE

Introduction

ApoL1 is a lipoprotein involved in innate immunity to parasites which is linked to and kidney disease risk in humans (see a model of the ApoL1 primary structure in Figure 4.1). As an essential component of trypanosome lytic factors (TLFs), ApoL1 prevents the veterinary parasite *Trypanosoma brucei brucei* from infecting humans. Much of the trypanosome work has been done using TLF-1, a subclass of high density

lipoprotein (HDL) particles which carries ApoL1 in human blood. The two subspecies of *T. brucei* which cause the deadly disease human African trypanosomiasis have evolved specific resistance mechanisms to evade the TLFs. *T. b. rhodesiense* resistance is conferred by a single serum resistance associated (SRA) protein which binds to a C-terminal domain on ApoL1. In a co-evolution reminiscent of sickle cell anemia and malaria parasites, ApoL1 alleles have evolved in humans to protect against human-infective *T. b. rhodesiense* trypanosomes. People with two copies of the trypanosome protective ApoL1 alleles (termed G1 and G2) have an increased risk of non-diabetic kidney disease (211). The G1 and G2 ApoL1 alleles are common in people of African ancestry, with nearly 15% of African Americans carrying 2 risk alleles (273).

Figure 4.1: **ApoL1 primary structure**. The secreted signal peptide is shown in green, the pore-forming domain is blue with the BH3 motif in purple, the membrane-addressing domain is red, the SRA-interacting domain is magenta, with the G1 amino acid substitutions indicated with arrows (S→G and I→M) and the G2 deletion bold and italicized (Δ***NY***). N_ is shown for the N-terminal and _C for the C-terminal ends of the protein.

The mechanisms ApoL1 uses to kill *T. brucei brucei* and causes kidney damage in humans are not well understood. Recently, several papers have emerged showing that ApoL1-induced osmotic stress at the plasma membrane of *T. b. brucei* and kidney cells is important for cell death (16, 47, 57, 274). This review will discuss how osmotic stress may be central to the mechanism of ApoL1 toxicity in both *T. b. brucei* and kidney cells.

ApoL1 causes osmotic lysis of trypanosomes

Osmotic swelling of *T. b. brucei* parasites has been recognized as a defining feature of human serum lysis of trypanosomes since before the discovery of ApoL1. The model for osmotic lysis of TLF-treated trypanosomes is shown in Figure 4.2. TLF-1 treated parasites appear identical to parasites exposed to hypotonic media, where osmotic stress causes water to flow into *T. b. brucei*, swelling its normally elongated cytoplasm into a rounded shape (47). Osmotic swelling appears necessary for lysis, because TLF-1 treated *T. b. brucei* lysis may be prevented by incubation in a buffer made hypertonic with sucrose (10, 47). Conversely, TLF-1 treatment for short periods of time make *T. b. brucei* extremely sensitive to hypotonic stress (47). Like *T. b. brucei* under hypotonic stress, TLF-1 induces calcium influx and potassium efflux (61). In addition to cation flux across the plasma membrane, chloride flux through plasma membrane channels is required for TLF-1 lysis of *T. b. brucei* (15, 57). The effects of

the different ApoL1 alleles on cell death in *T. b. brucei* are completely unknown.

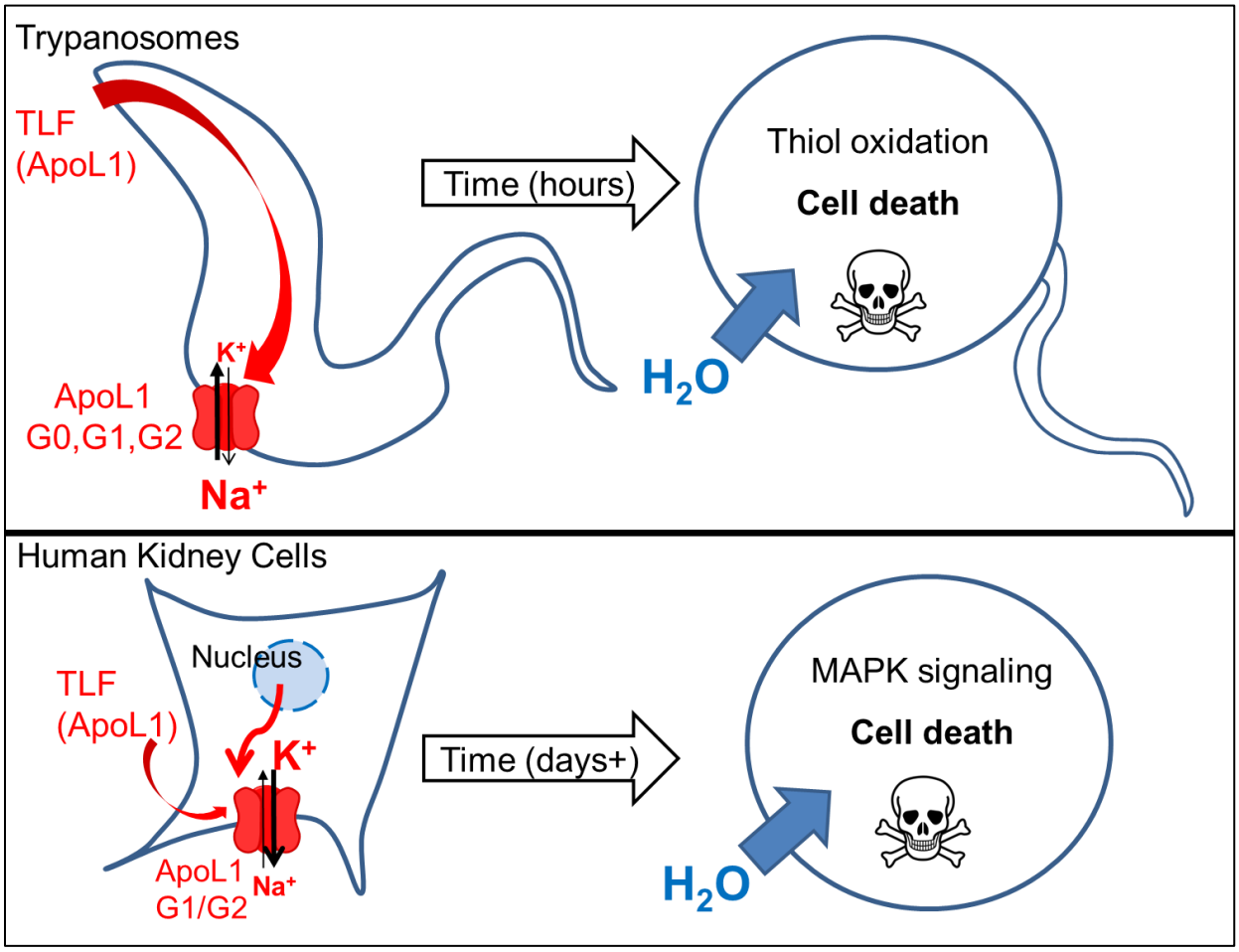

Figure 4.2: **Model for ApoL1-induced osmotic swelling and death** in human kidney cells (top) and *Trypanosoma brucei brucei* cells (bottom). ApoL1 localizations and signaling related to the osmotic model for ApoL1-induced cell death are depicted. ApoL1 endocytosis is indicated by the curved red arrows in both types of cells. Intracellular expression of ApoL1 may contribute to cell death in human kidney cells (thin red arrow from nucleus). In kidney cells, MAPK signaling is initiated by ApoL1-mediated K^+ efflux from the cells and contributes to cell death. In African trypanosomes, ApoL1-initiated sodium influx and thiol oxidation contributes to osmotic swelling and cell death.

Recently, oxidative processes in TLF-1 treated *T. b. brucei* were linked to cell swelling (47). Although oxidative stress has been implicated in TLF-1 killing for decades, the origin and effects of oxidative stress was not understood (13, 43, 48). It

appears that the osmotic and oxidative stress response pathways are linked in *T. b. brucei* so that oxidative stress exacerbates ApoL1-induced lysis. Under hypotonic stress, *T. b. brucei* treated with low concentrations of peroxides or thiol-binding reagents could not perform volume regulation and died. Similarly, peroxides and thiol-binding reagents make *T. b. brucei* extremely sensitive to TLF-1 lysis, while the lipophilic antioxidant DPPD rescues cell swelling and death. Because extensive oxidative damage or loss of free thiols was not observed, it seems that ApoL1 initiates specific oxidation of proteins involved in osmotic regulation. Thiol oxidation may initiate a signaling cascade for osmotic regulation in *T. b. brucei*. Further studies are necessary to determine the molecular details of osmotic cell death in TLF-1 treated *T. b. brucei.*

ApL1 causes osmotic swelling of human cells

Human cells experience swelling after overexpression of variant ApoL1 proteins or ApoL1 addition to the cell media. A model for osmotic lysis of human kidney cells is shown in Figure 4.2. In humans cells, overexpression of ApoL1 is commonly used to investigated ApoL1 toxicity. This is a reasonable approach because ApoL1 expression is naturally upregulated in response to immune stimulation from interferons (IFNα, IFNβ, and IFNγ), toll-like receptor agonists, and HIV infection (219, 228, 229). In podocytes from human kidneys, overexpression of ApoL1 variants leads to cytoplasmic swelling in a small percentage of G0 (wild-type allele) and 15-20% of G1 or G2-expressing cells. Many swollen cells were permeable to propidium iodide, suggesting necrotic cell death. Like trypanosomes, the chloride channel inhibitor DIDS prevented death of ApoL1-expressing podocytes (229). Similarly, human embryonic kidney (HEK) cells

overexpressing ApoL1 alleles showed a swollen phenotype (234). A fraction of ApoL1 localized to the plasma membrane of HEK cells, and ApoL1 variants mediated K^+ efflux from the cells. In fact, K^+ efflux was required for cell death, and a high-K^+ buffer prevented ApoL1-variant induced toxicity.

ApoL1 variant-induced K^+ efflux from HEK cells leads to the activation of stress-activated protein kinases including JNK, p38, and ERK and their downstream signaling pathways (234). The activation of these kinases is likely physiologically relevant because they are activated during clinical kidney disease (275). It is less clear how activation of MAPKs contributes to cell swelling or lysis. In their study, various experiments ruled out autophagy, pyroptosis, and apoptosis as the mechanism of lysis (234).

Kidney cells have evolved to respond dynamically to varying osmotic conditions, so it is intuitively appealing for ApoL1 variants to cause disease by disrupting osmotic response pathways (276). For instance, low dietary potassium intake leads to phosphorylation of ERK and p38, leading to changes in potassium flux in kidney cells (277). Similarly ERK and p38 regulate the secretion of K^+ through modulating the activity of calcium-activated big conductance channels (278). Therefore, interactions between stress activated protein kinases and ion transporters at the cell surface may play a role in osmotic swelling of kidney cells exposed to ApoL1.

Programmed cell death pathways initiated by ApoL1 in trypanosomes and humans

In both human cells and trypanosomes, ApoL1 can initiate programmed cell death pathways. In human cells, however, there is no consensus on what form of programmed cell death occurs, with different papers claiming that ApoL1 variants induces autophagic cell death, pyroptosis, necrosis, and overlapping cell death pathways (229, 232, 279). In bloodstream form trypanosomes, evolutionary divergence and the lack of an active mitochondrion contribute to unique and poorly understood programmed cell death pathways. Recent work in *T. b. brucei* showed that ApoL1 co-localizes with mitochondrial membranes of *T. b. brucei* leading to a release of endonuclease G from the mitochondrial matrix and DNA fragmentation (18). The apoptosis-like cell death model, however, does not explain why osmotic swelling rather than the apoptotic volume decrease occurs in *T. b. brucei*, and is programmed cell death is surprising given the rapid kinetics of trypanosome cell death (1-2 hours).

ApoL1 evolved from a class of apoptotic proteins and contains a BH3 domain in its pore-forming domain. The role of the BH3 domain in cell death in both trypanosomes and human cells is disputed. Trypanosomes do not have canonical bcl2 domain proteins to interact with BH3, and one study found that several mutants of the ApoL1 BH3 domain retained lytic activity, though total deletion of the BH3 domain made the protein non-functional (19). Surprisingly, Vanwalleghem *et al* found that one double amino acid mutation in the BH3 domain retained mitochondrial depolarization in *T. b. brucei* without downstream trypanosome lysis, suggesting that the BH3 domain may be important for downstream cell death signaling (18). In mammalian cells, total deletion of the BH3 domain or substitution of all the amino acids alanine abolished toxicity, but these mutations may interfere with the pore-forming activity of ApoL1 (222, 233). More

subtle mutations that interfere with protein interactions without perturbing the structure of the ApoL1 channel have not been published for human cell lines.

Current conundrums and osmotic connections

The conflicting data on the mechanisms of ApoL1 toxicity suggests that the cell death mechanism observed may be dependent on experimental variables. The type of cell death triggered may depend on the cell line used; the concentration ApoL1 or TLF-1 added or the level of intracellular ApoL1 expression; alternative splicing, glycosylation, or degradation of ApoL1; and the osmotic pressure and HDL content of the assay buffers. Until the mechanism initiating cell death in both trypanosome cells and human kidney cells is definitively determined, continuing to investigate downstream cell death and signaling pathways will only complicate the literature further. There are several core questions which, if answered, will clarify the mechanism of ApoL1 toxicity.

Firstly, it is important to resolve what cellular localization is important for ApoL1 activity. In trypanosomes, ApoL1 has been localized or inferred to reside in the endosomes, lysosome, kinesin-positive trafficking vesicles, mitochondrion, and plasma membrane (18, 44, 47, 57, 61, 97). In human cells, ApoL1 has been localized or inferred in the ER, lysosomes, and plasma membrane (228, 234, 279). It is probable that ApoL1 traffics to multiple organelles, but from which membrane does ApoL1 initiate cell death? In trypanosomes, the kinesin KIFC1 is involved in trafficking ApoL1 to extra-lysosomal localizations (18). Knocking down this protein in *T. b. brucei* led to lysosomal ApoL1 localization without significant lysis, suggesting that the lysosome is not important for the lytic mechanism. Similar experiments on other aspects of vesicular

trafficking might elucidate the important organelles for ApoL1 toxicity in human and trypanosome cells.

Secondly, the functional and structural differences between the G0, G1, and G2 alleles of ApoL1 must be elucidated. The G1 and G2 alleles of ApoL1 are able to kill human-infective *T. b. rhodesiense* parasites because they are not recognized by the parasite resistance protein SRA. It is not known whether the G1 and G2 variants of ApoL1 have other effects on lytic mechanism, even in *T. b. brucei* model parasites. In fact, the mechanism of ApoL1-induced cell death has not been studied in human infective *T. b. rhodesiense* or *T. b. gambiense* parasites. In human cells the relative toxicities of the three alleles have been compared to show that G1 and G2 are much more toxic than G0 ApoL1. There are several potential mechanisms for increased toxicity in the variants. The minor amino acid changes (G1) and deletion (G2) to the SRA-interacting domain in G1 and G2 may affect ApoL1 cation channel selectivity or activity. Post-transcriptional or post-translational processing may differ between the variants. Protein trafficking to the plasma membrane may be increased in the G1 and G2 variants compared to the G0, leading to increased toxicity. In fact, in a pull-down of surface-associated proteins in HEK cells, G1 and G2 ApoL1 appeared more abundant in the surface fraction than G0 ApoL1 (234). Finally, binding sites on G1 and G2 variants of ApoL1 for interacting proteins may be disrupted leading to inappropriate cellular signaling and toxicity.

Finally, osmotic swelling initiated by ApoL1 at the plasma membrane is supported by data from both trypanosomes and human kidney cell lines. If ApoL1 initiates osmotic swelling, it is predicted to shift the fluxes of ions and small molecules

across the plasma membrane, abolish the plasma membrane potential, activate plasma membrane channels such as aquaporins, and initiate osmoregulatory signaling cascades (280-282). Investigations of osmotic stress response pathways in both trypanosomes and human cells exposed to ApoL1 is likely to yield valuable insight into the connections between ApoL1 channel formation and cell death.

CHAPTER 5

MODEL FOR TLF-1 LYSIS OF *TRYPANOSOMA BRUCEI BRUCEI*

My Ph.D. research focused on the mechanism of human innate immunity against the eukaryotic pathogen *Trypanosoma brucei brucei*. I studied how human innate immune molecules called trypanosome lytic factors (TLFs) kill the veterinary parasite *T. b. brucei.* The disease African Sleeping Sickness is caused by human-infective parasites *T. b. gambiense* and *T. b. rhodesiense* which have evolved resistance against the TLFs. TLF- is a circulating high density lipoprotein (HDL) complex which contains the pore-forming toxin apolipoprotein L1 (ApoL1). Nanomolar concentrations of TLF-1 kill *T. b. brucei* within two hours, making TLF-1 an incredibly potent anti-parasitic agent. However, the mechanism of parasite cell death is poorly defined. Characterizing the mechanism which the human immune system uses to effectively kill the parasites may aid the development of more effective anti-parasitic agents for this neglected tropical disease.

My research elucidated important details concerning the mechanism of TLF-1 induced parasite death. After endocytosis of TLF-1 by *T. b. brucei*, ApoL1 inserts into an endosomal membrane, forming a cation channel. I showed that trafficking of ApoL1 from the endosomes to other membranes causes a loss of both the plasma membrane potential and the mitochondrial membrane potential within ten minutes after TLF-1 addition to the cells. The loss of plasma membrane potential requires the influx of

sodium ions and the opening of chloride channels in the plasma membrane. Furthermore, I discovered that TLF-1 induced lysis is involves oxidative regulation of the osmotic stress response in trypanosomes. Finally, TLF-1 causes uncontrolled swelling of the parasite cytosol leading directly to cell death.

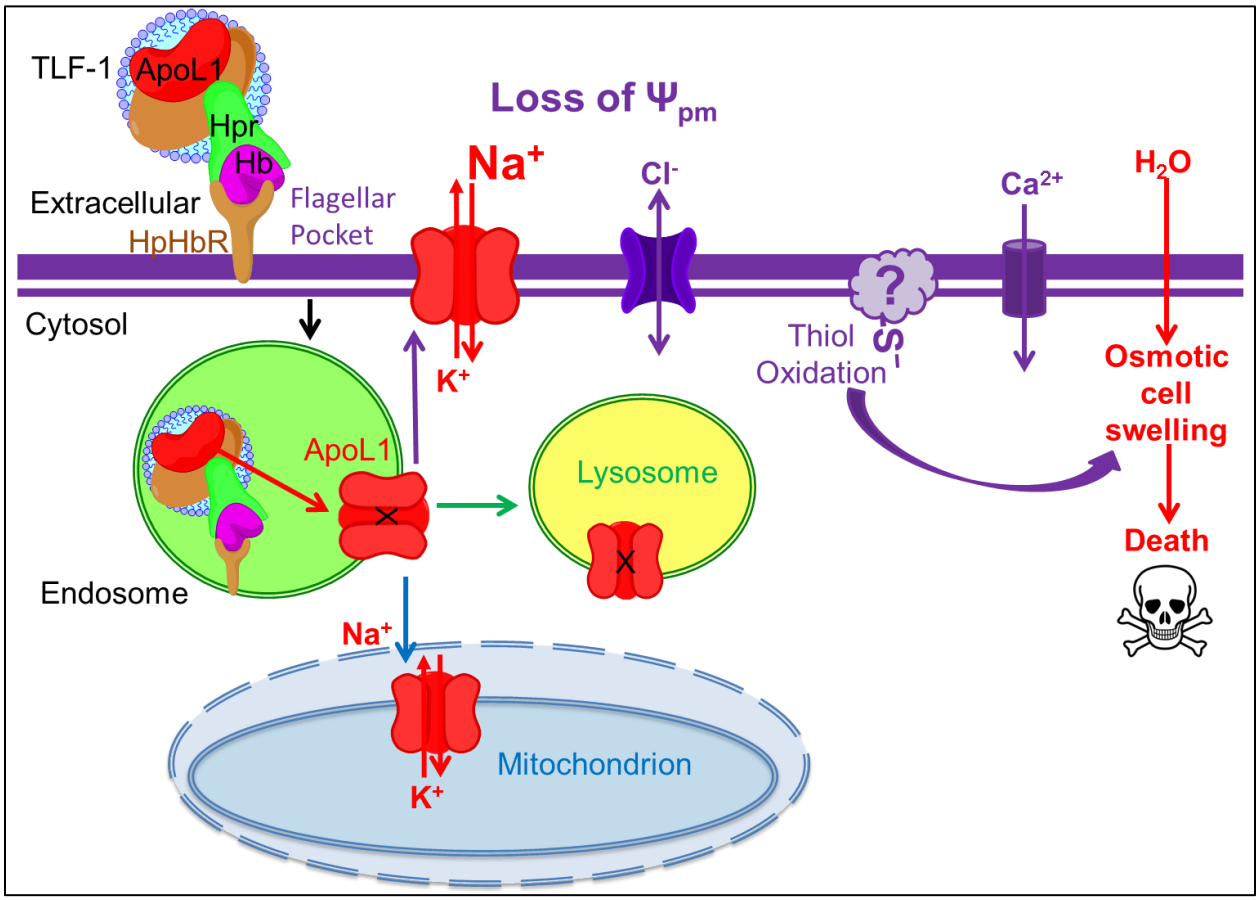

Figure 5.1: **TLF-1 kills *T. b. brucei* by causing osmotic stress via the plasma membrane.** TLF-1 is enters the parasite through high-affinity binding to the haptoglobin-hemoglobin receptor (HpHbR). In an acidic endosomal compartment, ApoL1 inserts into the membrane, forming a cation channel. While ApoL1 may travel to various the lysosome or the mitochondrion, my works shows that recycling to the plasma membrane is important for its activity. ApoL1 mediates the influx of sodium into the cell, causing a loss of plasma membrane potential Ψ_{PM}. The opening of chloride channels and thiol oxidation contributes to ApoL1-induced plasma membrane potential loss. These early TLF-1 mediated events lead to an influx of water resulting in osmotic lysis of *T. b. brucei.*

An illustration of our current model for TLF-1 lysis is illustrated in Figure 5.1. This model for cell death initiated by ApoL1 at the plasma membrane of *T. b. brucei* corresponds well with what is understood about ApoL1 function in both trypanosomes and human kidney cells where variant ApoL1 proteins cause disease. My contributions include discovering an intersection between oxidative and osmotic stress in trypanosomes to explain the disputed role of oxidative stress in TLF-1 lysis, and revealing the rapid kinetics of ApoL1 mediated effects at the plasma membrane including a loss of plasma membrane potential.

Many questions remain about the specific molecular details of TLF-1 induced cell death in *T. b. brucei.* It would be fascinating to determine what osmo-regulatory proteins are sensitive to regulation or inactivation by thiol oxidation. The intersecting cellular effects of ApoL1 in the lysosome, the mitochondrion, and the plasma membrane make the question of TLF-1 mechanism intriguing and difficult. It is possible that ApoL1-induced osmotic stress is critical for the observed apoptosis-like cell death, or even that programmed cell death induction is not necessary for TLF-1 lysis of *T. b. brucei*. Investigating TLF-1 mediated cell death in parasites with genetically impaired osmotic stress response such as aquaporin knockdown might yield insights into the relative importance of osmotic stress and other factors in TLF-1 lysis. An understanding of ApoL1 intracellular trafficking will also help answer outstanding questions about ApoL1-induced cell death in trypanosomes.

The precision and rapidity of the ApoL1-induced loss of plasma membrane potential and mitochondrial membrane potential allows ApoL1 to serve as a probe for investigating protein trafficking in trypanosomes. Vesicular connections between the

endosomes and mitochondria are unusual and controversial in any cell type (59). If KIFC1 is responsible only for mitochondrial trafficking, deletion or knockdown of KIFC1 would prevent mitochondrial membrane potential loss without effecting plasma membrane potential loss (18). Alternatively, if KIFC1 is responsible for recycling to the plasma membrane, KIFC1 knockdown would prevent loss of both plasma membrane and mitochondrial membrane potential.

In preliminary studies, I investigated TLF-1 induced loss of plasma membrane potential and lysis in *T. b. brucei* where the recycling-endosome associated Rab11 was inactive (double-negative cell line was donated by James Bangs, University of Buffalo). While the Rab11 mutant showed slightly reduced TLF-1 lysis, there was no effect on the rate of plasma membrane potential loss, suggesting that ApoL1 does not traffic not traffic through Rab11-positive vesicles, but utilize non-canonical recycling pathways in trypanosomes. Using ApoL1-induced membrane potential loss to study TLF-1 trafficking in *T. b. brucei* may enhance our understanding not only of the mechanism of ApoL1 lysis, but also of vesicular trafficking in other eukaryotes.

African trypanosomes represent an important global disease with limited therapeutic options. The surprising synergism I discovered between thiol oxidation and osmotic lysis of *T. b. brucei* is an aspect of my research applicable to drug development. The current eflornithine-nifurtimox combination therapy, while effective in terms of logistics and economics, does not increase parasite cure compared to the drugs given individually (262). Screening combinations of drugs for synergistic mechanisms, especially drug combinations which inhibit osmotic and oxidative processes in trypanosomes, may yield more effective treatment options. Alternatively,

ion channel forming drugs could be modelled off of ApoL1 and developed to target the extremely fluid membrane of African trypanosomes, letting the immune system provide the second hit of oxidative stress (23). Ultimately, I hope that the basic research advances I contributed to understanding the TLF-1 lytic mechanism will contribute to medical advances against Human African Trypanosomiasis.

ALL REFERENCES

1. Steverding D (2008) The history of African trypanosomiasis. *Parasit Vectors* 1(1):3.
2. Franco JR, Simarro PP, Diarra A, & Jannin JG (2014) Epidemiology of human African trypanosomiasis. *Clin Epidemiol* 6:257-275.
3. Mitashi P, *et al.* (2015) Integration of diagnosis and treatment of sleeping sickness in primary healthcare facilities in the Democratic Republic of the Congo. *Trop Med Int Health* 20(1):98-105.
4. Turner CM, *et al.* (2004) Human infectivity trait in Trypanosoma brucei: stability, heritability and relationship to sra expression. *Parasitology* 129(Pt 4):445-454.
5. Magez S, *et al.* (2008) The role of B-cells and IgM antibodies in parasitemia, anemia, and VSG switching in Trypanosoma brucei-infected mice. *PLoS Pathog* 4(8):e1000122.
6. Chaudhuri M, Ott RD, & Hill GC (2006) Trypanosome alternative oxidase: from molecule to function. *Trends Parasitol* 22(10):484-491.
7. Brown SV, Hosking P, Li J, & Williams N (2006) ATP synthase is responsible for maintaining mitochondrial membrane potential in bloodstream form Trypanosoma brucei. *Eukaryot Cell* 5(1):45-53.
8. Hide G (2008) Visualizing trypanosome sex. *Trends Parasitol* 24(10):425-428.
9. Hajduk SL, Hager KM, & Esko JD (1994) Human high density lipoprotein killing of African trypanosomes. *Annu Rev Microbiol* 48:139-162.
10. Rifkin MR (1978) Identification of the trypanocidal factor in normal human serum: high density lipoprotein. *Proc Natl Acad Sci U S A* 75(7):3450-3454.
11. Owen JS, Gillett MP, & Hughes TE (1992) Transgenic mice expressing human apolipoprotein A-I have sera with modest trypanolytic activity in vitro but remain susceptible to infection by Trypanosoma brucei brucei. *J Lipid Res* 33(11):1639-1646.
12. Tomlinson S, *et al.* (1995) High-density-lipoprotein-independent killing of Trypanosoma brucei by human serum. *Mol Biochem Parasitol* 70(1-2):131-138.
13. Smith AB, Esko JD, & Hajduk SL (1995) Killing of trypanosomes by the human haptoglobin-related protein. *Science* 268(5208):284-286.
14. Vanhamme L, *et al.* (2003) Apolipoprotein L-I is the trypanosome lytic factor of human serum. *Nature* 422(6927):83-87.
15. Perez-Morga D, *et al.* (2005) Apolipoprotein L-I promotes trypanosome lysis by forming pores in lysosomal membranes. *Science* 309(5733):469-472.
16. Thomson R & Finkelstein A (2015) Human trypanolytic factor APOL1 forms pH-gated cation-selective channels in planar lipid bilayers: relevance to trypanosome lysis. *Proc Natl Acad Sci U S A* 112(9):2894-2899.
17. Ridgley EL, Xiong ZH, & Ruben L (1999) Reactive oxygen species activate a Ca2+-dependent cell death pathway in the unicellular organism Trypanosoma brucei brucei. *Biochem J* 340 (Pt 1):33-40.
18. Vanwalleghem G, *et al.* (2015) Coupling of lysosomal and mitochondrial membrane permeabilization in trypanolysis by APOL1. *Nat Commun* 6:8078.

19. Heneghan JF, *et al.* (2015) BH3 domain-independent apolipoprotein L1 toxicity rescued by BCL2 prosurvival proteins. *Am J Physiol Cell Physiol* 309(5):C332-347.
20. Lecordier L, *et al.* (2009) C-terminal mutants of apolipoprotein L-I efficiently kill both Trypanosoma brucei brucei and Trypanosoma brucei rhodesiense. *PLoS Pathog* 5(12):e1000685.
21. Shiflett AM, Bishop JR, Pahwa A, & Hajduk SL (2005) Human high density lipoproteins are platforms for the assembly of multi-component innate immune complexes. *J Biol Chem* 280(38):32578-32585.
22. Molina-Portela MP, Samanovic M, & Raper J (2008) Distinct roles of apolipoprotein components within the trypanosome lytic factor complex revealed in a novel transgenic mouse model. *J Exp Med* 205(8):1721-1728.
23. Harrington JM, *et al.* (2012) Novel African trypanocidal agents: membrane rigidifying peptides. *PLoS One* 7(9):e44384.
24. Harrington JM, *et al.* (2010) The plasma membrane of bloodstream-form African trypanosomes confers susceptibility and specificity to killing by hydrophobic peptides. *J Biol Chem* 285(37):28659-28666.
25. Shiflett AM, Bishop, J.R., Pahwa, A., Hajduk, S.L. (2005) Human High Density Lipoproteins are Platforms for the Assembly of Multi-component Innate Immune Complexes. *JBC* 280(38):32578-32585.
26. Andersen CB, *et al.* (2012) Structure of the haptoglobin-haemoglobin complex. *Nature* 489(7416):456-459.
27. Nielsen MJ, *et al.* (2007) A unique loop extension in the serine protease domain of haptoglobin is essential for CD163 recognition of the haptoglobin-hemoglobin complex. *J Biol Chem* 282(2):1072-1079.
28. Harrington JM, *et al.* (2014) A retained secretory signal peptide mediates high density lipoprotein (HDL) assembly and function of haptoglobin-related protein. *J Biol Chem* 289(36):24811-24820.
29. Harrington JM, Howell S, & Hajduk SL (2009) Membrane permeabilization by trypanosome lytic factor, a cytolytic human high density lipoprotein. *J Biol Chem* 284(20):13505-13512.
30. Raper J, Fung R, Ghiso J, Nussenzweig V, & Tomlinson S (1999) Characterization of a novel trypanosome lytic factor from human serum. *Infect Immun* 67(4):1910-1916.
31. Raper J, Nussenzweig V, & Tomlinson S (1996) The main lytic factor of Trypanosoma brucei brucei in normal human serum is not high density lipoprotein. *J Exp Med* 183(3):1023-1029.
32. Bullard W, *et al.* (2012) Haptoglobin-hemoglobin receptor independent killing of African trypanosomes by human serum and trypanosome lytic factors. *Virulence* 3(1):72-76.
33. Vanhollebeke B, *et al.* (2008) A haptoglobin-hemoglobin receptor conveys innate immunity to Trypanosoma brucei in humans. *Science* 320(5876):677-681.
34. Muller N, Mansfield JM, & Seebeck T (1996) Trypanosome variant surface glycoproteins are recognized by self-reactive antibodies in uninfected hosts. *Infect Immun* 64(11):4593-4597.
35. Vanhollebeke B & Pays E (2010) The trypanolytic factor of human serum: many ways to enter the parasite, a single way to kill. *Mol Microbiol* 76(4):806-814.
36. Smith AB & Hajduk SL (1995) Identification of haptoglobin as a natural inhibitor of trypanocidal activity in human serum. *Proc Natl Acad Sci U S A* 92(22):10262-10266.

37. Raper J, Nussenzweig V, & Tomlinson S (1996) Lack of correlation between haptoglobin concentration and trypanolytic activity of normal human serum. *Mol Biochem Parasitol* 76(1-2):337-338.
38. Stodkilde K, Torvund-Jensen M, Moestrup SK, & Andersen CB (2014) Structural basis for trypanosomal haem acquisition and susceptibility to the host innate immune system. *Nat Commun* 5:5487.
39. DeJesus E, Kieft R, Albright B, Stephens NA, & Hajduk SL (2013) A single amino acid substitution in the group 1 Trypanosoma brucei gambiense haptoglobin-hemoglobin receptor abolishes TLF-1 binding. *PLoS Pathog* 9(4):e1003317.
40. Higgins MK, *et al.* (2013) Structure of the trypanosome haptoglobin-hemoglobin receptor and implications for nutrient uptake and innate immunity. *Proc Natl Acad Sci U S A* 110(5):1905-1910.
41. Lane-Serff H, MacGregor P, Lowe ED, Carrington M, & Higgins MK (2014) Structural basis for ligand and innate immunity factor uptake by the trypanosome haptoglobin-haemoglobin receptor. *Elife* 3:e05553.
42. Nielsen MJ, *et al.* (2006) Haptoglobin-related protein is a high-affinity hemoglobin-binding plasma protein. *Blood* 108(8):2846-2849.
43. Widener J, Nielsen MJ, Shiflett A, Moestrup SK, & Hajduk S (2007) Hemoglobin is a co-factor of human trypanosome lytic factor. *PLoS Pathog* 3(9):1250-1261.
44. Hager KM, *et al.* (1994) Endocytosis of a cytotoxic human high density lipoprotein results in disruption of acidic intracellular vesicles and subsequent killing of African trypanosomes. *J Cell Biol* 126(1):155-167.
45. Peck RF, *et al.* (2008) The LAMP-like protein p67 plays an essential role in the lysosome of African trypanosomes. *Mol Microbiol* 68(4):933-946.
46. Silverman JS, Schwartz KJ, Hajduk SL, & Bangs JD (2011) Late endosomal Rab7 regulates lysosomal trafficking of endocytic but not biosynthetic cargo in Trypanosoma brucei. *Mol Microbiol* 82(3):664-678.
47. Greene AS & Hajduk SL (2016) Trypanosome Lytic Factor-1 Initiates Oxidation-stimulated Osmotic Lysis of Trypanosoma brucei brucei. *J Biol Chem* 291(6):3063-3075.
48. Bishop JR, Shimamura M, & Hajduk SL (2001) Insight into the mechanism of trypanosome lytic factor-1 killing of Trypanosoma brucei brucei. *Mol Biochem Parasitol* 118(1):33-40.
49. Sadrzadeh SM, Graf E, Panter SS, Hallaway PE, & Eaton JW (1984) Hemoglobin. A biologic fenton reagent. *J Biol Chem* 259(23):14354-14356.
50. Molina Portela MP, Raper J, & Tomlinson S (2000) An investigation into the mechanism of trypanosome lysis by human serum factors. *Mol Biochem Parasitol* 110(2):273-282.
51. Reeder BJ & Wilson MT (2005) Hemoglobin and myoglobin associated oxidative stress: from molecular mechanisms to disease States. *Curr Med Chem* 12(23):2741-2751.
52. Banerjee S, *et al.* (2012) Haptoglobin alters oxygenation and oxidation of hemoglobin and decreases propagation of peroxide-induced oxidative reactions. *Free Radic Biol Med* 53(6):1317-1326.
53. Kapralov A, *et al.* (2009) Peroxidase activity of hemoglobin-haptoglobin complexes: covalent aggregation and oxidative stress in plasma and macrophages. *J Biol Chem* 284(44):30395-30407.

54. Miller YI, Altamentova SM, & Shaklai N (1997) Oxidation of low-density lipoprotein by hemoglobin stems from a heme-initiated globin radical: antioxidant role of haptoglobin. *Biochemistry* 36(40):12189-12198.
55. Cooper CE, Silaghi-Dumitrescu R, Rukengwa M, Alayash AI, & Buehler PW (2008) Peroxidase activity of hemoglobin towards ascorbate and urate: a synergistic protective strategy against toxicity of Hemoglobin-Based Oxygen Carriers (HBOC). *Biochim Biophys Acta* 1784(10):1415-1420.
56. Vanhollebeke B, Lecordier L, Perez-Morga D, Amiguet-Vercher A, & Pays E (2007) Human serum lyses Trypanosoma brucei by triggering uncontrolled swelling of the parasite lysosome. *J Eukaryot Microbiol* 54(5):448-451.
57. Molina-Portela Mdel P, Lugli EB, Recio-Pinto E, & Raper J (2005) Trypanosome lytic factor, a subclass of high-density lipoprotein, forms cation-selective pores in membranes. *Mol Biochem Parasitol* 144(2):218-226.
58. Delgado M, Anderson P, Garcia-Salcedo JA, Caro M, & Gonzalez-Rey E (2009) Neuropeptides kill African trypanosomes by targeting intracellular compartments and inducing autophagic-like cell death. *Cell Death Differ* 16(3):406-416.
59. Sheftel AD, Zhang AS, Brown C, Shirihai OS, & Ponka P (2007) Direct interorganellar transfer of iron from endosome to mitochondrion. *Blood* 110(1):125-132.
60. Dutoya S, *et al.* (2001) A novel C-terminal kinesin is essential for maintaining functional acidocalcisomes in Trypanosoma brucei. *J Biol Chem* 276(52):49117-49124.
61. Rifkin MR (1984) Trypanosoma brucei: biochemical and morphological studies of cytotoxicity caused by normal human serum. *Exp Parasitol* 58(1):81-93.
62. D'Hondt J, Van Meirvenne N, Moens L, & Kondo M (1979) Ca2+ is essential cofactor for trypanocidal activity of normal human serum. *Nature* 282(5739):613-615.
63. Kieft R, Stephens NA, Capewell P, MacLeod A, & Hajduk SL (2012) Role of expression site switching in the development of resistance to human Trypanosome Lytic Factor-1 in Trypanosoma brucei brucei. *Mol Biochem Parasitol* 183(1):8-14.
64. Xong HV, *et al.* (1998) A VSG expression site-associated gene confers resistance to human serum in Trypanosoma rhodesiense. *Cell* 95(6):839-846.
65. Gibson WC (2005) The SRA gene: the key to understanding the nature of Trypanosoma brucei rhodesiense. *Parasitology* 131(Pt 2):143-150.
66. Willett KC & Fairbairn H (1955) The Tinde experiment: a study of Trypanosoma rhodesiense during eighteen years of cyclical transmission. *Ann Trop Med Parasitol* 49(3):278-292.
67. Duffy CW, *et al.* (2013) Population genetics of Trypanosoma brucei rhodesiense: clonality and diversity within and between foci. *PLoS Negl Trop Dis* 7(11):e2526.
68. Stephens NA & Hajduk SL (2011) Endosomal localization of the serum resistance-associated protein in African trypanosomes confers human infectivity. *Eukaryot Cell* 10(8):1023-1033.
69. Bart JM, *et al.* (2015) Localization of serum resistance-associated protein in Trypanosoma brucei rhodesiense and transgenic Trypanosoma brucei brucei. *Cell Microbiol*.
70. Szempruch AJ, *et al.* (2016) Extracellular Vesicles from Trypanosoma brucei Mediate Virulence Factor Transfer and Cause Host Anemia. *Cell* 164(1-2):246-257.

71. Capewell P, Cooper A, Clucas C, Weir W, & Macleod A (2015) A co-evolutionary arms race: trypanosomes shaping the human genome, humans shaping the trypanosome genome. *Parasitology* 142 Suppl 1:S108-119.
72. Capewell P, *et al.* (2011) Differences between Trypanosoma brucei gambiense groups 1 and 2 in their resistance to killing by trypanolytic factor 1. *PLoS Negl Trop Dis* 5(9):e1287.
73. Kieft R, *et al.* (2010) Mechanism of Trypanosoma brucei gambiense (group 1) resistance to human trypanosome lytic factor. *Proc Natl Acad Sci U S A* 107(37):16137-16141.
74. Lecordier L, *et al.* (2014) Identification of Trypanosoma brucei components involved in trypanolysis by normal human serum. *Mol Microbiol* 94(3):625-636.
75. Alsford S, Currier RB, Guerra-Assuncao JA, Clark TG, & Horn D (2014) Cathepsin-L can resist lysis by human serum in Trypanosoma brucei brucei. *PLoS Pathog* 10(5):e1004130.
76. Uzureau P, *et al.* (2013) Mechanism of Trypanosoma brucei gambiense resistance to human serum. *Nature* 501(7467):430-434.
77. Capewell P, *et al.* (2013) The TgsGP gene is essential for resistance to human serum in Trypanosoma brucei gambiense. *PLoS Pathog* 9(10):e1003686.
78. Ortiz-Ordonez JC, Sechelski JB, & Seed JR (1994) Mechanism of lysis of Trypanosoma brucei gambiense by human serum. *J Parasitol* 80(6):924-930.
79. Moore DR, *et al.* (1995) Developmentally regulated sensitivity of Trypanosoma brucei brucei to the cytotoxic effects of human high-density lipoprotein. *Exp Parasitol* 81(2):216-226.
80. Natesan SK, Peacock L, Leung KF, Gibson W, & Field MC (2010) Evidence that low endocytic activity is not directly responsible for human serum resistance in the insect form of African trypanosomes. *BMC Res Notes* 3:63.
81. Engstler M, *et al.* (2004) Kinetics of endocytosis and recycling of the GPI-anchored variant surface glycoprotein in Trypanosoma brucei. *J Cell Sci* 117(Pt 7):1105-1115.
82. Silverman JS, Muratore KA, & Bangs JD (2013) Characterization of the late endosomal ESCRT machinery in Trypanosoma brucei. *Traffic* 14(10):1078-1090.
83. Manna PT, Boehm C, Leung KF, Natesan SK, & Field MC (2014) Life and times: synthesis, trafficking, and evolution of VSG. *Trends Parasitol* 30(5):251-258.
84. Leung KF, Riley FS, Carrington M, & Field MC (2011) Ubiquitylation and developmental regulation of invariant surface protein expression in trypanosomes. *Eukaryot Cell* 10(7):916-931.
85. Chung WL, Carrington M, & Field MC (2004) Cytoplasmic targeting signals in transmembrane invariant surface glycoproteins of trypanosomes. *J Biol Chem* 279(52):54887-54895.
86. Chung WL, Leung KF, Carrington M, & Field MC (2008) Ubiquitylation is required for degradation of transmembrane surface proteins in trypanosomes. *Traffic* 9(10):1681-1697.
87. Pal A, Hall BS, Nesbeth DN, Field HI, & Field MC (2002) Differential endocytic functions of Trypanosoma brucei Rab5 isoforms reveal a glycosylphosphatidylinositol-specific endosomal pathway. *J Biol Chem* 277(11):9529-9539.
88. Field H, Farjah M, Pal A, Gull K, & Field MC (1998) Complexity of trypanosomatid endocytosis pathways revealed by Rab4 and Rab5 isoforms in Trypanosoma brucei. *J Biol Chem* 273(48):32102-32110.

89. Ali M, Leung KF, & Field MC (2014) The ancient small GTPase Rab21 functions in intermediate endocytic steps in trypanosomes. *Eukaryot Cell* 13(2):304-319.
90. Benz C, Engstler M, Hillmer S, & Clayton C (2010) Depletion of 14-3-3 proteins in bloodstream-form Trypanosoma brucei inhibits variant surface glycoprotein recycling. *Int J Parasitol* 40(5):629-634.
91. Pal A, Hall BS, Jeffries TR, & Field MC (2003) Rab5 and Rab11 mediate transferrin and anti-variant surface glycoprotein antibody recycling in Trypanosoma brucei. *Biochem J* 374(Pt 2):443-451.
92. Overath P & Engstler M (2004) Endocytosis, membrane recycling and sorting of GPI-anchored proteins: Trypanosoma brucei as a model system. *Mol Microbiol* 53(3):735-744.
93. Kabiri M & Steverding D (2000) Studies on the recycling of the transferrin receptor in Trypanosoma brucei using an inducible gene expression system. *Eur J Biochem* 267(11):3309-3314.
94. Steverding D, Stierhof YD, Fuchs H, Tauber R, & Overath P (1995) Transferrin-binding protein complex is the receptor for transferrin uptake in Trypanosoma brucei. *J Cell Biol* 131(5):1173-1182.
95. McConville MJ, Mullin KA, Ilgoutz SC, & Teasdale RD (2002) Secretory pathway of trypanosomatid parasites. *Microbiol Mol Biol Rev* 66(1):122-154; table of contents.
96. Shimamura M, Hager KM, & Hajduk SL (2001) The lysosomal targeting and intracellular metabolism of trypanosome lytic factor by Trypanosoma brucei brucei. *Mol Biochem Parasitol* 115(2):227-237.
97. Shiflett AM, *et al.* (2007) African trypanosomes: intracellular trafficking of host defense molecules. *J Eukaryot Microbiol* 54(1):18-21.
98. Tripodi KE, Menendez Bravo SM, & Cricco JA (2011) Role of heme and heme-proteins in trypanosomatid essential metabolic pathways. *Enzyme Res* 2011:873230.
99. Koreny L, *et al.* (2012) Aerobic kinetoplastid flagellate Phytomonas does not require heme for viability. *Proc Natl Acad Sci U S A* 109(10):3808-3813.
100. McCann AK, Schwartz KJ, & Bangs JD (2008) A determination of the steady state lysosomal pH of bloodstream stage African trypanosomes. *Mol Biochem Parasitol* 159(2):146-149.
101. Scott CC & Gruenberg J (2011) Ion flux and the function of endosomes and lysosomes: pH is just the start: the flux of ions across endosomal membranes influences endosome function not only through regulation of the luminal pH. *Bioessays* 33(2):103-110.
102. Welburn SC, Macleod E, Figarella K, & Duzensko M (2006) Programmed cell death in African trypanosomes. *Parasitology* 132 Suppl:S7-S18.
103. Proto WR, Coombs GH, & Mottram JC (2013) Cell death in parasitic protozoa: regulated or incidental? *Nat Rev Microbiol* 11(1):58-66.
104. Worthen C, Jensen BC, & Parsons M (2010) Diverse effects on mitochondrial and nuclear functions elicited by drugs and genetic knockdowns in bloodstream stage Trypanosoma brucei. *PLoS Negl Trop Dis* 4(5):e678.
105. Duszenko M, Figarella K, Macleod ET, & Welburn SC (2006) Death of a trypanosome: a selfish altruism. *Trends Parasitol* 22(11):536-542.
106. Gannavaram S, Vedvyas C, & Debrabant A (2008) Conservation of the pro-apoptotic nuclease activity of endonuclease G in unicellular trypanosomatid parasites. *J Cell Sci* 121(Pt 1):99-109.

107. Alvarez VE, *et al.* (2008) Autophagy is involved in nutritional stress response and differentiation in Trypanosoma cruzi. *J Biol Chem* 283(6):3454-3464.
108. Williams RA, Woods KL, Juliano L, Mottram JC, & Coombs GH (2009) Characterization of unusual families of ATG8-like proteins and ATG12 in the protozoan parasite Leishmania major. *Autophagy* 5(2):159-172.
109. Duszenko M, *et al.* (2011) Autophagy in protists. *Autophagy* 7(2):127-158.
110. Brennand A, *et al.* (2015) ATG24 Represses Autophagy and Differentiation and Is Essential for Homeostasy of the Flagellar Pocket in Trypanosoma brucei. *PLoS One* 10(6):e0130365.
111. Michaeli S (2015) The response of trypanosomes and other eukaryotes to ER stress and the spliced leader RNA silencing (SLS) pathway in Trypanosoma brucei. *Crit Rev Biochem Mol Biol* 50(3):256-267.
112. Michaeli S (2012) Spliced leader RNA silencing (SLS) - a programmed cell death pathway in Trypanosoma brucei that is induced upon ER stress. *Parasit Vectors* 5:107.
113. Hope R, *et al.* (2014) Phosphorylation of the TATA-binding protein activates the spliced leader silencing pathway in Trypanosoma brucei. *Sci Signal* 7(341):ra85.
114. Goldshmidt H, *et al.* (2010) Persistent ER stress induces the spliced leader RNA silencing pathway (SLS), leading to programmed cell death in Trypanosoma brucei. *PLoS Pathog* 6(1):e1000731.
115. Tiengwe C, Brown AE, & Bangs JD (2015) Unfolded Protein Response Pathways in Bloodstream Form Trypanosoma brucei? *Eukaryot Cell*.
116. Babokhov P, Sanyaolu AO, Oyibo WA, Fagbenro-Beyioku AF, & Iriemenam NC (2013) A current analysis of chemotherapy strategies for the treatment of human African trypanosomiasis. *Pathog Glob Health* 107(5):242-252.
117. Mathis AM, *et al.* (2006) Accumulation and intracellular distribution of antitrypanosomal diamidine compounds DB75 and DB820 in African trypanosomes. *Antimicrob Agents Chemother* 50(6):2185-2191.
118. Fidalgo LM & Gille L (2011) Mitochondria and trypanosomatids: targets and drugs. *Pharm Res* 28(11):2758-2770.
119. Baker N, *et al.* (2012) Aquaglyceroporin 2 controls susceptibility to melarsoprol and pentamidine in African trypanosomes. *Proc Natl Acad Sci U S A* 109(27):10996-11001.
120. Munday JC, Settimo L, & de Koning HP (2015) Transport proteins determine drug sensitivity and resistance in a protozoan parasite, Trypanosoma brucei. *Front Pharmacol* 6:32.
121. Alsford S, Field MC, & Horn D (2013) Receptor-mediated endocytosis for drug delivery in African trypanosomes: fulfilling Paul Ehrlich's vision of chemotherapy. *Trends Parasitol* 29(5):207-212.
122. Vansterkenburg EL, *et al.* (1993) The uptake of the trypanocidal drug suramin in combination with low-density lipoproteins by Trypanosoma brucei and its possible mode of action. *Acta Trop* 54(3-4):237-250.
123. Alsford S, *et al.* (2012) High-throughput decoding of antitrypanosomal drug efficacy and resistance. *Nature* 482(7384):232-236.
124. Kelley RJ, Alexander DL, Cowan C, Balber AE, & Bangs JD (1999) Molecular cloning of p67, a lysosomal membrane glycoprotein from Trypanosoma brucei. *Mol Biochem Parasitol* 98(1):17-28.

125. Pepin J, *et al.* (1995) Risk factors for encephalopathy and mortality during melarsoprol treatment of Trypanosoma brucei gambiense sleeping sickness. *Trans R Soc Trop Med Hyg* 89(1):92-97.
126. Baker N, de Koning HP, Maser P, & Horn D (2013) Drug resistance in African trypanosomiasis: the melarsoprol and pentamidine story. *Trends Parasitol* 29(3):110-118.
127. Fairlamb AH, Henderson GB, & Cerami A (1989) Trypanothione is the primary target for arsenical drugs against African trypanosomes. *Proc Natl Acad Sci U S A* 86(8):2607-2611.
128. Sapra A, Ramadan D, & Thorpe C (2015) Multivalency in the inhibition of oxidative protein folding by arsenic(III) species. *Biochemistry* 54(2):612-621.
129. Steverding D & Sexton DW (2013) Trypanocidal activity of salinomycin is due to sodium influx followed by cell swelling. *Parasit Vectors* 6:78.
130. Steglich C & Schaeffer SW (2006) The ornithine decarboxylase gene of Trypanosoma brucei: Evidence for horizontal gene transfer from a vertebrate source. *Infect Genet Evol* 6(3):205-219.
131. Iten M, *et al.* (1997) Alterations in ornithine decarboxylase characteristics account for tolerance of Trypanosoma brucei rhodesiense to D,L-alpha-difluoromethylornithine. *Antimicrob Agents Chemother* 41(9):1922-1925.
132. Vincent IM, *et al.* (2010) A molecular mechanism for eflornithine resistance in African trypanosomes. *PLoS Pathog* 6(11):e1001204.
133. Priotto G, *et al.* (2009) Nifurtimox-eflornithine combination therapy for second-stage African Trypanosoma brucei gambiense trypanosomiasis: a multicentre, randomised, phase III, non-inferiority trial. *Lancet* 374(9683):56-64.
134. Baker N, Alsford S, & Horn D (2011) Genome-wide RNAi screens in African trypanosomes identify the nifurtimox activator NTR and the eflornithine transporter AAT6. *Mol Biochem Parasitol* 176(1):55-57.
135. Boiani M, *et al.* (2010) Mode of action of nifurtimox and N-oxide-containing heterocycles against Trypanosoma cruzi: is oxidative stress involved? *Biochem Pharmacol* 79(12):1736-1745.
136. Taylor MC, McLatchie AP, & Kelly JM (2013) Evidence that transport of iron from the lysosome to the cytosol in African trypanosomes is mediated by a mucolipin orthologue. *Mol Microbiol* 89(3):420-432.
137. Carvalho S, *et al.* (2009) Heme as a source of iron to Leishmania infantum amastigotes. *Acta Trop* 109(2):131-135.
138. Koreny L, Lukes J, & Obornik M (2010) Evolution of the haem synthetic pathway in kinetoplastid flagellates: an essential pathway that is not essential after all? *Int J Parasitol* 40(2):149-156.
139. Horakova E, Changmai P, Paris Z, Salmon D, & Lukes J (2015) Simultaneous depletion of Atm and Mdl rebalances cytosolic Fe-S cluster assembly but not heme import into the mitochondrion of Trypanosoma brucei. *FEBS J* 282(21):4157-4175.
140. Krishnamurthy G, *et al.* (2005) Hemoglobin receptor in Leishmania is a hexokinase located in the flagellar pocket. *J Biol Chem* 280(7):5884-5891.
141. Singh SB, *et al.* (2003) Rab5-mediated endosome-endosome fusion regulates hemoglobin endocytosis in Leishmania donovani. *EMBO J* 22(21):5712-5722.

142. Schaer DJ, *et al.* (2005) Soluble hemoglobin-haptoglobin scavenger receptor CD163 as a lineage-specific marker in the reactive hemophagocytic syndrome. *Eur J Haematol* 74(1):6-10.
143. Merli ML, *et al.* (2016) The Trypanosoma cruzi Protein TcHTE Is Critical for Heme Uptake. *PLoS Negl Trop Dis* 10(1):e0004359.
144. Patel N, Singh SB, Basu SK, & Mukhopadhyay A (2008) Leishmania requires Rab7-mediated degradation of endocytosed hemoglobin for their growth. *Proc Natl Acad Sci U S A* 105(10):3980-3985.
145. Sengupta S, *et al.* (1999) Hemoglobin endocytosis in Leishmania is mediated through a 46-kDa protein located in the flagellar pocket. *J Biol Chem* 274(5):2758-2765.
146. Huynh C, *et al.* (2012) Heme uptake by Leishmania amazonensis is mediated by the transmembrane protein LHR1. *PLoS Pathog* 8(7):e1002795.
147. Hamza I (2006) Intracellular trafficking of porphyrins. *ACS Chem Biol* 1(10):627-629.
148. Chang KP, Chang CS, & Sassa S (1975) Heme biosynthesis in bacterium-protozoon symbioses: enzymic defects in host hemoflagellates and complemental role of their intracellular symbiotes. *Proc Natl Acad Sci U S A* 72(8):2979-2983.
149. Rossi BC & Dean RT (1988) Trypanosoma brucei: susceptibility to hydrogen peroxide and related products of activated macrophages. *Exp Parasitol* 65(1):131-140.
150. Penketh PG & Klein RA (1986) Hydrogen peroxide metabolism in Trypanosoma brucei. *Mol Biochem Parasitol* 20(2):111-121.
151. Flohe L (2012) The trypanothione system and its implications in the therapy of trypanosomatid diseases. *Int J Med Microbiol* 302(4-5):216-220.
152. Krauth-Siegel RL & Comini MA (2008) Redox control in trypanosomatids, parasitic protozoa with trypanothione-based thiol metabolism. *Biochim Biophys Acta* 1780(11):1236-1248.
153. Comini MA, Krauth-Siegel RL, & Flohe L (2007) Depletion of the thioredoxin homologue tryparedoxin impairs antioxidative defence in African trypanosomes. *Biochem J* 402(1):43-49.
154. Wilkinson SR, Horn D, Prathalingam SR, & Kelly JM (2003) RNA interference identifies two hydroperoxide metabolizing enzymes that are essential to the bloodstream form of the african trypanosome. *J Biol Chem* 278(34):31640-31646.
155. Comini MA, *et al.* (2004) Validation of Trypanosoma brucei trypanothione synthetase as drug target. *Free Radic Biol Med* 36(10):1289-1302.
156. Ariyanayagam MR, Oza SL, Guther ML, & Fairlamb AH (2005) Phenotypic analysis of trypanothione synthetase knockdown in the African trypanosome. *Biochem J* 391(Pt 2):425-432.
157. Wyllie S, *et al.* (2009) Dissecting the essentiality of the bifunctional trypanothione synthetase-amidase in Trypanosoma brucei using chemical and genetic methods. *Mol Microbiol* 74(3):529-540.
158. Torrie LS, *et al.* (2009) Chemical validation of trypanothione synthetase: a potential drug target for human trypanosomiasis. *J Biol Chem* 284(52):36137-36145.
159. Diechtierow M & Krauth-Siegel RL (2011) A tryparedoxin-dependent peroxidase protects African trypanosomes from membrane damage. *Free Radic Biol Med* 51(4):856-868.

160. Hiller C, Nissen A, Benitez D, Comini MA, & Krauth-Siegel RL (2014) Cytosolic peroxidases protect the lysosome of bloodstream African trypanosomes from iron-mediated membrane damage. *PLoS Pathog* 10(4):e1004075.
161. Krieger S, *et al.* (2000) Trypanosomes lacking trypanothione reductase are avirulent and show increased sensitivity to oxidative stress. *Mol Microbiol* 35(3):542-552.
162. Ceylan S, *et al.* (2010) The dithiol glutaredoxins of african trypanosomes have distinct roles and are closely linked to the unique trypanothione metabolism. *J Biol Chem* 285(45):35224-35237.
163. Comini MA, *et al.* (2008) Monothiol glutaredoxin-1 is an essential iron-sulfur protein in the mitochondrion of African trypanosomes. *J Biol Chem* 283(41):27785-27798.
164. Wilkinson SR, *et al.* (2006) Functional characterisation of the iron superoxide dismutase gene repertoire in Trypanosoma brucei. *Free Radic Biol Med* 40(2):198-209.
165. Prathalingham SR, Wilkinson SR, Horn D, & Kelly JM (2007) Deletion of the Trypanosoma brucei superoxide dismutase gene sodb1 increases sensitivity to nifurtimox and benznidazole. *Antimicrob Agents Chemother* 51(2):755-758.
166. Shlomai J (2010) Redox control of protein-DNA interactions: from molecular mechanisms to significance in signal transduction, gene expression, and DNA replication. *Antioxid Redox Signal* 13(9):1429-1476.
167. Sela D, Yaffe N, & Shlomai J (2008) Enzymatic mechanism controls redox-mediated protein-DNA interactions at the replication origin of kinetoplast DNA minicircles. *J Biol Chem* 283(46):32034-32044.
168. Dormeyer M, Reckenfelderbaumer N, Ludemann H, & Krauth-Siegel RL (2001) Trypanothione-dependent synthesis of deoxyribonucleotides by Trypanosoma brucei ribonucleotide reductase. *J Biol Chem* 276(14):10602-10606.
169. Alibu VP, *et al.* (2006) The role of Trypanosoma brucei MRPA in melarsoprol susceptibility. *Mol Biochem Parasitol* 146(1):38-44.
170. Nolan DP & Voorheis HP (2000) Factors that determine the plasma-membrane potential in bloodstream forms of Trypanosoma brucei. *Eur J Biochem* 267(15):4615-4623.
171. Van der Heyden N & Docampo R (2002) Significant differences between procyclic and bloodstream forms of Trypanosoma brucei in the maintenance of their plasma membrane potential. *J Eukaryot Microbiol* 49(5):407-413.
172. Anonymous (Blood Glucose.
173. Gruenberg J, Sharma PR, & Deshusses J (1978) D-Glucose transport in Trypanosoma brucei. D-Glucose transport is the rate-limiting step of its metabolism. *Eur J Biochem* 89(2):461-469.
174. Landon J, Fawcett JK, & Wynn V (1962) Blood pyruvate concentration measured by a specific method in control subjects. *J Clin Pathol* 15:579-584.
175. Wiemer EA, Michels PA, & Opperdoes FR (1995) The inhibition of pyruvate transport across the plasma membrane of the bloodstream form of Trypanosoma brucei and its metabolic implications. *Biochem J* 312 (Pt 2):479-484.
176. Isokawa M, Kanamori T, Funatsu T, & Tsunoda M (2014) Analytical methods involving separation techniques for determination of low-molecular-weight biothiols in human plasma and blood. *J Chromatogr B Analyt Technol Biomed Life Sci* 964:103-115.
177. Raper J, Portela MP, Lugli E, Frevert U, & Tomlinson S (2001) Trypanosome lytic factors: novel mediators of human innate immunity. *Curr Opin Microbiol* 4(4):402-408.

178. Halliwell B, Clement MV, & Long LH (2000) Hydrogen peroxide in the human body. *FEBS Lett* 486(1):10-13.
179. Lau A, Chan, LN (2013) *Basic skills in interpreting laboratory data: Chapter 6 Electrolytes, other minerals, and trace elements / Alan Lau, Lingtak- Neander Chan* (ASHSP, Bethesda, MD).
180. Anonymous (Blood bicarbonate.
181. Ruben L, Akins CD, Haghighat NG, & Xue L (1996) Calcium influx in Trypanosoma brucei can be induced by amphiphilic peptides and amines. *Mol Biochem Parasitol* 81(2):191-200.
182. Vanderheyden N, Wong J, & Docampo R (2000) A pyruvate-proton symport and an H+-ATPase regulate the intracellular pH of Trypanosoma brucei at different stages of its life cycle. *Biochem J* 346 Pt 1:53-62.
183. Defrise-Quertain F, Fraser-L'Hostis C, Coral D, & Deshusses J (1996) Kinetic study of the plasma-membrane potential in procyclic and bloodstream forms of Trypanosoma brucei brucei using the fluorescent probe bisoxonol. *Biochem J* 314 (Pt 2):595-601.
184. Mosimann M, *et al.* (2010) A Trk/HKT-type K+ transporter from Trypanosoma brucei. *Eukaryot Cell* 9(4):539-546.
185. Sanchez MA (2013) Molecular identification and characterization of an essential pyruvate transporter from Trypanosoma brucei. *J Biol Chem* 288(20):14428-14437.
186. Poole RC & Halestrap AP (1993) Transport of lactate and other monocarboxylates across mammalian plasma membranes. *Am J Physiol* 264(4 Pt 1):C761-782.
187. Tepel M, Nesbit O, Tokmak F, & Zidek W (1998) Sodium-dependent Cl-/HCO3- exchange in patients with chronic renal failure: correlation with renal function. *Kidney Int* 53(2):432-438.
188. Luo S, Fang J, & Docampo R (2006) Molecular characterization of Trypanosoma brucei P-type H+-ATPases. *J Biol Chem* 281(31):21963-21973.
189. Stiles JK, *et al.* (2003) Identification of surface-membrane P-type ATPases resembling fungal K(+)- and Na(+)-ATPases, in Trypanosoma brucei, Trypanosoma cruzi and Leishmania donovani. *Ann Trop Med Parasitol* 97(4):351-366.
190. Docampo R & Huang G (2015) Calcium signaling in trypanosomatid parasites. *Cell Calcium* 57(3):194-202.
191. Luo S, Rohloff P, Cox J, Uyemura SA, & Docampo R (2004) Trypanosoma brucei plasma membrane-type Ca(2+)-ATPase 1 (TbPMC1) and 2 (TbPMC2) genes encode functional Ca(2+)-ATPases localized to the acidocalcisomes and plasma membrane, and essential for Ca(2+) homeostasis and growth. *J Biol Chem* 279(14):14427-14439.
192. Bursell JD, Kirk J, Hall ST, Gero AM, & Kirk K (1996) Volume-regulatory amino acid release from the protozoan parasite Crithidia luciliae. *J Membr Biol* 154(2):131-141.
193. Munday JC, *et al.* (2014) Trypanosoma brucei aquaglyceroporin 2 is a high-affinity transporter for pentamidine and melaminophenyl arsenic drugs and the main genetic determinant of resistance to these drugs. *J Antimicrob Chemother* 69(3):651-663.
194. Uzcategui NL, *et al.* (2013) Trypanosoma brucei aquaglyceroporins facilitate the uptake of arsenite and antimonite in a pH dependent way. *Cell Physiol Biochem* 32(4):880-888.
195. Bassarak B, Uzcategui NL, Schonfeld C, & Duszenko M (2011) Functional characterization of three aquaglyceroporins from Trypanosoma brucei in osmoregulation and glycerol transport. *Cell Physiol Biochem* 27(3-4):411-420.

196. LeFurgey A, Ingram P, & Blum JJ (2001) Compartmental responses to acute osmotic stress in Leishmania major result in rapid loss of Na+ and Cl. *Comp Biochem Physiol A Mol Integr Physiol* 128(2):385-394.
197. Scott DA, Docampo R, Dvorak JA, Shi S, & Leapman RD (1997) In situ compositional analysis of acidocalcisomes in Trypanosoma cruzi. *J Biol Chem* 272(44):28020-28029.
198. Ruiz FA, Rodrigues CO, & Docampo R (2001) Rapid changes in polyphosphate content within acidocalcisomes in response to cell growth, differentiation, and environmental stress in Trypanosoma cruzi. *J Biol Chem* 276(28):26114-26121.
199. Rohloff P, Rodrigues CO, & Docampo R (2003) Regulatory volume decrease in Trypanosoma cruzi involves amino acid efflux and changes in intracellular calcium. *Mol Biochem Parasitol* 126(2):219-230.
200. Hashimoto M, *et al.* (2013) Inositol 1,4,5-trisphosphate receptor regulates replication, differentiation, infectivity and virulence of the parasitic protist Trypanosoma cruzi. *Mol Microbiol* 87(6):1133-1150.
201. Eintracht J, Maathai R, Mellors A, & Ruben L (1998) Calcium entry in Trypanosoma brucei is regulated by phospholipase A2 and arachidonic acid. *Biochem J* 336 (Pt 3):659-666.
202. Pyana Pati P, *et al.* (2014) Melarsoprol sensitivity profile of Trypanosoma brucei gambiense isolates from cured and relapsed sleeping sickness patients from the Democratic Republic of the Congo. *PLoS Negl Trop Dis* 8(10):e3212.
203. Bienert GP & Chaumont F (2014) Aquaporin-facilitated transmembrane diffusion of hydrogen peroxide. *Biochim Biophys Acta* 1840(5):1596-1604.
204. Gordon SM, Hofmann S, Askew DS, & Davidson WS (2011) High density lipoprotein: it's not just about lipid transport anymore. *Trends Endocrinol Metab* 22(1):9-15.
205. Zannis VI, Chroni A, & Krieger M (2006) Role of apoA-I, ABCA1, LCAT, and SR-BI in the biogenesis of HDL. *J Mol Med-Jmm* 84(4):276-294.
206. Muranjan M, Nussenzweig V, & Tomlinson S (1998) Characterization of the human serum trypanosome toxin, haptoglobin-related protein. *J Biol Chem* 273(7):3884-3887.
207. Chou MY, *et al.* (2009) Oxidation-specific epitopes are dominant targets of innate natural antibodies in mice and humans. *J Clin Invest* 119(5):1335-1349.
208. Binder CJ (2010) Natural IgM antibodies against oxidation-specific epitopes. *J Clin Immunol* 30 Suppl 1:S56-60.
209. Mott GA, Costales JA, & Burleigh BA (2011) A soluble factor from Trypanosoma cruzi inhibits transforming growth factor-ss-induced MAP kinase activation and gene expression in dermal fibroblasts. *PLoS One* 6(9):e23482.
210. Chang MK, *et al.* (1999) Monoclonal antibodies against oxidized low-density lipoprotein bind to apoptotic cells and inhibit their phagocytosis by elicited macrophages: evidence that oxidation-specific epitopes mediate macrophage recognition. *Proc Natl Acad Sci U S A* 96(11):6353-6358.
211. Genovese G, *et al.* (2010) Association of trypanolytic ApoL1 variants with kidney disease in African Americans. *Science* 329(5993):841-845.
212. Limou S, *et al.* (2015) Sequencing rare and common APOL1 coding variants to determine kidney disease risk. *Kidney Int*.
213. Friedman DJ, Kozlitina J, Genovese G, Jog P, & Pollak MR (2011) Population-based risk assessment of APOL1 on renal disease. *J Am Soc Nephrol* 22(11):2098-2105.

214. Johnstone DB, *et al.* (2012) APOL1 null alleles from a rural village in India do not correlate with glomerulosclerosis. *PLoS One* 7(12):e51546.
215. Gutierrez OM, *et al.* (2015) APOL1 nephropathy risk variants are associated with altered high-density lipoprotein profiles in African Americans. *Nephrol Dial Transplant*.
216. Ma L, *et al.* (2015) Localization of APOL1 protein and mRNA in the human kidney: nondiseased tissue, primary cells, and immortalized cell lines. *J Am Soc Nephrol* 26(2):339-348.
217. Madhavan SM, *et al.* (2011) APOL1 localization in normal kidney and nondiabetic kidney disease. *J Am Soc Nephrol* 22(11):2119-2128.
218. Kruzel-Davila E, Wasser WG, Aviram S, & Skorecki K (2015) APOL1 nephropathy: from gene to mechanisms of kidney injury. *Nephrol Dial Transplant*.
219. Nichols B, *et al.* (2015) Innate immunity pathways regulate the nephropathy gene Apolipoprotein L1. *Kidney Int* 87(2):332-342.
220. Larsen CP, Beggs ML, Saeed M, & Walker PD (2013) Apolipoprotein L1 risk variants associate with systemic lupus erythematosus-associated collapsing glomerulopathy. *J Am Soc Nephrol* 24(5):722-725.
221. Taylor HE, Khatua AK, & Popik W (2014) The innate immune factor apolipoprotein L1 restricts HIV-1 infection. *J Virol* 88(1):592-603.
222. Zhaorigetu S, Wan G, Kaini R, Jiang Z, & Hu CA (2008) ApoL1, a BH3-only lipid-binding protein, induces autophagic cell death. *Autophagy* 4(8):1079-1082.
223. Lee BT, *et al.* (2012) The APOL1 genotype of African American kidney transplant recipients does not impact 5-year allograft survival. *Am J Transplant* 12(7):1924-1928.
224. Reeves-Daniel AM, *et al.* (2011) The APOL1 gene and allograft survival after kidney transplantation. *Am J Transplant* 11(5):1025-1030.
225. Freedman BI, *et al.* (2015) Apolipoprotein L1 gene variants in deceased organ donors are associated with renal allograft failure. *Am J Transplant* 15(6):1615-1622.
226. Bruggeman LA, *et al.* (2014) Plasma apolipoprotein L1 levels do not correlate with CKD. *J Am Soc Nephrol* 25(3):634-644.
227. Thomson R, *et al.* (2014) Evolution of the primate trypanolytic factor APOL1. *Proc Natl Acad Sci U S A* 111(20):E2130-2139.
228. Lan X, *et al.* (2014) APOL1 risk variants enhance podocyte necrosis through compromising lysosomal membrane permeability. *Am J Physiol Renal Physiol* 307(3):F326-336.
229. Lan X, *et al.* (2015) Vascular smooth muscle cells contribute to APOL1-induced podocyte injury in HIV milieu. *Exp Mol Pathol* 98(3):491-501.
230. Khatua AK, *et al.* (2015) Exon 4-encoded sequence is a major determinant of cytotoxicity of apolipoprotein L1. *Am J Physiol Cell Physiol* 309(1):C22-37.
231. Cheng D, *et al.* (2015) Biogenesis and cytotoxicity of APOL1 renal-risk variant proteins in hepatocytes and hepatoma cells. *J Lipid Res*.
232. Wan G, *et al.* (2008) Apolipoprotein L1, a novel Bcl-2 homology domain 3-only lipid-binding protein, induces autophagic cell death. *J Biol Chem* 283(31):21540-21549.
233. Lan X, *et al.* (2015) Protein domains of APOL1 and its risk variants. *Exp Mol Pathol* 99(1):139-144.
234. Olabisi OA, *et al.* (2016) APOL1 kidney disease risk variants cause cytotoxicity by depleting cellular potassium and inducing stress-activated protein kinases. *Proc Natl Acad Sci U S A* 113(4):830-837.

235. Duchateau PN, *et al.* (1997) Apolipoprotein L, a new human high density lipoprotein apolipoprotein expressed by the pancreas. Identification, cloning, characterization, and plasma distribution of apolipoprotein L. *J Biol Chem* 272(41):25576-25582.
236. Sharma AK, Friedman DJ, Pollak MR, & Alper SL (2016) Structural characterization of the C-terminal coiled coil domains of wild-type and kidney disease associated mutants of Apolipoprotein L1. *FEBS J.*
237. Ito K, *et al.* (2014) Increased burden of cardiovascular disease in carriers of APOL1 genetic variants. *Circ Res* 114(5):845-850.
238. Freedman BI, *et al.* (2015) APOL1 associations with nephropathy, atherosclerosis, and all-cause mortality in African Americans with type 2 diabetes. *Kidney Int* 87(1):176-181.
239. Samanovic M, Molina-Portela MP, Chessler AD, Burleigh BA, & Raper J (2009) Trypanosome lytic factor, an antimicrobial high-density lipoprotein, ameliorates Leishmania infection. *PLoS Pathog* 5(1):e1000276.
240. McLaren PJ, *et al.* (2015) Identification of potential HIV restriction factors by combining evolutionary genomic signatures with functional analyses. *Retrovirology* 12:41.
241. Cossarizza A, *et al.* (2009) Simultaneous analysis of reactive oxygen species and reduced glutathione content in living cells by polychromatic flow cytometry. *Nat. Protoc.* 4(12):1790-1797.
242. Reczek CR & Chandel NS (2015) ROS-dependent signal transduction. *Curr Opin Cell Biol* 33:8-13.
243. Waks M & Beychok S (1974) Induced conformational states in human apohemoglobin on binding of haptoglobin 1--1. Effect of added heme as a probe of frozen structures. *Biochemistry* 13(1):15-22.
244. Niki E & Noguchi N (2000) Evaluation of antioxidant capacity. What capacity is being measured by which method? *IUBMB Life* 50(4-5):323-329.
245. Niki E (2010) Assessment of antioxidant capacity in vitro and in vivo. *Free Radic Biol Med* 49(4):503-515.
246. Hajduk SL, Hager K, & Esko JD (1992) High-density lipoprotein-mediated lysis of trypanosomes. *Parasitol Today* 8(3):95-98.
247. Uzcategui NL, *et al.* (2004) Cloning, heterologous expression, and characterization of three aquaglyceroporins from Trypanosoma brucei. *J. Biol. Chem.* 279(41):42669-42676.
248. Vanhollebeke B, *et al.* (2007) Distinct roles of haptoglobin-related protein and apolipoprotein L-I in trypanolysis by human serum. *Proc. Natl. Acad. Sci. U. S. A.* 104(10):4118-4123.
249. Hansen DB, Friis MB, Hoffmann EK, & Lambert IH (2012) Downregulation of the taurine transporter TauT during hypo-osmotic stress in NIH3T3 mouse fibroblasts. *J. Membr. Biol.* 245(2):77-87.
250. Diaz-Elizondo J, *et al.* (2006) Reactive oxygen species inhibit hyposmotic stress-dependent volume regulation in cultured rat cardiomyocytes. *Biochem. Biophys. Res. Commun.* 350(4):1076-1081.
251. Rojas-Rivera D, *et al.* (2009) Regulatory volume decrease in cardiomyocytes is modulated by calcium influx and reactive oxygen species. *FEBS Lett.* 583(21):3485-3492.
252. Roggy JL & Bangs JD (1999) Molecular cloning and biochemical characterization of a VCP homolog in African trypanosomes. *Mol. Biochem. Parasitol.* 98(1):1-15.

253. Wright VP, Reiser PJ, & Clanton TL (2009) Redox modulation of global phosphatase activity and protein phosphorylation in intact skeletal muscle. *J. Physiol.* 587(Pt 23):5767-5781.
254. Cosentino-Gomes D, *et al.* (2009) Modulation of Trypanosoma rangeli ecto-phosphatase activity by hydrogen peroxide. *Free Radic. Biol. Med.* 47(2):152-158.
255. Tamma G, *et al.* (2014) Glutathionylation of the aquaporin-2 water channel: a novel post-translational modification modulated by the oxidative stress. *J Biol Chem* 289(40):27807-27813.
256. Lambert IH, Klausen TK, Bergdahl A, Hougaard C, & Hoffmann EK (2009) ROS activate KCl cotransport in nonadherent Ehrlich ascites cells but K+ and Cl- channels in adherent Ehrlich Lettre and NIH3T3 cells. *Am. J. Physiol. Cell Physiol.* 297(1):C198-206.
257. Lambert IH (2003) Reactive oxygen species regulate swelling-induced taurine efflux in NIH3T3 mouse fibroblasts. *J. Membr. Biol.* 192(1):19-32.
258. Zhu L, *et al.* (2013) Involvement of volume-activated chloride channels in H2O 2 preconditioning against oxidant-induced injury through modulating cell volume regulation mechanisms and membrane permeability in PC12 cells. *Mol. Neurobiol.* 48(1):205-216.
259. Adragna NC, Di Fulvio M, & Lauf PK (2004) Regulation of K-Cl cotransport: from function to genes. *J. Membr. Biol.* 201(3):109-137.
260. Ren Z, Raucci FJ, Jr., Browe DM, & Baumgarten CM (2008) Regulation of swelling-activated Cl(-) current by angiotensin II signalling and NADPH oxidase in rabbit ventricle. *Cardiovasc Res* 77(1):73-80.
261. Lutje V, Seixas J, & Kennedy A (2010) Chemotherapy for second-stage Human African trypanosomiasis. *Cochrane Database Syst Rev* (8):CD006201.
262. Vincent IM, *et al.* (2012) Untargeted metabolomics reveals a lack of synergy between nifurtimox and eflornithine against Trypanosoma brucei. *PLoS Negl Trop Dis* 6(5):e1618.
263. Meshnick SR, Blobstein SH, Grady RW, & Cerami A (1978) An approach to the development of new drugs for African trypanosomiasis. *J. Exp. Med.* 148(2):569-579.
264. Jimenez V, Paredes R, Sosa MA, & Galanti N (2008) Natural programmed cell death in T. cruzi epimastigotes maintained in axenic cultures. *J Cell Biochem* 105(3):688-698.
265. Irigoin F, *et al.* (2009) Mitochondrial calcium overload triggers complement-dependent superoxide-mediated programmed cell death in Trypanosoma cruzi. *Biochem J* 418(3):595-604.
266. Dolai S, Pal S, Yadav RK, & Adak S (2011) Endoplasmic reticulum stress-induced apoptosis in Leishmania through Ca2+-dependent and caspase-independent mechanism. *J Biol Chem* 286(15):13638-13646.
267. Ascoli F, Fanelli MR, & Antonini E (1981) Preparation and properties of apohemoglobin and reconstituted hemoglobins. *Methods Enzymol.* 76:72-87.
268. Lustbader JW, Arcoleo JP, Birken S, & Greer J (1983) Hemoglobin-binding site on haptoglobin probed by selective proteolysis. *J. Biol. Chem.* 258(2):1227-1234.
269. Keij JF, Bell-Prince C, & Steinkamp JA (1999) Simultaneous analysis of relative DNA and glutathione content in viable cells by phase-resolved flow cytometry. *Cytometry* 35(1):48-54.
270. Ariyanayagam MR & Fairlamb AH (2001) Ovothiol and trypanothione as antioxidants in trypanosomatids. *Mol. Biochem. Parasitol.* 115(2):189-198.

271. De Greef C, Chimfwembe E, Kihang'a Wabacha J, Bajyana Songa E, & Hamers R (1992) Only the serum-resistant bloodstream forms of Trypanosoma brucei rhodesiense express the serum resistance associated (SRA) protein. *Ann Soc Belg Med Trop* 72 Suppl 1:13-21.
272. Jeffries TR, Morgan GW, & Field MC (2001) A developmentally regulated rab11 homologue in Trypanosoma brucei is involved in recycling processes. *J Cell Sci* 114(Pt 14):2617-2626.
273. Zhang J, *et al.* (2016) Analytical Validation of a Personalized Medicine APOL1 Genotyping Assay for Nondiabetic Chronic Kidney Disease Risk Assessment. *J Mol Diagn* 18(2):260-266.
274. Edwards JK (2016) Chronic kidney disease: Potassium efflux in APOL1 nephropathy. *Nat Rev Nephrol* 12(3):124.
275. Jaiman S, Sharma AK, Singh K, & Khanna D (2013) Signalling mechanisms involved in renal pathological changes during cisplatin-induced nephropathy. *Eur J Clin Pharmacol* 69(11):1863-1874.
276. Wang WH & Giebisch G (2009) Regulation of potassium (K) handling in the renal collecting duct. *Pflugers Arch* 458(1):157-168.
277. Babilonia E, *et al.* (2006) Mitogen-activated protein kinases inhibit the ROMK (Kir 1.1)-like small conductance K channels in the cortical collecting duct. *J Am Soc Nephrol* 17(10):2687-2696.
278. Li D, *et al.* (2006) Inhibition of MAPK stimulates the Ca2+ -dependent big-conductance K channels in cortical collecting duct. *Proc Natl Acad Sci U S A* 103(51):19569-19574.
279. Cheng D, *et al.* (2015) Biogenesis and cytotoxicity of APOL1 renal risk variant proteins in hepatocytes and hepatoma cells. *J Lipid Res* 56(8):1583-1593.
280. Docampo R, Jimenez V, Lander N, Li ZH, & Niyogi S (2013) New insights into roles of acidocalcisomes and contractile vacuole complex in osmoregulation in protists. *Int Rev Cell Mol Biol* 305:69-113.
281. Waldegger S, *et al.* (1998) Mechanisms and clinical significance of cell volume regulation. *Nephrol Dial Transplant* 13(4):867-874.
282. Zhou X (2016) How do kinases contribute to tonicity-dependent regulation of the transcription factor NFAT5? *World J Nephrol* 5(1):20-32.

SDG.